The Analyst

The Analytical Journal
of The Chemical Society

A monthly international publication dealing with all branches of analytical chemistry

Volume 103 No 1231 Pages 1009–1088 October 1978

THE ANALYST

THE ANALYTICAL JOURNAL OF THE CHEMICAL SOCIETY

Published by The Chemical Society

Editorial: The Director of Publications, The Chemical Society, Burlington House, London, W1V 0BN. Telephone 01-734 9864. Telex No. 268001

Advertisements: Advertisement Department, The Chemical Society, Burlington House, Piccadilly, London, W1V 0BN. Telephone 01-734 9864

Subscriptions (non-members): The Chemical Society, Distribution Centre, Blackhorse Road, Letchworth, Herts., SG6 1HN

Volume 103 No 1231 October 1978

Summaries of Papers in this Issue

Methods for the Quantitative Determination of Asbestos and Quartz in Bulk Samples Using X-ray Diffraction

Procedures are described for the quantitative determination of the asbestos and α-quartz contents of bulk samples by use of X-ray powder diffractometry. The method gives satisfactory results for several different types of asbestos and for mixtures of two or more different types. Problems with sample grinding and preferred-orientation effects have been largely overcome. An effective procedure has been developed for grinding samples to a suitable particle size for accurate quantitative work. This procedure works equally well for all the types of asbestos studied and the sample is intimately mixed with the internal standard, nickel(II) oxide, at the same time. A sample press has been designed that enables the same pressure to be applied to each sample when sample holders are filled for the diffractometer, giving the same degree of preferred orientation each time. Calibration lines have been calculated for chrysotile, amosite, crocidolite and anthophyllite, and results are given for mixtures containing two or more types of asbestos as well as other commonly occurring minerals.

Similar techniques are used to grind samples containing quartz and to mix them with internal standard. Work on both synthetic and real samples is described and results are compared with those obtained by use of an infrared spectroscopic method.

Keywords: *Asbestos determination*; *quartz determination*; *X-ray diffraction*

M. TAYLOR

Health & Safety Executive, The Occupational Medicine and Hygiene Laboratories, 403–405 Edgware Road, London, NW2 6LN.

Analyst, 1978, **103**, 1009–1020.

Application of the Faraday Effect to the Trace Determination of Cadmium by Atomic Spectroscopy with an Electrothermal Atomiser

As a technique for the trace determination of elements, the Faraday effect has been applied to atomic spectroscopy with the use of electrothermal atomisers. The atomiser was located between two crossed plane-polarisers (called the polariser and the analyser). An electromagnet magnetised the atomised sample and, as a result of the Faraday effect, the source radiation could, in the presence of the atomic vapour, pass through the optical system. A simple theoretical treatment was developed to explain the dependence of the transmitted intensity on the magnetic field strength and the source intensity and the ability to eliminate the effects of background scattering.

Measurements on cadmium were carried out at a wavelength of 228.8 nm, dispensing into the atomiser 5-μl samples, which, after drying, were atomised at 1000–1800 °C. The calibration graphs demonstrated a square-law dependence. At high concentrations the calibration graphs were corrected for atomic absorption. The technique gave a detection limit of 5×10^{-13} g for cadmium.

Keywords: *Magneto-optical rotation*; *atomic spectroscopy*; *electrothermal atomisation*; *Faraday effect*; *cadmium determination*

K. KITAGAWA, T. SHIGEYASU and T. TAKEUCHI

Department of Synthetic Chemistry, Faculty of Engineering, Nagoya University, Furo-cho, Chikusa-ku, Nagoya, Japan.

Analyst, 1978, **103**, 1021–1030.

Flotation of Sub-microgram Amounts of Arsenic Coprecipitated with Iron(III) Hydroxide from Natural Waters and Determination of Arsenic by Atomic-absorption Spectrophotometry Following Hydride Generation

A method is described for the flotation and determination of sub-microgram levels of arsenic in water. A sub-microgram amount of arsenic(III, V) in a 500-ml sample of water is coprecipitated with iron(III) hydroxide at pH 8–9. The precipitate is floated with the aid of sodium oleate and small air bubbles, then separated and dissolved in 5 M hydrochloric acid, and finally the arsenic content is determined by generation of arsine using sodium tetrahydroborate(III) as a reductant and atomic-absorption spectrophotometry with a long absorption cell (60 × 1.2 cm i.d.). This separation technique has been successfully applied to the determination of sub-microgram amounts of arsenic(III, V) in natural waters.

Keywords: *Arsenic · determination*; *flotation*; *natural waters*; *atomic-absorption spectrophotometry*; *hydride generation*

SUSUMU NAKASHIMA

Institute for Agricultural and Biological Sciences, Okayama University, Kurashiki-shi 710, Japan.

Analyst, 1978, **103**, 1031–1036.

Extraction - Spectrophotometric Determination of Tin in Lead and Lead-based Alloys with 5,7-Dichloroquinolin-8-ol

A method is described for the direct spectrophotometric determination of micro-amounts of tin, by extraction into a chloroform solution of 5,7-dichloroquinolin-8-ol from a solution containing sulphuric acid. The influence of the different experimental parameters on the formation and extraction of the complex were studied and optimum conditions for the determination of tin were established. The precision of the extraction - spectrophotometric procedure, expressed in terms of relative standard deviation, was 1.4%.

It is shown that two different complexes (with $\lambda_{max.}$ 403 or 390 nm) can be extracted into the chloroform, depending on the presence or absence of chloride and on the pH of the solution.

The method has been tested on six standard lead-based samples with tin contents ranging from 0.05 to 1%. The average relative error (mean error) of the results lies within the range ±1.4%, which shows that the accuracy is good and that systematic errors are absent.

Keywords: *Tin determination*; *5,7-dichloroquinolin-8-ol extraction*; *spectrophotometry*; *lead-based alloys*

A. SANZ-MEDEL and A. M. GUTIÉRREZ CARRERAS

Departamento de Química Analítica, Facultad de Ciencias Químicas, Universidad Complutense, Ciudad Universitaria, Madrid-3, Spain.

Analyst, 1978, **103**, 1037–1045.

Method for the Determination of Methanol in Binary Methanol - Water Mixtures by Use of Ion-selective Electrodes

For a given concentration of indicator ion X (X = F^-, Cl^-, Br^-, I^-, OH^-, S^{2-}, Ag^+ or H^+), the systematic change of cell potential, E, with variation in the concentration of methanol provides a graphical method for the rapid determination of methanol in methanol - water mixtures. Readings obtained by direct potentiometry show good reproducibility and stability. In 99.0–99.9% *m/m* methanol, containing 10^{-2} M hydrochloric acid, trace amounts of water can be determined accurately owing to a potential "anomaly."

Keywords: *Methanol determination*; *methanol - water mixtures*; *ion-selective electrodes*; *trace water determination*

G. J. KAKABADSE, H. ABDULAHED MALEILA, M. N. KHAYAT, G. TASSOPOULOS and A. VAHDATI

Department of Chemistry, University of Manchester Institute of Science and Technology, P.O. Box 88, Manchester, M60 1QD.

Analyst, 1978, **103**, 1046–1052.

OCTOBER 1978 Vol. 103 No. 1231

The Analyst

Methods for the Quantitative Determination of Asbestos and Quartz in Bulk Samples Using X-ray Diffraction

M. Taylor

Health & Safety Executive, The Occupational Medicine and Hygiene Laboratories, 403–405 Edgware Road, London, NW2 6LN

Procedures are described for the quantitative determination of the asbestos and α-quartz contents of bulk samples by use of X-ray powder diffractometry. The method gives satisfactory results for several different types of asbestos and for mixtures of two or more different types. Problems with sample grinding and preferred-orientation effects have been largely overcome. An effective procedure has been developed for grinding samples to a suitable particle size for accurate quantitative work. This procedure works equally well for all the types of asbestos studied and the sample is intimately mixed with the internal standard, nickel(II) oxide, at the same time. A sample press has been designed that enables the same pressure to be applied to each sample when sample holders are filled for the diffractometer, giving the same degree of preferred orientation each time. Calibration lines have been calculated for chrysotile, amosite, crocidolite and anthophyllite, and results are given for mixtures containing two or more types of asbestos as well as other commonly occurring minerals.

Similar techniques are used to grind samples containing quartz and to mix them with internal standard. Work on both synthetic and real samples is described and results are compared with those obtained by use of an infrared spectroscopic method.

Keywords: *Asbestos determination*; *quartz determination*; *X-ray diffraction*

Inhalation of asbestos dust can cause fatal lung diseases such as cancer and asbestosis and also mesothelioma of the pleura and abdominal cavity linings. X-ray diffraction (XRD) is an established procedure for the qualitative determination of asbestos, by which it is possible to identify the different crystalline types (chrysotile, amosite, crocidolite and anthophyllite), and to distinguish crocidolite from amosite even though the two have very similar diffraction patterns. The technique is less satisfactory when accurate quantitative results for asbestos are required; one of the main problems is that the preferred-orientation effects of fibrous materials cause large variations in diffraction-peak intensities.[1] Also, it is difficult to obtain a truly representative portion from the bulk of the sample submitted for analysis because sample mixtures are often inhomogeneous and the fibrous nature of asbestos inhibits mechanical mixing and stirring. Asbestos generally, and the chrysotile form in particular is difficult to grind to the optimum size for accurate quantitative work (Crable and Knott used a particle size of less than 3.5 μm in their work on amosite and crocidolite[2]). Preparation of an intimate mixture of the ground asbestos with an internal standard, *e.g.*, calcium fluoride or nickel(II) oxide, is also difficult. The method described here substantially overcomes these problems. Crable and Knott used a powder diffractometer in their work on amosite and crocidolite, and also on chrysotile.[3] Goodhead and Martindale used a powder camera technique.[4] The proposed method is substantially different and is applicable to all types of asbestos and also to mixtures containing several types in conjunction with other minerals. Nickel(II) oxide as purchased and without pre-sizing is used as the internal standard. Mixing and grinding are carried out reproducibly in grinding mills. The grinding procedures adopted reduce the length of the asbestos fibres to below 5.0 μm, irrespective of asbestos type or the complexity of the mixture being ground, which helps to reduce preferred-orientation problems.

It was found that the intensities of the asbestos diffraction peaks were dependent upon the pressure used in preparing the samples for scanning in the diffractometer. A sample press has been constructed to enable the same pressure and thus the same degree of preferred orientation to be applied to each sample.

The method has been used to analyse a large variety of asbestos-containing samples, including complex mixtures. Analytical results obtained by analysts experienced at this type of work gave good agreement with those obtained by others new to the method. A similar analytical procedure has been used to prepare quartz samples for XRD analysis. Inhalation of quartz particles in the respirable range of below 5.0 μm can, over many years, cause the lung disease silicosis, so dust samples are analysed in order to help predict if the use of a particular material in a factory could cause a quartz hazard. The analysis of asbestos-containing samples will be described first and then the related procedures for the analysis of quartz will be discussed.

Determination of Asbestos

Apparatus

Philips PW 1011/00 X-ray generator. A vertical powder diffractometer fitted with a graphite-crystal focusing monochromator and proportional counter. Copper Kα X-radiation is produced with generator settings of 44 kV, 36 mA, 1° divergence slit and $\frac{1}{4}$° anti-scatter used as receiving slit.

Chart recorder. The chart recorder used for recording the XRD traces has a zero suppression facility, which has proved invaluable when traces at very low attenuations are recorded in order to measure very low percentages by mass of asbestos.

Glen Creston microhammer mill. Fitted with a 3.0 mm mesh diameter screen. The microhammer mill has been modified by replacing with a screw the retaining clip that normally holds the hammers in place on the central shaft, thus facilitating removal of the hammers for cleaning.

Analytical mixer mill. Obtained from Glen Creston Ltd. With a 5-ml hardened stainless-steel grinding cylinder and steel ball pestle, and a 5-ml agate grinding cylinder and matching ball pestle.

Sample press. Specially constructed (see below).

Reagents

Union Internationale Contre le Cancer (UICC) standard reference asbestos samples. Chrysotile A, chrysotile B, amosite, crocidolite and anthophyllite.

Nickel(II) oxide (NiO). Johnson Matthey Specpure.

γ-Aluminium(III) oxide (γ-Al_2O_3). Aluminium oxide 90 active, neutral for column chromatography (E. Merck).

Acetic acid, 1 N. Analytical-reagent grade diluted with de-mineralised water.

Cyclohexane. Analytical-reagent grade.

Cellulose powder. Whatman CF 11.

Procedure

Samples as received are often very inhomogeneous and are ground in two stages. First, a microhammer mill fitted with a 3 mm mesh screen is used to grind all, or a substantial portion (several grams), of the sample material to an average fibre length of 1–2 mm. Asbestos fibres in bulk samples are usually much longer than this and must be reduced in length before the mixer mill can be used to grind them to a size suitable for analysis. After the first grinding a representative portion can be taken from the bulk sample and a qualitative XRD pattern obtained. Comparison with reference patterns shows the types of asbestos present.

If chrysotile is detected a rough visual estimate is made of whether the percentage by mass is likely to exceed 60%. Chrysotile is the most difficult type of asbestos to grind and a larger mass of γ-aluminium(III) oxide must be used in the second grinding to give the required fibre length if the percentage by mass is over 60%. Any carbonates present, *e.g.*, calcium carbonate, should be removed by treatment with 1 N acetic acid.

For the second grinding the steel cylinder of the mixer mill is used. An amount of sample weighing 0.1000 ± 0.0005 g, 0.1000 ± 0.0005 g of γ-aluminium(III) oxide [0.1500 ± 0.0005 g of γ-aluminium(III) oxide should be used if the percentage by mass of chrysotile is estimated to be above 60%], 0.0333 ± 0.0001 g of nickel(II) oxide and 0.5 ml of cyclohexane (added by pipette) are placed in the cylinder with the steel ball pestle, the ends of the cylinder are taped with poly(vinyl chloride) tape in order to prevent leakage and the mixture is ground for 25 min (see Note). The mixer mill is thus used both to grind the sample and to mix it intimately with the nickel(II) oxide, the internal standard, in one operation. If the specified amount of sample cannot easily be weighed out because of handling problems, a slightly smaller amount is weighed and the combined mass of sample plus γ-aluminium(III) oxide is made up to 0.2000 ± 0.0010 g (or 0.2500 ± 0.0010 g for samples containing more than 60% of chrysotile) by adding more γ-aluminium(III) oxide. The necessary correction is applied to the result.

NOTE—

The γ-aluminium(III) oxide acts as a grinding agent and is effective in reducing the asbestos fibres to the required length, particularly with cyclohexane present. It also helps to ensure that the grinding is uniform; without γ-aluminium(III) oxide present the asbestos is not uniformly ground and a sizeable proportion of it merely becomes packed into the end caps of the grinding cylinder. γ-Aluminium(III) oxide gives a very weak diffraction peak, which does not interfere with that of asbestos.

Close control of the mass loading of the grinding cylinder and of the length of the grinding period helps to ensure that samples are reproducibly ground so that most of the fibres are of a length below 5.0 μm. That the grinding is reproducible has been verified by optical microscopy.

The material is removed from the cylinder and the cyclohexane is allowed to evaporate. The dry residue is ground in the mixer mill in an agate grinding cylinder with an agate ball pestle for a further 5 min in order to break up the lumps left when the cyclohexane has evaporated, and to improve homogeneity.

Samples are pressed in standard Philips sample holders with a specially constructed sample press (see below). A 0.620 ± 0.001-g amount of cellulose powder is used for each pressing. The sample is then scanned in the diffractometer over the relevant asbestos peaks and also over two nickel(II) oxide peaks. The primary peaks for chrysotile, amosite, crocidolite and anthrophyllite are 7.36, 8.33, 8.42 and 3.24 Å, respectively. The secondary peaks are 3.66, 3.07, 3.09 and 3.05 Å, respectively. These peaks are used in conjunction with the nickel(II) oxide 2.09- and 2.41-Å peaks (1 Å = 10^{-10} m). Scanning speed is normally ½° min^{-1} but should be slower if the percentage by mass of asbestos is low. Three separate portions of each sample mixture are scanned. The asbestos to nickel(II) oxide peak-height ratios are calculated and the percentage by mass of asbestos in the sample is determined from calibration graphs. Four values are generally obtained for each type of asbestos present in the sample, from the permutations of (asbestos primary or secondary peak height)/[nickel(II) oxide 2.09- or 2.41-Å peak height]. These four values are averaged to give the concentration of asbestos.

Sample Press

Standard Philips sample holders for the powder diffractometer were used and sample mixtures were pressed in place with cellulose powder. In the early stages of the work two analysts prepared calibration mixtures, pressing sample slides in the usual way and independently constructing calibration graphs.

It was found, however, that calibration graphs produced by one analyst could not be used by the other; each analyst had to produce calibration graphs for his own use only. It was realised that the asbestos to nickel(II) oxide peak-height ratios obtained were dependent upon the pressure used to press the samples. To ensure that the same pressure was applied to each sample, a press (Fig. 1) based on a small portable electric drill stand was designed and constructed. The press is made of steel and is plated to prevent corrosion. Two locating pins, B, fit into holes in the base plate, A, and the locating plate, C, for the metal sample holder, H, and the block, D, fits on to these. A fixed mass of cellulose powder is pressed to a fixed volume each time, the volume being controlled by two adjustable stops, E, which screw into the block and which arrest the downwards movement of the plunger. It was found by trial and error that a press with the dimensions shown required 0.620 ± 0.001 g of cellulose powder to obtain good pressings, and this mass of powder was used each

time. A piece of Mylar film placed between the locating and base plates prevents the sample sticking to the base plate; a fresh piece is used for each sample. The sample press enabled different analysts to use one set of calibration graphs.

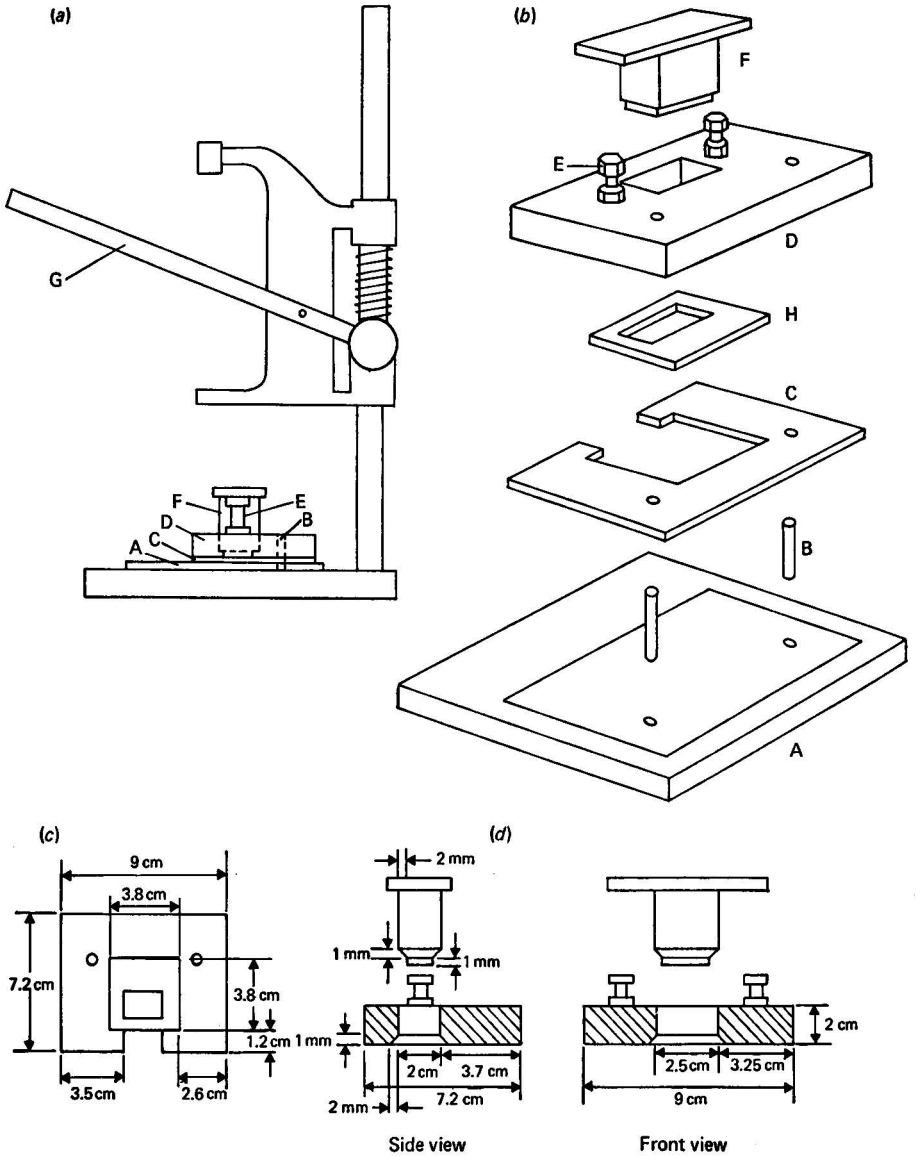

Fig. 1. Diagrams showing the construction of the sample press (not to scale). (*a*), Side view. (*b*), Exploded view. A, Base plate, bolted to the base of the drill stand; B, locating pins; C, locating plate for sample holder; D, block; E, adjustable stops; F, plunger; G, strengthened arm for the drill stand; H, sample holder. (*c*), Locating plate with sample holder *in situ* (plate thickness and sample-holder thickness both approximately 1 mm). (*d*), Cross-sections through the block and plunger.

Operation of the press is as follows. The locating plate is placed over the locating pins and the sample holder is fitted into place. A thin layer of sample mixture is spread evenly over the hole in the sample holder. The block is fitted into place, the cellulose powder is poured over the sample through the hole in the block and its surface is roughly levelled with

a microspatula. Lowering the handle of the drill stand moves the plunger down until its progress is arrested by the stops. The bevelled edges prevent the sample from sticking within the block. The plunger is slowly withdrawn and the block removed from the locating pins: the pressed sample can then be removed for scanning in the powder diffractometer. The cellulose becomes compacted by the action of the press and it does not stick to the plunger when the latter is withdrawn.

Calibration Graphs

The UICC standard reference samples supplied by the Pneumoconiosis unit of the Medical Research Council[5] were used to prepare mixtures for the construction of calibration graphs. These samples were received already ground to an average fibre length of approximately 1–2 mm, which makes them directly comparable with real samples that have been ground by the microhammer mill fitted with the 3.0 mm mesh diameter screen. It was therefore only necessary to grind them in the mixer mill by means of the procedure given above. Calibration graphs were constructed for all of the reference materials; at least nine mixtures were prepared for each material.

For any mixture the total mass of asbestos plus γ-aluminium(III) oxide as primary diluent was 0.1000 $\pm$ 0.0005 g. [For example, a 60% amosite mixture would contain 0.0600 $\pm$ 0.0003 g of amosite diluted with 0.0400 $\pm$ 0.0002 g of γ-aluminium(III) oxide.] To this would be added 0.0333 $\pm$ 0.0001 g of nickel(II) oxide and a further 0.1000 $\pm$ 0.0005 g of γ-aluminium(III) oxide as grinding agent; chrysotile is a special case as it is particularly difficult to grind and for mixtures containing more than 0.0600 $\pm$ 0.0003 g of chrysotile (*i.e.*, more than 60% of chrysotile), the amount of γ-aluminium(III) oxide as grinding agent had to be increased to 0.1500 $\pm$ 0.0005 g.

The absorption coefficient of the asbestos being analysed differs from that of the matrix. If an internal standard is added in a constant proportion, the concentration of the asbestos component is a linear function of the asbestos to internal standard peak-height ratio.[6]

Three separate portions of each mixture were scanned and the peak-height ratios calculated. Average values for the ratios were used to construct the graphs. A calibration graph is shown for the 7.36-Å chrysotile A diffraction peak in Fig. 2. All the calibration graphs were straight lines and the coefficients m and c for the straight-line equation $y = mx + c$, calculated by linear regression, are given in Table I for each line.

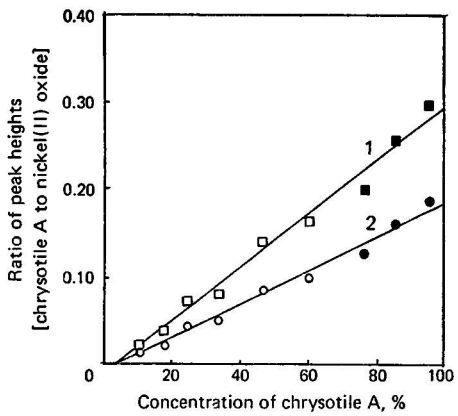

Fig. 2. Calibration graphs for chrysotile A using the 7.36-Å chrysotile A peak. Wavelength of nickel(II) oxide peak: 1, 2.41 Å; 2, 2.09 Å. Amount of γ-aluminium(III) oxide added as grinding agent: □ and ○, 0.100 g; ■ and ●, 0.150 g. For each mixture the combined mass of chryostile A and γ-aluminium(III) oxide added as primary diluent is 0.1000 $\pm$ 0.0005 g, with 0.0333 $\pm$ 0.0001 g of nickel(II) oxide added as internal standard.

Asbestos does not give particularly intense diffraction peaks. Calibration lines do not pass through the origin as the peak heights are measured from a "noisy" base line; a significant peak cannot be detected until a few per cent. of asbestos are present. Fig. 3 shows how the base lines were drawn for the relevant peaks in order to measure the peak heights.

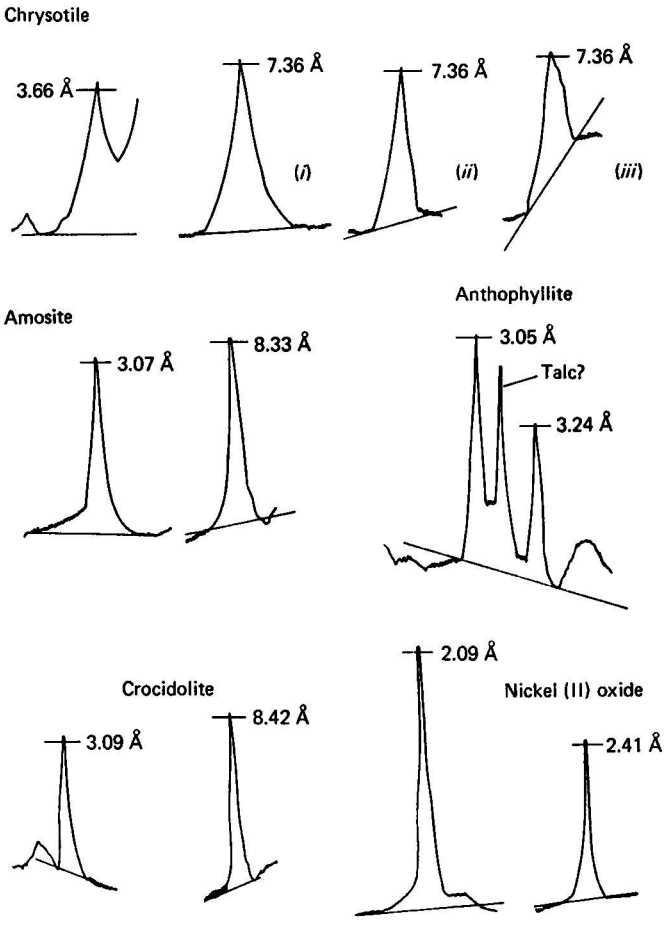

Fig. 3. Peak shapes for asbestos and nickel(II) oxide showing base lines drawn for measurement of peak height. Three alternative shapes are shown for the chrysotile 7.36-Å peak.

Results and Discussion

Correlation coefficients were calculated for the calibration lines (Table I). The coefficients were generally better than 0.990, except for the chryostile A lines based on the 3.66-Å chrysotile peak and the anthophyllite lines based on the 3.05-Å anthophyllite peak, which gave slightly lower values. For all the calibration lines other than these exceptions there is a 95% probability that the true value will lie within $\pm 8\%$ of the value determined. In the worst case, *i.e.*, for the anthophyllite lines based on the 3.05-Å peak, this figure drops to $\pm 12\%$; for the chrysotile A lines based on the 3.66-Å chrysotile peak it is $\pm 10\%$.

The lower accuracy found for calibration lines based on the 3.05-Å anthophyllite diffraction peak is due to overlap of the peak with a spurious one at 3.12 Å; this last peak is not listed for anthophyllite in the ASTM index and it causes calibration lines based on the 3.05-Å peak to intersect the y-axis at a point a little above the origin. The presence of talc as an impurity would explain the 3.12-Å peak.

Goodhead and Martindale[4] state that samples of a particular type of asbestos mined from different locations can have slightly different chemical compositions and that this can alter the diffraction pattern, so that calibration lines may be somewhat dependent upon the origin of the sample. The calibration lines obtained for UICC chrysotile A mined in Rhodesia and UICC chrysotile B (which originates in Canada) demonstrate this effect. Ideally, therefore, specimens of pure asbestos should be taken at each sampling site and should be used to determine whether or not the existing calibration graphs can be used without correction. In practice, however, it is rarely possible to obtain these specimens of "pure" asbestos when sampling and the unmodified graphs must be used.

TABLE I

VALUES OF THE COEFFICIENTS m AND c IN THE ASBESTOS CALIBRATION LINES $y = mx + c$

y = asbestos to nickel(II) oxide peak-height ratio and x = percentage of asbestos.

Type of asbestos	Asbestos peak/Å	Nickel(II) oxide peak/Å	m	c
Chrysotile A	7.36	2.41	0.00309	−0.0128
	7.36	2.09	0.00197	−0.00948
	3.66	2.41	0.00258	−0.00491
	3.66	2.09	0.00165	−0.00427
Chrysotile B	7.36	2.41	0.00277	−0.0148
	7.36	2.09	0.00173	−0.00874
	3.66	2.41	0.00255	−0.00905
	3.66	2.09	0.00158	−0.00488
Amosite	8.33	2.41	0.00888	−0.0206
	8.33	2.09	0.00535	−0.0134
	3.07	2.41	0.00706	−0.00372
	3.07	2.09	0.00424	−0.00256
Crocidolite	8.42	2.41	0.00964	−0.0306
	8.42	2.09	0.00566	−0.0173
	3.09	2.41	0.00610	−0.0146
	3.09	2.09	0.00358	−0.00792
Anthopyilite	3.24	2.41	0.00185	−0.00264
	3.24	2.09	0.00115	−0.00202
	3.05	2.41	0.00264	+0.0149
	3.05	2.09	0.00163	+0.00946

Factors affecting the determination of chrysotile

Generally four results are calculated for each type of asbestos in the sample. These results arise from the permutations of the primary and secondary asbestos peaks with the two nickel(II) oxide peaks. The cellulose used to hold the sample in place can give a peak that partially overlaps the 3.66-Å chrysotile peak. If cellulose shows on the surface of the sample pressing it is safest to use only ratios based on the 7.36-Å peak to calculate the result, because the height of the 3.66-Å chrysotile peak may have been affected. The height of the 3.66-Å peak is usually slightly less than that of the 7.36-Å primary peak. The mineral kaolinite gives a diffraction pattern which overlaps that of chrysotile, and no way has yet been found of overcoming its interference with the chrysotile trace.

Mixtures containing crocidolite and amosite

If crocidolite and amosite occur together in a sample, results must be based on the 3.09-Å secondary peak for crocidolite and the 3.07-Å secondary peak for amosite. The primary peaks for crocidolite and amosite at 8.42 and 8.33 Å, respectively, cannot readily be resolved.

Removal of carbonates

A large proportion of asbestos-containing samples received by this laboratory are taken during de-lagging operations and often contain a high proportion of calcium carbonate or other carbonates. Calcium carbonate gives an intense diffraction peak at 3.035 Å, which

overlaps the 3.09- and 3.07-Å secondary peaks of crocidolite and amosite, respectively. If, therefore, it is not removed from samples containing amosite or crocidolite, results must be based on the primary asbestos lines only. Treatment with 1 N acetic acid removes the carbonates, so that the sample mixture is concentrated and simplified and secondary asbestos lines can be used in the determination. It was not known, however, whether the different types of asbestos were completely immune to attack by this reagent. Portions of UICC standard reference asbestos samples were subjected to the treatment with 1 N acetic acid and were then analysed for asbestos content. It was found that the percentage remaining of amosite, chrysotile A, crocidolite and anthophyllite was 85.5, 92, 94 and 97, respectively. These results suggest that amosite in particular is not completely free from attack by this acid.

Analysis of synthetic mixtures

Test mixtures containing two or three different types of asbestos, and some containing asbestos plus quartz or calcium carbonate, were analysed and the results are shown in Table II. For mixtures containing both amosite and crocidolite their concentrations have been calculated using the 3.07- and 3.09-Å secondary peaks and no allowance has been made for the overlap between these two peaks. It can be seen that the largest deviations between actual and calculated values occur for chrysotile and in some instances the actual value is not within $\pm 10\%$ of the value determined.

TABLE II

RESULTS OF THE ANALYSIS OF TEST MIXTURES CONTAINING ASBESTOS

Mixture	Composition, % *m/m*	Amount of asbestos determined, % *m/m*
1	Amosite, 18 Chrysotile A, 28.5 Calcium carbonate, 46.6 γ-Aluminium(III) oxide, 6.9	Amosite, 17 Chrysotile, 22.5
2	Crocidolite, 8.3 Chrysotile B, 74 γ-Aluminium(III) oxide, 17.7	Crocidolite, 11 Chrysotile, 73
3	Quartz, 13 Amosite, 14 Calcium carbonate, 73	Amosite, 13.5
4	Quartz, 14.6 Chrysotile A, 32 γ-Aluminium(III) oxide, 53.4	Chrysotile, 25.5
5	Crocidolite, 16 Chrysotile A, 36 Amosite, 48	Crocidolite, 23.5* Chrysotile, 37 Amosite, 53
6	Crocidolite, 38 Chrysotile B, 24.5 Amosite, 15 γ-Aluminium(III) oxide, 22.5	Crocidolite, 42* Chrysotile, 29.5 Amosite, 17
7	Crocidolite, 42 Chrysotile B, 25 Amosite, 28 γ-Aluminium(III) oxide, 5	Crocidolite, 44.5* Chrysotile, 23 Amosite, 27

* There was considerable overlap between the 3.07-Å amosite and 3.09-Å crocidolite peaks used.

It was invariably found with the test mixtures that the 7.36-Å chrysotile peak had the non-symmetrical profile shown in Fig. 3 (*iii*), making it impossible to measure the peak height accurately. The peak shapes shown in Fig. 3 (*i*) and (*ii*) were found with the chrysotile calibration mixtures. It was thought that the non-symmetrical peak shape was due to some

overlap between the chrysotile peak and the primary amosite and crocidolite diffraction peaks, but it occurred even with mixture 4 in Table II, which contained no amosite or crocidolite.

Limits of detection

The lowest percentages by mass of asbestos used to plot the calibration graphs were approximately 10%. These percentages were readily measurable for all the different types of asbestos. The average primary peak heights obtained for the mixtures of lowest asbestos content are shown in Table III.

TABLE III

PEAK HEIGHTS OBTAINED WITH THE CALIBRATION MIXTURES OF LOWEST ASBESTOS CONTENT

Asbestos type and percentage	Peak height/ counts s^{-1}	Peak position/ Å
11% Chrysotile A	36	7.36
13.5% Chrysotile B	38	7.36
10.5% Amosite	80	8.33
12.8% Crocidolite	138	8.42
10% Anthophyllite	23	3.24
10% Anthophyllite	62	3.05

The limit of detection is less good for chrysotile than for the other forms of asbestos, *i.e.*, about 6% by mass of chrysotile should be just detectable whereas 2 or 3% of amosite or crocidolite is clearly detectable. Six per cent. of chrysotile should give a rather diffuse peak about 20 counts s^{-1} in height and a very slow scanning speed and relatively long associated time constant are needed to measure it. Two or three per cent. of amosite or crocidolite would give a more clearly defined peak. Anthophyllite is rarely found in the absence of interfering minerals but its limit of detection should again be about 3%. If the mixture can be cleaned with acetic acid detection limits will correspondingly improve.

The X-ray generator used had a maximum power rating of 1600 W. The latest diffraction tubes are designed for use at up to 2700 W. Use of a more powerful generator that could take advantage of this higher tube rating would considerably increase the signal and improve the detection limits.

Determination of Quartz

The main use of XRD at the Health & Safety Executive laboratories in London is in the analysis of samples for quartz. The samples are largely of airborne dust collected on filters, but bulk samples are also examined and these are prepared in much the same way as asbestos samples. Nickel(II) oxide is again used as internal standard[7] and γ-aluminium(III) oxide is also used, acting as a buffer to even out the grinding so that the quartz and nickel(II) oxide particles will be ground to the same extent for each sample, independently of sample composition. The sample press is not used as there is no problem of preferred orientation with quartz particles.

Gordon and Harris[8] have demonstrated that the determination of quartz by use of XRD is dependent on particle size. Nenadic and Crable[9] have suggested that for quantitative work the quartz mean particle diameter should be of the order of 5 μm. Hand grinding and mixing with a mortar and pestle is subjective and a grinding procedure based on the analytical mixer mill was found to give more reliable results and to make it possible to grind consistently to the recommended particle size.

Procedure

The microhammer mill can be used to grind the bulk sample so that a representative portion can be taken. A qualitative XRD scan on the sample shows the presence of quartz and other minerals. Chemical clean-up procedures are used to concentrate the quartz in the sample and to remove minerals that interfere with the quartz 3.343-Å diffraction peak.

Samples from foundries commonly contain iron; this is removed by treatment with a warm solution of hydrochloric acid - water (1 + 2). The mixture is filtered through a pulp pad, which is then ignited. Silicates such as mullite ($3Al_2O_3.2SiO_2$), which give a strong diffraction peak at 3.39 Å, close to the 3.343-Å α-quartz primary peak, are removed by fusing the sample with analytical-reagent grade potassium hydrogen sulphate and dissolving the melt in hot water to which a few millilitres of hydrochloric acid - water (1 + 2) have been added. The solution is filtered through a pulp pad, which is then ignited, and again any quartz is left as a residue.

The cleaned sample is ground initially with a mortar and pestle in order to remove extreme roughness. A 0.200 ± 0.001-g amount of sample, 0.200 ± 0.001 g of nickel(II) oxide and 0.1000 ± 0.0005 g of γ-aluminium(III) oxide are placed in the steel cylinder of the analytical mixer mill with 0.5 ml of cyclohexane and ground for 30 min with the steel ball pestle. The ends of the cylinder are taped to prevent leakage. At the end of the grinding period the material is scraped from the cylinder, the cyclohexane is allowed to evaporate and the lumps in the dried mixture are gently broken up with a pestle and mortar but without further grinding. Optical microscopy has shown that this grinding procedure reduces the mean diameter of the quartz and nickel(II) oxide particles to below 5.0 μm.

The sample mixture is then ready for scanning on the diffractometer. As with asbestos, cellulose powder is used as the backing material to hold the sample in place in the diffractometer sample holder. Results are not pressure dependent and so samples can be pressed by hand. The same diffractometer scanning conditions are used for quartz as are described for the quantitative work on asbestos. A scanning speed of $\frac{1}{2}°$ min^{-1} is usual. The 2.09- and 2.41-Å nickel(II) oxide peaks are again used, in conjunction with the 3.343-Å quartz peak; quartz to nickel(II) oxide peak-height ratios are calculated and the percentage of quartz in the sample is determined from a straight-line calibration graph. Quartz sample mixtures are scanned in duplicate as the precision of peak-height measurements is better for quartz than for asbestos.

Calibration Graph

The calibration graph used for quartz was constructed with mixtures of quartz, γ-aluminium(III) oxide and nickel(II) oxide. No iron was present. Two types of pure quartz were used in 21 standard mixtures; in each instance the total mass of quartz plus γ-aluminium(III) oxide as diluent was 0.2 g [for example, a 10% quartz mixture would be 0.02 g of quartz diluted with 0.18 g of γ-aluminium(III) oxide]. To this would be added 0.2 g of nickel(II) oxide and a further 0.1 g of γ-aluminium(III) oxide as grinding agent. Duplicate portions of each mixture were scanned and the average values for the relevant peak-height ratios were used to construct the calibration graphs. The calculated values of m and c in the straight-line equation $y = mx + c$ were $m = 0.0199$, $c = -0.0196$ for the α-quartz 3.343-Å/nickel(II) oxide 2.41-Å line and $m = 0.0123$, $c = -0.0073$ for the α-quartz 3.343-Å/nickel(II) oxide 2.09-Å line. Peak-height ratio was again plotted along the y-axis and percentage of quartz along the x-axis. The spread of the points about these graphs was less than in Fig. 5, though the gradient was virtually the same. Both graphs have correlation coefficients of 0.995 and in 95% of cases the true quartz concentration should lie within ±6% of the value determined. The mean quartz and nickel(II) oxide particle size for these mixtures was again below 5.0 μm; optical microscopy showed no noticeable difference between mean particle size in mixtures used to prepare the calibration graph and those used to prepare Fig. 5. The degree of grinding would appear to be the same for both graphs; the wider spread of the points in Fig. 5 is attributed to the difficulty of obtaining a uniform mixture when more components are present. This demonstrates the advisability of carrying out clean-up procedures to reduce the number of components to be mixed.

Results and Discussion

Analysis of synthetic mixtures

In order to determine the effects of γ-aluminium(III) oxide on the grinding process, synthetic mixtures were prepared from two different samples of relatively pure quartz. The first, known as Snowit X6403, comes from a Belgian deposit and is used by the Safety

in Mines Research Establishment (SMRE) as a reference quartz. The other is a commercially available Redhill sand, reference T3/300. Both samples showed a wide range of particle sizes.

Figs. 4 and 5 demonstrate the effect of the γ-aluminium(III) oxide on the grinding process for samples containing quartz. Fig. 4 shows results obtained with synthetic mixtures of quartz and iron powder, but with no γ-aluminium(III) oxide present. The combined mass of quartz and iron was 0.2 g for each mixture and the mass of nickel(II) oxide was 0.2 g in each instance. The graph is not a straight line for the entire concentration range up to 100% of quartz, which suggests that the quartz particles are ground to a different extent at the upper and lower regions of the graph. For higher concentrations of quartz there is less iron present to cushion the grinding. Optical microscopy showed that the mean size of the quartz particles in both the upper and lower region was below 5.0 μm, but in the upper region of the graph the quartz was more vigorously ground and the spread of particle size was very narrow: all the particles of quartz observed in this region were below 5.0 μm. In the lower region of the graph there was a wider spread of quartz particle size.

For Fig. 5 the total mass of quartz and iron used for each mixture was again 0.2 g, with 0.2 g of nickel(II) oxide, but 0.1 g of γ-aluminium(III) oxide was added to each mixture before the grinding and mixing. The presence of γ-aluminium(III) oxide evens out the grinding so that the resulting graph is linear, but the spread of the points about the lines is still fairly wide. The mean particle size for quartz and nickel(II) oxide in these mixtures was again below 5.0 μm.

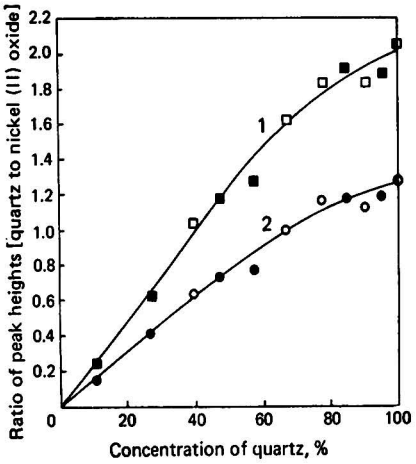

Fig. 4. Effect of grinding quartz with no γ-aluminium(III) oxide present. For each mixture the combined mass of quartz and iron is 0.2 g, with 0.2 g of nickel(II) oxide added as internal standard. Wavelength of quartz peak, 3.343 Å. Wavelength of nickel(II) oxide peak: 1, 2.41 Å; 2, 2.09 Å. Quartz sample: ■ and ●, Snowit X6403; □ and ○, T3/300 ground silica.

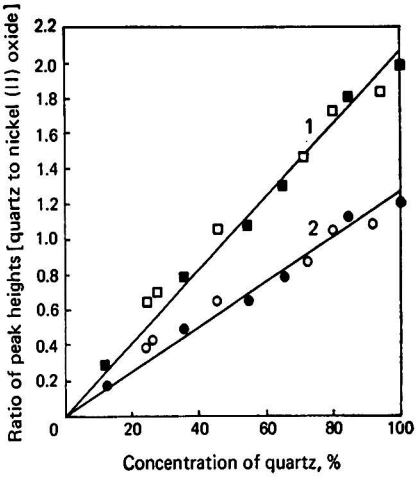

Fig. 5. Effect of grinding quartz with γ-aluminium(III) oxide. Details as for Fig. 4, except that 0.1 g of γ-aluminium(III) oxide is added to each mixture.

Analysis of real samples

Fourteen real samples were analysed for quartz content by the above method, and also independently at SMRE, Sheffield, by an infrared spectroscopic technique. The samples included dusts from foundries, brickworks, potteries and roofing-felt manufacture. Particle size is even more critical for infrared methods than it is for XRD. The presence of kaolinite in some of the pottery samples and talc in the roofing-felt samples caused the analyst who was carrying out the infrared spectroscopy some difficulty. SMRE claim an accuracy of 10% for their infrared determinations on samples with quartz content greater than 30%.

Table IV compares the results obtained with the two techniques. An optical examination using optical microscopy of several of the samples prepared for XRD showed that the quartz and nickel(II) oxide particle size was uniform and generally below 5 μm.

TABLE IV

COMPARISON OF RESULTS FOR QUARTZ OBTAINED ON REAL SAMPLES BY XRD AND INFRARED SPECTROSCOPY

Factory type	Amount of quartz, %	
	XRD	Infrared spectroscopy
Foundry	76	84
	57	59
	69	78
Brickworks	66	69
	79	70
	18	12–16
	39	38
Pottery	8	8
	15	12
	42	49
Roofing felt	7	2
	26	27
(Sand)	94	93
White powder (source unknown) ..	85	93

The author gratefully acknowledges the help of various members of the Health & Safety Executive staff, particularly Messrs. Black, Evans and Revell. This paper is contributed by permission of the Director of the Research and Laboratory Services Division, Health & Safety Executive.

References

1. Klug, H. P., and Alexander, L. E., "X-ray Diffraction Procedures for Polycrystalline and Amorphous Materials," Second Edition, Wiley-Interscience, New York, 1974, p. 368.
2. Crable, J. V., and Knott, M. T., *Am. Ind. Hyg. Ass. J.*, 1966, **27**, 449.
3. Crable, J. V., and Knott, M. T., *Am. Ind. Hyg. Ass. J.*, 1966, **27**, 383.
4. Goodhead, K., and Martindale, R. W., *Analyst*, 1969, **94**, 985.
5. Timbrell, V., and Rendall, R. E. G., *Powder Technol.*, 1971/72, **5**, 279.
6. Klug, H. P., and Alexander, L. E., "X-ray Diffraction Procedures for Polycrystalline and Amorphous Materials," Second Edition, Wiley-Interscience, New York, 1974, p. 536.
7. Klug, H. P., Alexander, L., and Kummer, E., *J. Ind. Hyg. Toxicol.*, 1948, **30**, 166.
8. Gordon, R. L., and Harris, G. W., *Nature, Lond.*, 1955, **175**, 1135.
9. Nenadic, C. M., and Crable, J. V., *in* Simmons, I. L., and Ewing, G. W., *Editors*, "Progress in Analytical Chemistry," Volume 6, Plenum, New York, 1972, p. 81.

Received *February 23rd*, 1978
Accepted *April 25th*, 1978

Analyst, October, 1978, Vol. 103, pp. 1021–1030

Application of the Faraday Effect to the Trace Determination of Cadmium by Atomic Spectroscopy with an Electrothermal Atomiser

K. Kitagawa, T. Shigeyasu and T. Takeuchi

Department of Synthetic Chemistry, Faculty of Engineering, Nagoya University, Furo-cho, Chikusa-ku, Nagoya, Japan

As a technique for the trace determination of elements, the Faraday effect has been applied to atomic spectroscopy with the use of electrothermal atomisers. The atomiser was located between two crossed plane-polarisers (called the polariser and the analyser). An electromagnet magnetised the atomised sample and, as a result of the Faraday effect, the source radiation could, in the presence of the atomic vapour, pass through the optical system. A simple theoretical treatment was developed to explain the dependence of the transmitted intensity on the magnetic field strength and the source intensity and the ability to eliminate the effects of background scattering.

Measurements on cadmium were carried out at a wavelength of 228.8 nm, dispensing into the atomiser 5-μl samples, which, after drying, were atomised at 1000–1800 °C. The calibration graphs demonstrated a square-law dependence. At high concentrations the calibration graphs were corrected for atomic absorption. The technique gave a detection limit of 5×10^{-13} g for cadmium.

Keywords: *Magneto-optical rotation*; *atomic spectroscopy*; *electrothermal atomisation*; *Faraday effect*; *cadmium determination*

Atomic-fluorescence spectroscopy[1–3] has been developed as a useful technique for the determination of trace amounts of elements. It requires no thermal excitation of atoms and consequently can reduce the known inter-element effects due to variations in the excitation temperature or the degree of ionisation of atoms, that may be encountered in atomic-emission spectroscopy.[4] Compared with atomic-absorption spectroscopy, the noise in the light source does not contribute to the noise on the base line. Further, the intensity of the re-emitted radiation increases with increasing source intensity and the development of intense light sources may therefore enable the analytical sensitivity to be improved. As the re-emitted light has a very narrow band width, the construction of a non-dispersive detection system and multi-element detectors is feasible.

However, two problems in the practical application of atomic-fluorescence spectroscopy must be pointed out: the difficulty of collecting the re-emitted radiation necessitates the use of a sensitive detector, such as a photoelectron counter, and the background signal produced by scattering of the source radiation by non-atomic species produced in the atomiser, for example water droplets in a total consumption burner or smoke generated by pyrolysis of organic substances in the sample matrix in a furnace atomiser.

In this work, a spectroscopic method utilising the Faraday effect is proposed for overcoming these problems. A magnetic field is applied to an electrothermal atomiser in the direction parallel to the propagation of the source radiation, as shown in Fig. 1. The electrothermal atomiser is located between two plane-polarising prisms in a crossed configuration. When the atomic vapour is absent or not magnetised, the source radiation is blocked by the analyser. Owing to the Faraday effect, the magnetised atomic vapour rotates the plane of polarisation of the incident light, which then passes through the analyser. By this means we can detect the presence of analyte atoms.

Macaluso and Corbino,[5] in 1898, stated that a rotation of the plane of polarisation was observed when a magnetic field was applied to sodium vapour. They employed solar light or an arc discharge as the source. A stainless-steel tube containing sodium metal was placed between crossed Nicol prisms and a magnetic field was applied by means of a solenoid coil. They heated the tube with a burner to vaporise the sodium metal and measured the

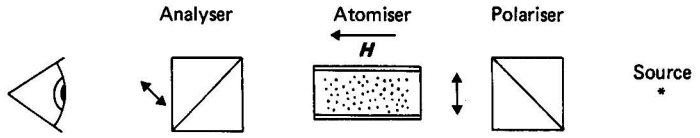

Fig. 1. Schematic diagram of the Faraday configuration.

angle of rotation by revolving the analyser. The found that magnetic rotation occurred in the atomic vapour of sodium as well as in the molecular vapour of Na_2. Later, Ladenburg[6] discussed magnetic rotation by hydrogen atoms. More recently, Corney *et al.*[7] applied dispersion theory to this phenomenon and to the Voigt effect for atomic vapour. They called the phenomenon "forward scattering of resonance radiation." Making use of the fact that the forward-scattered light is coherent, Hackett and Series[8] studied the line crossings (see under Principle) of the isotope-shifted lines in Hg I 253.65 nm. Church and Hadeishi[9] studied the line crossings and pointed out the possibility that the phenomenon was applicable to the trace determination of mercury vapour in air. The Faraday effect applied to molecular spectroscopy is called magneto-optical rotation (MOR), and is expected to be useful for the determination of molecules that are optically inactive and difficult to examine by optical rotatory dispersion. Buckingham and Stephens[10] described the theoretical aspects of MOR in detail. Although this principle has been used for the modulation of a laser beam, its development for analytical purposes has, to date, been limited. The Faraday effect applied to atomic spectroscopy can be called "atomic magneto-optical rotation" (AMOR).

Principle

The phenomenon that the plane of polarisation rotates owing to asymmetric carbon atoms in certain organic substances when located between crossed Nicol prisms is called optical rotatory dispersion (ORD) and has been developed for molecular analysis.[11] In certain instances, and only if external magnetic forces are applied to the substance, the source radiation can pass through the optical system. The associated effects are named after the original workers involved. In the Faraday effect, the plane of polarisation rotates through the substance to which the magnetic force is applied in the direction parallel to the propagation of the source radiation. Another example in which the magnetic force is applied transversely is the Cotton - Mouton effect or the Voigt effect.[12] In this instance, the source radiation can pass through the optical system because the propagating light wave is elliptically polarised through the magnetised substance. An application of the Voigt effect to the trace determination of elements has been reported.[13]

The Faraday effect is related to the longitudinal Zeeman effect. As illustrated in Fig. 2, when the atomic vapour is magnetised the absorption line splits into σ^-, π and σ^+ components due to the Zeeman effect, which correspond to the transitions $\Delta M = -1$, 0 and $+1$, respectively, where ΔM is the difference in magnetic quantum number between the upper and lower energy levels. When the optical system is viewed in the direction of the magnetic field, the σ^- and σ^+ components are circularly polarised with clockwise and counter-clockwise motion, respectively. The π components are not observed from this position as they vibrate along the lines of magnetic force. Because plane-polarised light can be considered to be the resultant of opposite circular motions of the same frequency, the plane-polarised source radiation can be resolved into clockwise and counter-clockwise rotations. Fig. 3 shows the correlation of the refractive indices of the σ^- and σ^+ components of the source radiation with the absorption coefficient, α, and the angle of rotation, ϕ. As the refractive index is inversely proportional to the propagating velocity of the motion, the clockwise motion travels slower outside and faster inside the region between the σ^- and σ^+ components. For the counter-clockwise motion, the reverse applies. Owing to the coherence, the two circular motions are synthesised to yield a plane-polarised wave. Because of the difference in velocity, the plane of the resulting light is at an angle to that of the incident light. Hence the rotatory power arises from the difference in refractive index or, in other words, it is caused by the double refraction of two circularly polarised waves through the Zeeman components σ^+ and σ^-. If there is no difference in frequency between the σ^+ and σ^- components,

the refraction curves are superimposed on each other, and there is no difference between them, resulting in no rotation. This is called line crossing. The line crossings among hyperfine components and isotope-shifted components in the mercury line at 253.65 nm have been studied in detail.[8,9]

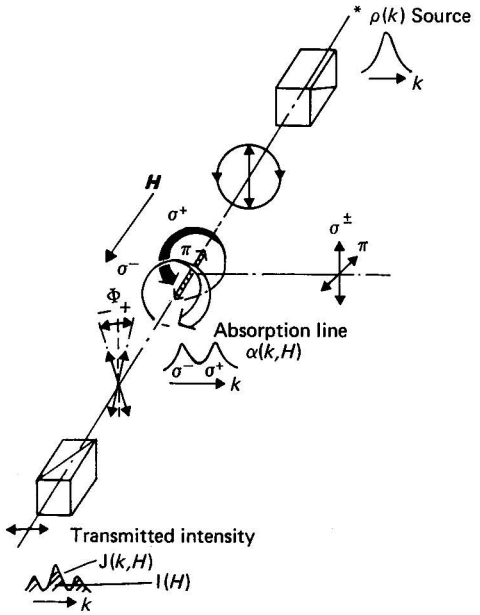

Fig. 2. Relation between the Faraday effect and the Zeeman effect.

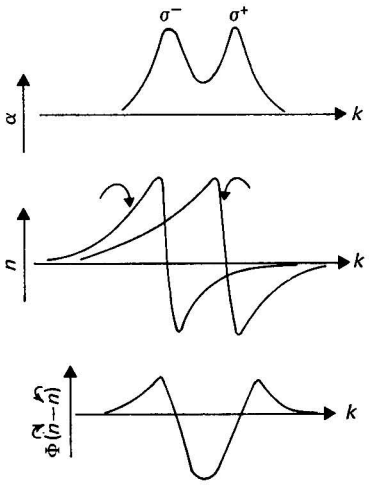

Fig. 3. Correlation of the angle of rotation, Φ, with the absorption coefficient, α, and the refractive index, *n*. $k = 2\pi\nu$, where ν is the frequency of the radiation.

Theoretical

According to Malus's law, the fraction of the light energy passing through the analyser is expressed as $\sin^2\phi$, where ϕ is the angle of rotation compared with the plane of the incident polarised light. As factors determining the transmitted intensity we must take into account the profile of the source radiation, $\rho(k)$, and the damping by atomic absorption. Thus, if the frequency is expressed in terms of angular velocity $k = 2\pi\nu$, the transmitted intensity at k, $J(k)$, can be expressed as follows:

$$J(k) = \rho(k)|\sin\phi(k)|^2\exp[-\alpha(k)L] \quad .. \quad .. \quad .. \quad (1)$$

where $\alpha(k)$ is the absorption coefficient and L the length of the atomic vapour in the atomiser. In practice, we detect the integrated intensity, I:

$$I = \int_s \rho(k)|\sin\phi(k)|^2\exp[-\alpha(k)L]\,dk \quad .. \quad .. \quad .. \quad (2)$$

where s is the band pass of the monochromator. According to the analysis based on dispersion theory by Corney *et al.*[7] and Buckingham and Stephens,[10] the rotatory power is proportional to the number of atoms in the light beam, NL, where N is the number of atoms per cubic centimetre, and the oscillator strength, f. As stated above, the rotatory power arises from the difference in refractive index, so it includes the difference between the two dispersion functions, which is called the Faraday function, $F(k,H)$. In addition, applying the Zeeman splitting to the dispersion functions, ϕ is expressed as follows:

$$\phi(k,H) \propto NLfF(k,H) \quad .. \quad .. \quad .. \quad .. \quad (3)$$

where H is the magnetic field strength.

If the number of atoms in the light beam, NL, is small enough, we can make approximations such as $\sin \phi \approx \phi$ and $\exp[-\alpha(k)L] \approx 1$. Consequently, the transmitted intensity becomes

$$I \propto (NL)^2 f^2 \int_s \rho(k) |F(k,H)|^2 \, dk \quad .. \quad .. \quad .. \quad .. \quad (4)$$

As $\rho(k)$ can be normalised as $\rho'(k) = f(k)/I_0$, where I_0 is the source intensity integrated over the band pass of the monochromator, $\int_s \rho(k) dk$, the transmitted intensity is expressed as follows:

$$I \propto (NL)^2 f^2 I_0 M(H) \quad .. \quad .. \quad .. \quad .. \quad .. \quad (5)$$

where $M(H) = \int_s \rho'(k) |F(k,H)|^2 \, dk$.

Thus, the transmitted intensity is theoretically expected to be proportional to the square of the number of atoms in the light beam and to the source intensity, and to change as a function of the applied magnetic field strength and the line profile of the source radiation. In experimental calibration of the instrument, it is convenient to use an intensity normalised by the source intensity:

$$T = I/I_0 \text{ or } T = K(NL)^2 f^2 M(H)/\int_s \rho(k) dk \; .. \quad .. \quad .. \quad (6)$$

where K is a constant defined by the instrumental factors. If NL is so large that the atomic absorption is not negligible, the calibration should be made after a correction for the absorption has been applied. The corrected transmitted intensity, T_c, is given by substituting the reduced source intensity for the source intensity I_0:

$$T_c = I/\int_s \rho(k) \exp[-\alpha(k,H)L] \, dk \quad .. \quad .. \quad .. \quad (7)$$

In order to apply this principle in practical analysis, we combined the Faraday configuration with an electrothermal atomiser, and studied several fundamental characteristics of the system for cadmium, namely the dependence of the transmitted intensity on the magnetic field strength and its proportionality to the square of the number of atoms in the light beam and to the source intensity.

Use of the Faraday effect is expected to have the following advantages:

1. Those similar to atomic-fluorescence spectroscopy. As found in the above equations, the transmitted intensity increases proportionally to the source radiance, and the base-line noise is independent of the source noise.
2. Unless depolarisation occurs, the light scattered by non-atomic species is blocked by the analyser. Therefore, it has the ability to remove the positive background signal, which is a significant problem in non-dispersive atomic-fluorescence spectroscopy.
3. As the optical system is aligned, it is easy to measure the source radiation.

Experimental

Fig. 4 illustrates the apparatus constructed for this work. It consists of a light source, polariser, electromagnet, atomiser, analyser, monochromator, photomultiplier tube (RCA 1P28), power supply for the atomiser, d.c. amplifier (Sanei Sokki Co.), power supply for the coils of the electromagnet, power supply for the light source, flow controller for argon gas and strip-chart recorder. A cadmium hollow-cathode lamp (Hitachi) and a cadmium electrodeless discharge lamp (EMI) were used as light sources. The former was operated in the d.c. mode and the latter mounted in a tuned cavity[14] through which microwave power of 2450 MHz was supplied. The electromagnet generated a maximum field strength of 17 kG between the pole pieces 10 mm apart with a coil current of 10 A. The pole pieces have a diameter of 20 mm and a central aperture of 3 mm diameter.

The strength of magnetic field was calibrated against the coil current by using a gauss meter (Yokokawa Co.). Glan-type prisms were employed as polariser and analyser (Karl Lambrecht Co.). A prism monochromator was chosen for the dispersing element in order

to prevent the polarisation that can arise with some grating monochromators. The slit width of the monochromator was 2 mm, giving a band pass of 2.5 nm. The photocurrent due to black-body radiation from the atomiser was negligibly small.

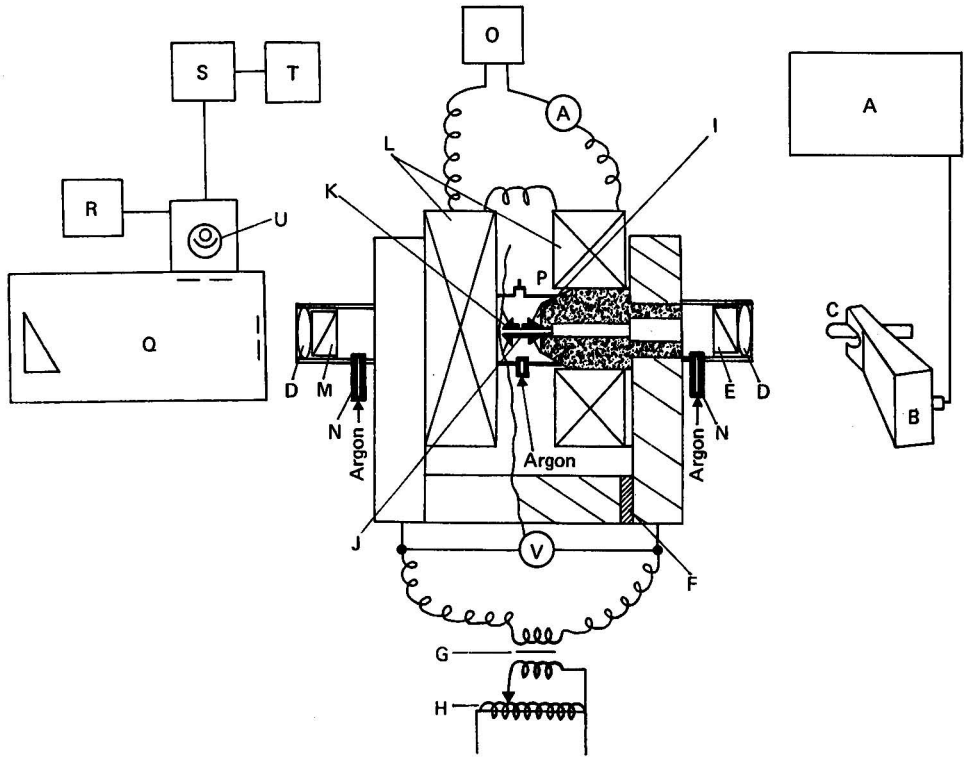

Fig. 4. Schematic diagram of the optical system: A, microwave power supply for the electrodeless discharge lamp; B, microwave cavity; C, electrodeless discharge lamp; D, lens; E, polariser; F, insulator; G, transformer; H, variable transformer; I, pole piece; J, graphite tube atomiser; K, graphite cone; L, solenoid coil; M, analyser; N, gas inlet; O, power supply for the solenoid coil; P, chamber; Q, prism monochromator; R, stabiliser for high-voltage supply for the photomultiplier tube; S, d.c. amplifier; T, strip-chart recorder; and U, photomultiplier tube.

Two types of electrothermal atomiser were located in turn between the pole pieces. One was an M-shaped strip atomiser of tungsten, 2 mm in width,[15] and the other was a graphite tube atomiser of 3 mm i.d., 5 mm o.d. and 18 mm long. The strip atomiser was attached to brass rod electrodes 4 mm in diameter, through which the atomiser was supplied with electric current. An aliquot of the sample solution was placed on the bottom of the M-shape. The incident beam was focused on the atomic vapour. The graphite tube atomiser was fitted to the pole pieces of the electromagnet through graphite cones, which served as thermal insulators, as shown in Fig. 5. The atomiser was supplied with electric current through the pole pieces. The sample solution was dispersed on to the bottom of the graphite tube with a syringe through a sampling port of diameter 1 mm in the middle of the lateral face of the tube. Both atomisers were enclosed in a chamber of 70 mm i.d. Argon gas was passed into the chamber and the graphite tube for purging at flow-rates of 1 l min^{-1} and 50 ml min^{-1}, respectively. The latter plays an important role in reducing the contamination on the inside surface of the graphite tube by the atomic vapour. The flow of argon gas carries the atomic vapour generated by electrical heating out of the tube through the sampling port. As the temperature of the tube atomiser is highest at the port, the atomic vapour does not condense there. Thus, contamination at the edges of the tube can be prevented.

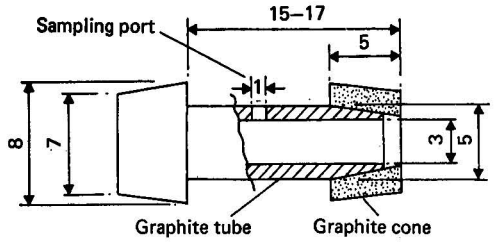

Fig. 5. Schematic diagram of the graphite tube atomiser fitted with graphite cones. All dimensions are given in millimetres.

A stock solution with a cadmium concentration of 1000 μg ml^{-1} was prepared by dissolving cadmium metal in 6 N hydrochloric acid purified by distillation. Standard solutions were prepared by dilution and the acidity was adjusted to 0.1 N. Sample solution (5 μl) was removed with a microsyringe (SGE), dried at 120 °C for 1 min and atomised at an equilibrium temperature of 1000 °C for the strip atomiser and 1800 °C for the carbon tube atomiser. Because of the large capacity of the latter, its equilibrium temperature was chosen to be higher than that of the strip atomiser. A cylindrical air - acetylene flame was also examined for comparison purposes. A burner was constructed by fitting a stainless-steel tube of 6 mm i.d. to a mounting block of 30 mm o.d. The burner was connected to a conventional nebuliser for atomic-absorption spectroscopy and operated at flow-rates of 7 and 2 l min^{-1} for air and acetylene, respectively. The Cd I line at 228.8 nm was chosen as the analytical line.

Results and Discussion

Dependence of Transmitted Intensity on Magnetic Field Strength

Fig. 6 shows the dependence of the transmitted intensity (T) on magnetic field strength. The curve A presents the results obtained with the hollow-cathode lamp (discharge current 10 mA) and curve B those for the electrodeless discharge lamps (100 W; reflected power $\leqslant$5 W). These curves have a maximum value at a field strength of about 3–5 kG, which we interpret as follows.

When no magnetic field is applied to the atomic vapour, the frequency of the σ^+ and σ^- Zeeman components are the same, so line crossings occur. For this reason, the source radiation is not transmitted by the optical system. As the field strength is increased, the rotatory power is enhanced owing to the change in the relative velocity of the σ^+ and σ^- components, corresponding to the change in the term $\phi(k,H)$ in equation (2). Thus, an increasing amount of source radiation is allowed to pass through the optical system. However, too strong a field causes such a large displacement of the σ components that the source line cannot superimpose upon them. In this event, there is no region of frequency in which the source radiation is affected by the influence of the σ components, which leads to a decrease in the transmitted intensity. This corresponds to a decrease in the product $\rho(k)[\sin\phi(k,H)]^2$ in equation (3). Thus, the curve presents a maximum value, depending on the profile of the source radiation. On comparing curves A and B, it is evident that the maximum of the latter lies at a higher field strength and that its profile is broader than that of the former. Recalling the superimposition effect, the results suggest that the line profile of the radiation from the electrodeless discharge lamp is broader than that from the hollow-cathode lamp under the given conditions. This was also examined by calculating curves C and D according to equation (2). The parameters for curve C are as follows: the width of the source line was 0.2 pm, that of the absorption line 1.8 pm, the Doppler width of the absorption line 2.3 $\times$ 10^9 rad s^{-1} and the number of atoms 5 $\times$ 10^7 cm^{-2}. The parameters for curve D were the same as those for curve C, except that the width of the source radiation was larger (0.5 pm).

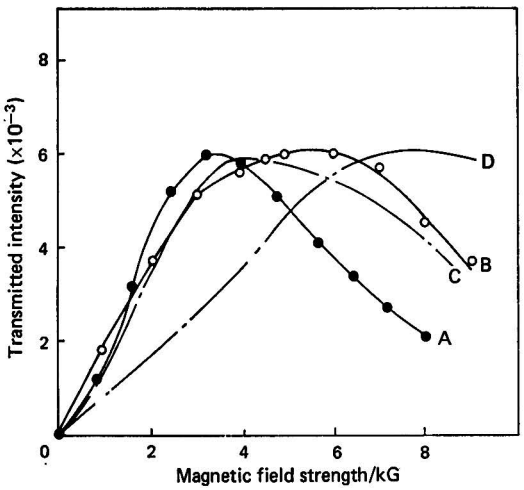

Fig. 6. Dependence of the transmitted intensity (T) on the magnetic field strength: A, observed curve with the hollow-cathode lamp; B, with the electrodeless discharge lamp; C and D, the calculated curves.

These calculated curves also indicate that a broader source line gives a broader curve and that the curve maximum shifts to a stronger field. Another factor that determines the curve profile is line crossing. The effect of hyperfine structure on line crossing was taken into account and the Zeeman splitting pattern estimated for the analytical line at 228.8 nm. The natural abundance of cadmium is 0.875% of ^{108}Cd, 12.39% of ^{110}Cd, 12.75% of ^{111}Cd, 24.07% of ^{112}Cd, 12.26% of ^{113}Cd, 28.86% of ^{114}Cd and 9.58% of ^{116}Cd. The splitting pattern can be readily calculated for the isotopes of even relative atomic mass as they possess no nuclear spin. However, the situation is complicated for those of odd relative atomic mass because their spin momenta contribute to the Zeeman splitting. In weak fields, the nuclear spin momentum, **I**, is coupled with the electronic momentum, **J**, to yield a resultant momentum, **F**, leading to $2F + 1$ Zeeman levels in the magnetic field, where F is the total momentum quantum number. On the other hand, in a strong field, they cannot be coupled together owing to the Back - Goudsmit effect,[16] but independently yield their magnetic momenta. In practice, an intermediate case exists between the two extremes.

Fig. 7 shows the calculated splitting pattern for the case based on the perturbation method.[17] It is expected from Fig. 7 that a line crossing may occur at a field strength near 0.2 kG. However, contrary to expectation, no minima can be found on the curves in Fig. 6. Presumably because of Lorentz broadening of the absorption line at atmospheric pressure, the zero-field line crossings cannot be separated from the line crossings in question. In addition, because the natural abundance of the isotopes of odd relative atomic mass is only a quarter of the total, they have no significant effect on the shape of the curve. Another problem concerned with line crossings is created by isotope shifts.[8] If any isotope shift exists with a displacement comparable to the broadening of the absorption line, the fall might be found on the observed curve. The results suggest that such a large shift does not occur in the cadmium line at 228.8 nm.

Calibration Graphs and Atomic Fluorescence

Fig. 8 shows the relationship between the square root of the transmitted intensity and the amount of cadmium in the atomiser, *i.e.*, the calibration graphs. The lower graph (un-

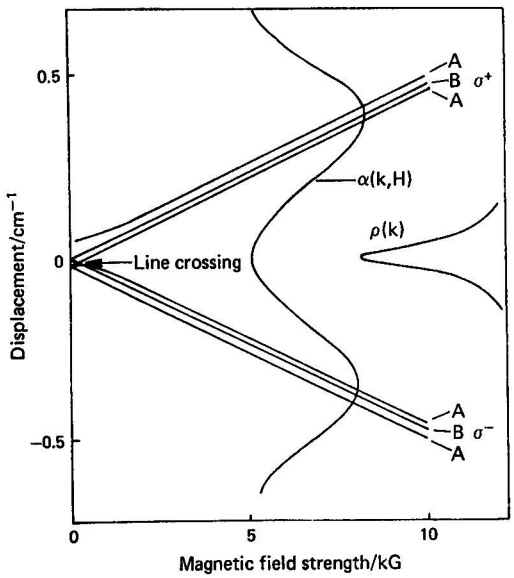

Fig. 7. Zeeman splitting pattern calculated for cadmium isotopes with the nuclear spin quantum numbers, $I = \frac{1}{2}$ (A) and $I = 0$ (B).

corrected) bends at high cadmium concentrations. The $\sqrt{T_c}$ graph is the corrected graph defined by equation (7), which includes the correction for atomic absorption. The atomic absorption was measured by setting the polariser and the analyser in a parallel configuration. The results indicate that the transmitted intensity is proportional to the square of the number of atoms. The relationship is important in measuring the phenomena observed in this work.

From the above theoretical discussion, only the rotatory dispersion induced under the magnetic field is taken into account. Atomic fluorescence of the Zeeman components might contribute to the phenomena observed. Two cases are possible. If the fluorescent radiation yields plane-polarised light synthesised in a fashion similar to that in the Faraday effect, the expression for the detected light should be

$$I = \int_s \rho(k) |\sin\phi_1 (k,H)|^2 \exp[-\alpha(k,H)L]\mathrm{d}k + \int_s \rho(k) |\sin\phi_2 (k,H)|^2 \gamma\{1 - \exp[-\alpha(k,H]L\}\mathrm{d}k \quad \ldots \quad \ldots \quad \ldots \quad (8)$$

where γ is the quantum yield. The first term corresponds to the Faraday effect and the second to rotation via atomic fluorescence. If the number of atoms is small enough, the second term on the right-hand side can be reduced to the expression $I_2 =$ constant $\times$ $(NL)^3 f^3 \gamma I_0$ (under a constant field). Thus, if the fluorescence has an important role, the transmitted intensity should change as a function $C_1(NL)^2 + C_2(NL)^3$ under a constant field, where C_1 and C_2 are constants. The results indicate that the transmitted intensity is almost proportional to $(NL)^2$, in contrast to the above expression.

The other case, which may be the more likely, is partial depolarisation by inelastic collision between photons and atoms. For this reason, the plane-polarised radiation may become elliptically polarised and could pass through the analyser. However, this process could also occur under zero magnetic field. The results (Fig. 6) indicate that no radiation is detected under such conditions and it therefore appears that either the fluorescent energy is negligible compared with that due to the Faraday effect, or the plane of polarisation of the fluorescent radiation is the same as that of the exciting radiation and hence is blocked by the analyser.

This discussion is valid for small N, but under conditions when the number of atoms in the light beam is large the fluorescence could predominate. In the future, a detailed examination of this question will be made by checking a decay curve, using a temporal disperser of picosecond response.

Proportionality of the Transmitted Intensity to the Source Radiance

Fig. 9 shows the dependence of the transmitted intensity on the intensity of the source radiation. Contrary to the prediction by equation (5), the resulting graph is not rectilinear but is concave at high source radiance, probably because the increase in lamp current causes an increase in line width. As the line width of the source radiation increases, the convolution term $\rho(k)|\sin\phi|^2$ in equation (2) becomes larger, leading to an increase in the transmitted intensity. Consequently, it could be suggested that a source radiation of higher band width is more suitable for this technique. However, theoretical calculations using equation (2) predict that too broad a line causes an increase in the rotatory power of molecular species and thus results in an unfavourable background. This was verified by introducing cigarette smoke into the graphite tube atomiser and using a D_2 lamp as the light source. Macaluso and Corbino[5] also demonstrated that magneto-optical rotation of a continuum source occurred through magnetised diatomic sodium (Na_2) as well as through the atomic vapour of sodium.

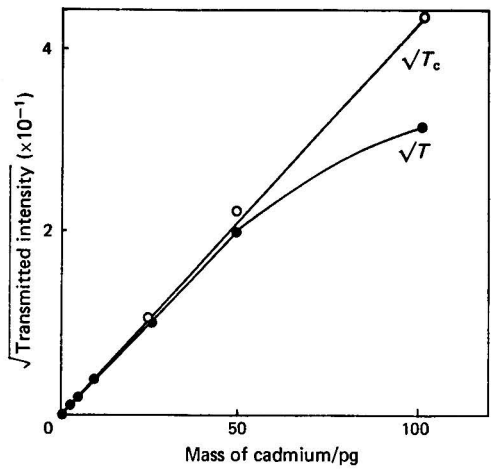

Fig. 8. Calibration graphs: $\sqrt{T}$, uncorrected for the atomic absorption and $\sqrt{T_c}$, corrected.

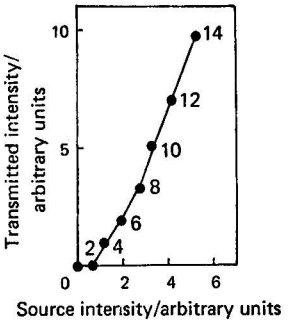

Fig. 9. Dependence of the transmitted intensity on the source intensity. The figures on the curve indicate the discharge lamp current in milliamperes.

Elimination of Background

Cigarette smoke was introduced into the graphite tube atomiser with the flow of argon in order to examine the ability of the system to overcome background effects. The source radiation was decreased to half of the incident power, but no background magnetic rotation signal was detected. In this technique, the depolarisation of the incident radiation through the scattering process is significant for the background. However, in practice, it was found that the transmitted radiation was negligible. When 5 μl of 25 mg ml^{-1} sodium chloride solution was introduced in order to generate background, the result was the same. Thus, this technique proved to be insensitive to those background components of scattered light from which conventional atomic-absorption or atomic-fluorescence spectrometers may suffer. In this technique, there is a problem associated with a loss of incident power and transmitted energy attributable to background components, which leads to a negative interference. Nevertheless, the correction method, using T_c, enables us to overcome the interference. The operational circuits for a correction system will be described elsewhere.

Detection Limit and Reproducibility

On the basis of a signal to noise ratio of 2, the cylindrical flame atomiser gave a detection limit for cadmium of 1 μg ml^{-1}, the tungsten strip atomiser with the hollow-cathode lamp 5×10^{-12} g and the graphite tube atomiser with the electrodeless discharge lamp 5×10^{-13} g, the discharge current for the hollow-cathode lamp being 15 mA and the microwave power for the electrodeless discharge lamp 120 W. In the flame atomiser, the number of atoms in the light beam is much smaller than that in the electrothermal atomisers and therefore, owing to the dependence of the transmitted intensity on the number of atoms, *i.e.*, $I =$ constant $\times$ $(NL)^2$, the latter atomiser is the more suitable for the present technique, as it can produce a pulse of condensed atomic cloud in the light beam. Although the tungsten strip atomiser had the advantage of less contamination, it gave less reproducible signals (the relative standard deviation was 10%) than the graphite tube atomiser (4%).

Finally, it should be emphasised that the present technique is applicable to trace analyses for elements other than cadmium and applications to copper and lead are being developed.

This work was supported by a grant from the Ministry of Education of Japan. We thank Dr. J. B. Dawson and Professor T. S. West for helpful discussions and advice.

References

1. Winefordner, J. D., and Vickers, T. J., *Analyt. Chem.*, 1964, **36**, 161.
2. Dagnall, R. M., Thompson, K. C., and West, T. S., *Analytica Chim. Acta*, 1966, **36**, 269.
3. Marshall, G. B., and West, T. S., *Analytica Chim. Acta*, 1970, **51**, 179.
4. Kitagawa, K., and Takeuchi, T., *Analytica Chim. Acta*, 1972, **60**, 309.
5. Macaluso, D., and Corbino, O. M., *C. R. Hebd. Séanc. Acad. Sci., Paris*, 1898, **127**, 548.
6. Ladenburg, R., *Annln Phys.*, 1912, **38**, 249.
7. Corney, A., Kibble, B. P., and Series, G. W., *Proc. R. Soc.*, 1966, **A248**, 701.
8. Hackett, R. Q., and Series, G. W., *Opt. Commun.*, 1970, **2**, 93.
9. Church, D. A., and Hadeishi, T., *Phys. Rev.*, 1973, **A8**, 1864.
10. Buckingham, A. D., and Stephens, P. J., *A. Rev. Phys. Chem.*, 1971, **22**, 259.
11. Wong, K. P., *J. Chem. Educ.*, 1975, **52**, A83.
12. Wood, R. W., "Physical Optics," Third Edition, Dover, New York, 1961.
13. Ito, M., Murayama, S., Kayama, K., and Yamamoto, M., *Spectrochim. Acta*, 1977, **32B**, 347.
14. Broida, H. P., and Chapman, M. W., *Analyt. Chem.*, 1958, **30**, 2049.
15. Hasegawa, T., Yanagisawa, M., and Takeuchi, T., *Analytica Chim. Acta*, 1977, **89**, 217.
16. White, H. E., "Introduction to Atomic Spectra," International Student Edition, McGraw-Hill Kogakusha Ltd., Tokyo, 1934.
17. Bersohn, M., and Baird, J. C., "Introduction to Electron Paramagnetic Resonance," W. A. Benjamin, New York, 1966.

Received *March 6th*, 1978
Accepted *April 4th*, 1978

Analyst, October, 1978, Vol. 103, pp. 1031–1036

Flotation of Sub-microgram Amounts of Arsenic Coprecipitated with Iron(III) Hydroxide from Natural Waters and Determination of Arsenic by Atomic-absorption Spectrophotometry Following Hydride Generation

Susumu Nakashima

Institute for Agricultural and Biological Sciences, Okayama University, Kurashiki-shi 710, Japan

A method is described for the flotation and determination of sub-microgram levels of arsenic in water. A sub-microgram amount of arsenic(III, V) in a 500-ml sample of water is coprecipitated with iron(III) hydroxide at pH 8–9. The precipitate is floated with the aid of sodium oleate and small air bubbles, then separated and dissolved in 5 M hydrochloric acid, and finally the arsenic content is determined by generation of arsine using sodium tetrahydroborate(III) as a reductant and atomic-absorption spectrophotometry with a long absorption cell (60 × 1.2 cm i.d.). This separation technique has been successfully applied to the determination of sub-microgram amounts of arsenic(III, V) in natural waters.

Keywords: Arsenic determination; flotation; natural waters; atomic-absorption spectrophotometry; hydride generation

Arsenic probably exists at the 1 $\mu g\ l^{-1}$ level in natural water samples. At such concentrations a precise direct determination is impracticable even by atomic-absorption spectrophotometry of arsine, which has a high sensitivity.[1–4] Accordingly, the arsenic must be concentrated from the water prior to determination.

Coprecipitation with iron(III) hydroxide is commonly used as a pre-concentration technique for the determination of arsenic in water.[5] This bulky amorphous precipitate, however, is difficult to filter, and centrifugation is cumbersome for larger volumes.

Therefore, a flotation technique[6,7] in which the precipitate of iron(III) hydroxide is floated with the aid of sodium oleate and small air bubbles (0.1–0.5 mm diameter) has been used for the pre-concentration of arsenic. The precipitate is readily separated from the mother liquor and then dissolved in hydrochloric acid for the atomic-absorption spectrophotometry of arsine using sodium tetrahydroborate(III) as a reductant. Various parameters, such as the pH of the solution, the amounts of iron(III) and surfactant added, stirring time, sample volume and foreign ions, have been investigated in order to obtain optimum conditions for the flotation and determination of the arsenic. For the atomic-absorption determination of arsenic a technique involving a long absorption cell and the argon - hydrogen flame system has been used.

The proposed method is simple and rapid, and applicable to the determination of arsenic at the low parts per billion (10^9) level in water.

Experimental

Apparatus

A Nippon Jarrell-Ash, Model AA-1, Mark II atomic-absorption spectrophotometer equipped with a Westinghouse arsenic hollow-cathode lamp and a custom-made silica absorption cell (60 × 1.2 cm i.d.) was used with a Beckman burner supplied with argon and hydrogen.

The apparatus used for hydride generation was a modified Nippon Jarrell-Ash, Model ASD-1A, arsenic measurement unit coupled to a custom-made hydride generating cell approximately 40 ml in volume. A schematic diagram of the analytical system is illustrated in Fig. 1.

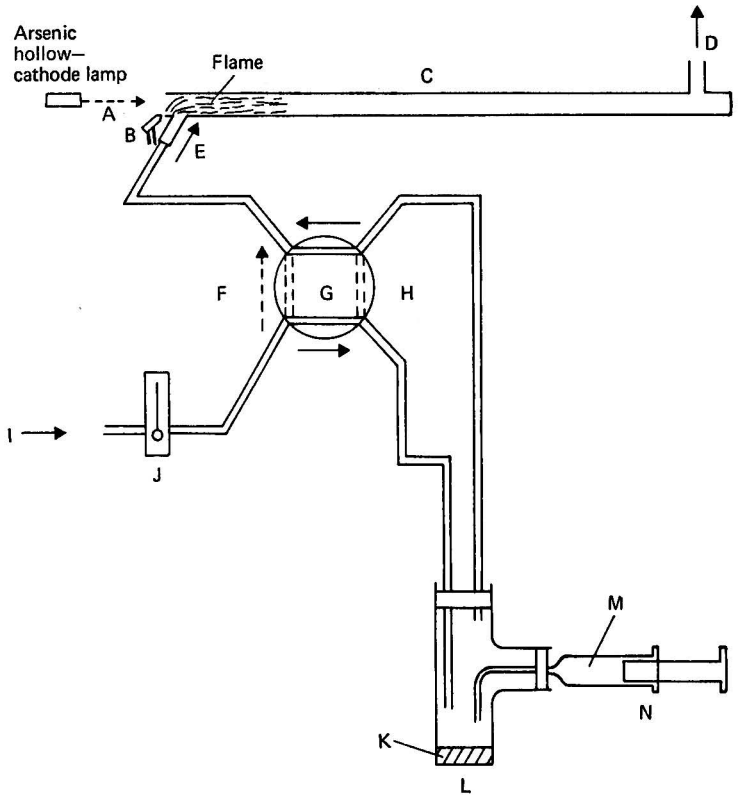

Fig. 1. Schematic diagram of analytical system. A, Light from hollow-cathode lamp; B, Beckman burner; C, silica absorption tube (60 × 1.2 cm i.d.); D, outlet from tube; E, argon gas flow containing arsine; F, by-pass; G, four-way stopcock, alternative gas passages shown by broken lines; H, gas flow with valve in sweep position; I, argon supply; J, flow meter; K, sodium tetrahydroborate(III) solution; L, hydride generating cell; M, sample solution; and N, syringe.

All pH readings were made with a Hitachi-Horiba, Model M-5, pH meter together with a combined glass electrode.

The flotation and separation apparatus was similar to that described by Mizuike and co-workers.[6,7] The flotation cell, shown in Fig. 2, was a glass cylinder, 40 × 6.5 cm i.d., which was fitted with a sintered-glass filter (No. 4) to generate small bubbles.

The air that served as the inert gas was supplied by a Nippon Jarrell-Ash, Model AMD-B1, air pump unit.

Reagents

All reagents were of analytical-reagent grade except for sodium oleate. Aqueous reagents were prepared in de-ionised, distilled water. Arsenic standard solutions were freshly prepared by diluting stock solutions before use.

Arsenic(III) stock solution, 1 mg ml^{-1}. Dissolve 1.321 g of diarsenic trioxide in a minimum amount of 20% *m/V* sodium hydroxide solution, acidify with 5 M hydrochloric acid and dilute to 1000 ml with water.

Arsenic(V) stock solution, 1 mg ml^{-1}. Dissolve 4.165 g of sodium arsenate ($Na_2HAsO_4 \cdot 7H_2O$) in 1000 ml of water.

Iron(III) solution, 5 mg ml^{-1}. Dissolve 43.17 g of ammonium iron(III) sulphate [$Fe_2(SO_4)_3(NH_4)_2SO_4.24H_2O$] in water and dilute to 1000 ml in 1 M hydrochloric acid with hydrochloric acid and water.

Sodium oleate solution, 1 mg ml^{-1}. Dissolve sodium oleate (powder, extra-pure reagent, Wako Pure Chemicals Co.) in 99.5% *V*/*V* ethanol with magnetic stirring.

Sodium tetrahydroborate(III) solution, 5% *m*/*V*. Dissolve sodium tetrahydroborate(III) in water.

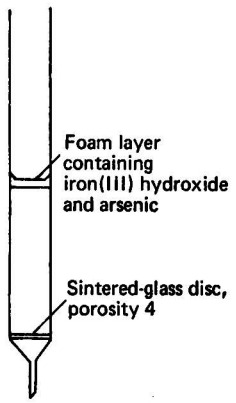

Fig. 2. Flotation cell for pre-concentration of arsenic.

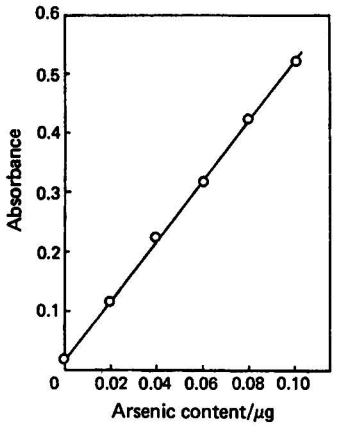

Fig. 3. Typical calibration graph for determination of arsenic in 1 ml of solution.

Recommended Procedure for the Determination of Arsenic

Transfer 1 ml of freshly prepared 5% *m*/*V* sodium tetrahydroborate(III) solution into an arsine-generating cell and attach the cell to the apparatus. Insert the needle of a plastic syringe containing 1 ml of sample solution that contains less than 0.10 μg of arsenic through the side-arm seal of the cell. Turn the four-way stopcock of the apparatus to the sweep position in order to introduce argon into the system and inject the sample into the cell. Sweep the arsine thus generated into the long absorption cell with the argon so that it is atomised in the argon - hydrogen flame and record the absorption signal on a recorder. Return the stopcock to the by-pass position. Rinse the cell carefully with distilled water and re-charge with sodium tetrahydroborate(III) solution ready for the next sample. If the concentration of arsenic exceeds 0.10 μg ml^{-1}, dilute the solution further, adjusting the hydrochloric acid and iron(III) concentrations accordingly.

Construct a calibration graph using 5 M hydrochloric acid solutions containing 1 mg ml^{-1} of iron(III) and 0–0.10 μg ml^{-1} of arsenic(III). A typical calibration graph for arsenic is illustrated in Fig. 3, which is linear up to 0.10 μg of arsenic. The same result was obtained by using an arsenic(V) solution containing 1 mg ml^{-1} of iron(III) as a standard. The coefficient of variation based on 10 replicate runs of a solution containing 0.05 μg ml^{-1} of arsenic was within 1.5%.

The atomic-absorption equipment was operated under the following conditions: wavelength, 193.7 nm; lamp current, 16 mA; gas flow-rates, argon 1.5, hydrogen 1.5 and auxiliary argon 6 l min^{-1}; slit (spectral band width), 1 nm.

The 60-cm tube system described in this paper cannot be used with most commercial atomic-absorption spectrophotometer units. However, the arsenic in a sample solution can also be determined by atomic-absorption spectrophotometry, using an arsine generation - electrically or flame-heated silica tube. Moreover, nitrogen can be substituted for the more expensive argon.

Procedure Recommended for the Flotation Step

Place 500 ml of the water sample in a 500-ml beaker and add 2 ml of iron(III) solution and 1 ml of sodium oleate solution. Adjust the pH to 8–9 with aqueous ammonia solution (5 and 0.1 M) in order to precipitate iron(III) hydroxide, while stirring magnetically, and stir the solution for 15 min. Transfer the contents of the beaker (excluding the stirring bar) to a flotation cell and wash the residue in the beaker into the cell by using two small portions of water. Pass air at a flow-rate of 50 ml min^{-1} from the lower end of the cell for about 30 s, in order to obtain complete mixing and flotation of the precipitate. Suck off the mother liquor through the sintered-glass disc and wash the precipitate with 30 ml of water. Add 5 ml of 5 M hydrochloric acid to the cell to dissolve the precipitate, collect the filtrate by suction in a 10-ml calibrated flask, wash the sintered-glass disc with hydrochloric acid, add the washings to the flask and dilute to the mark with 5 M hydrochloric acid.

Results and Discussion

Determination of the Optimum pH for Collection of Arsenic

The effect of the pH of the 500 ml of solution containing 0.5 μg of arsenic(III, V), 10 mg of iron(III) and 1.0 mg of sodium oleate on the coprecipitation of arsenic was studied. Hydrochloric acid and aqueous ammonia solution were used to adjust the pH to values within the range 4–10. As a result satisfactory recoveries of both trivalent and pentavalent states of arsenic were obtained over this range. The most stable layer of surface foam supporting the precipitate of iron(III) hydroxide was formed within the pH range 7–9.5; the pH range of 8–9 was used throughout the work.

At a pH below about 6.5, a stable surface-foam layer was obtained by using sodium lauryl sulphate as a surfactant.

Determination of Optimum Amounts of Iron(III) and Surfactant

Table I shows the percentage of arsenic recovered as a function of the amount of iron(III) added to the solution. Quantitative recoveries of arsenic were obtained above 2.5 mg of iron(III). In this work 10 mg of iron(III) were added to 500 ml of the solution.

The amount of sodium oleate required for complete flotation of the precipitate was investigated. Quantitative recoveries of arsenic were obtained between 0.2 and 4.0 mg of sodium oleate and 1.0 mg in 500 ml of solution was adopted in further work.

TABLE I

RELATIONSHIP BETWEEN AMOUNT OF IRON(III) ADDED AND RECOVERY OF ARSENIC

Solution contained 0.5 μg of As(III) and 1 mg of sodium oleate; pH, 8–9; volume, 500 ml.

Fe(III) added/mg	2.5	5.0	7.5	10.0	15.0	20.0
As recovered, %	98	100	101	100	98	99

Stirring Time

The relation between stirring time and recovery of arsenic was investigated. The results are shown in Table II. Coprecipitation was quantitative over the range 5–40 min and stirring for 15 min was found to be best.

TABLE II

RELATIONSHIP BETWEEN STIRRING TIME AND RECOVERY OF ARSENIC

Solution contained 0.5 μg of As(III) and 10 mg of Fe(III); pH, 8–9; volume, 500 ml.

Stirring time/min	5	10	15	20	25	30	40
As recovered, %	99	101	101	100	98	99	97

Solution Volume

The effect of variation of the volume of solution containing 0.5 μg of arsenic(III), 10 mg of iron(III) and 1.0 mg of surfactant was studied. Arsenic was recovered quantitatively from volumes of up to at least 1000 ml. Taking the arsenic content (1 μg l^{-1} level) in natural waters and the sensitivity of analytical equipment into account, 500 ml of water sample was considered to be a suitable volume.

Effect of Foreign Ions

By following the recommended procedure, the effect of various ions on the separation and determination of arsenic was investigated. Table III shows permissible amounts of foreign ions for the determination of 0.5 μg of arsenic(III) in 500 ml of solution with 10 mg of iron(III) added. As can be seen, the determination of arsenic is scarcely affected by the amounts of foreign ions normally present in natural waters. Of these ions, hydride-forming elements such as selenium(IV), antimony(III) and tin(IV) are coprecipitated with iron(III) hydroxide in the same way as arsenic and would have a relatively strong effect on the arsine generation. However, these ions occur at extremely low levels in natural waters in comparison with arsenic. Therefore, this method can be employed for the determination of arsenic in natural waters without any interference from co-existing ions.

TABLE III

PERMISSIBLE AMOUNTS OF FOREIGN IONS FOR DETERMINATION OF ARSENIC

Solution contained 0.5 μg of As(III) and 10 mg of Fe(III); volume, 500 ml.

Ion	Limit [Ion]/[As]	Ion	Limit [Ion]/[As]	Ion	Limit [Ion]/[As]
Na^{+}	20 000	Cd^{2+}	2 000	Co^{2+}	2 000
K^{+}	20 000	Zn^{2+}	2 000	PO_4^{3-}	2 000
Ca^{2+}	20 000	Mn^{2+}	2 000	V^{5+}	1 000
Mg^{2+}	20 000	Al^{3+}	2 000	Bi^{3+}	400
Cl^{-}	20 000	Cr^{3+}	2 000	Te^{4+}	400
NO_3^{-}	20 000	Cr^{6+}	2 000	Ni^{2+}	400
SO_4^{2-}	20 000	Mo^{6+}	2 000	Cu^{2+}	200
SiO_3^{2-}	20 000	Pb^{2+}	2 000	Sb^{3+}	60
Sr^{2+}	2 000	Hg^{2+}	2 000	Sn^{4+}	60
Ba^{2+}	2 000	Se^{6+}	2 000	Se^{4+}	10

Recovery of Arsenic

Solutions (500 ml) at pH 8–9 containing 10 mg of iron(III), 1.0 mg of sodium oleate and 0.2, 0.5, 1.0, 2.0, 3.0, 4.0, 5.0, 7.0 and 10.0 μg of arsenic(III, V) were analysed by the recommended procedure. Recoveries of the arsenic that had been added were greater than 95% in all instances. Recommended conditions, therefore, appear to be optimum for 500-ml volumes of solutions containing up to at least 10 μg of arsenic.

The relative standard deviation of 10 analyses of solutions containing 0.5 μg of arsenic(III) per 500 ml was less than 3%.

Determination of Trace Amounts of Arsenic in Natural Water

The analyses were carried out on 500-ml aliquots of clear, uncontaminated water (river, well and tap waters), filtered through 0.45-μm Millipore filters after addition of 10 ml of hydrochloric acid per 1000 ml of sample immediately after collection.

Table IV presents analytical results for natural water samples by the procedure recommended. A known amount of arsenic(III) was added to water samples and the recovery was measured. In these instances the recoveries were from 94 to 103%. The arsenic concentrations in the waters analysed were 1.59, 0.63 and 0.71 μg l^{-1} for Takahashi River water (Okayama Prefecture, Japan), well water and laboratory tap water, respectively.

TABLE IV

DETERMINATION OF ARSENIC IN NATURAL WATER SAMPLES

Volume of sample, 500 ml.

Sample	Amount of arsenic/μg Added	Found	Recovered	Recovery, %	Arsenic in sample/μg l^{-1}
River water	None	0.795			1.59
	0.200	1.001	0.206	103	
	0.400	1.200	0.405	101	
Well water	None	0.315			0.63
	0.200	0.502	0.187	94	
	0.400	0.700	0.385	96	
Tap water	None	0.357			0.71
	0.200	0.560	0.203	102	
	0.400	0.734	0.377	94	

Conclusions

The flotation of sub-microgram amounts of arsenic coprecipitated with iron(III) hydroxide is useful as a pre-concentration technique for extraction of arsenic from a large volume of water, and subsequent atomic-absorption spectrophotometry in a long absorption cell of the arsine generated from the arsenic is an accurate method for the determination of arsenic.

The method offers a rapid and precise procedure for the routine determination of arsenic in natural fresh waters. This method is also applicable to the flotation of arsenic in artificial sea water. With suitable modifications, the procedure can be applied to determining sub-microgram levels of metals, such as tin(IV), antimony(III, V) and selenium(IV), which readily form volatile hydrides in water.

The author thanks Professor Atsushi Mizuike and Dr. Masataka Hiraide of Nagoya University for their helpful advice on the flotation technique, and Assistant Professor Fuji Morii of Okayama University for useful discussions.

References

1. Yamamoto, Y., Kumamaru, T., Hayashi, Y., and Kamada, T., *Bunseki Kagaku*, 1973, **22**, 876.
2. Yamamoto, Y., Kumamaru, T., Edo, T., and Takemoto, J., *Bunseki Kagaku*, 1976, **25**, 770.
3. Thompson, K. C., and Thomerson, D. R., *Analyst*, 1974, **99**, 595.
4. Goulden, P. D., and Brooksbank, P., *Analyt. Chem.*, 1974, **46**, 1431.
5. Sugawara, K., Tanaka, M., and Kanamori, S., *Bull. Chem. Soc. Japan*, 1956, **29**, 670.
6. Hiraide, M., and Mizuike, A., *Bunseki Kagaku*, 1977, **26**, 47.
7. Hiraide, M., Yoshida, Y., and Mizuike, A., *Analytica Chim. Acta*, 1976, **81**, 185.

Received *February 9th*, 1978
Accepted *April 12th*, 1978

Analyst, October, 1978, Vol. 103, pp. 1037–1045

Extraction - Spectrophotometric Determination of Tin in Lead and Lead-based Alloys with 5,7-Dichloroquinolin-8-ol

A. Sanz-Medel and A. M. Gutiérrez Carreras

Departamento de Química Analítica, Facultad de Ciencias Químicas, Universidad Complutense, Ciudad Universitaria, Madrid-3, Spain

A method is described for the direct spectrophotometric determination of micro-amounts of tin, by extraction into a chloroform solution of 5,7-dichloroquinolin-8-ol from a solution containing sulphuric acid. The influence of the different experimental parameters on the formation and extraction of the complex were studied and optimum conditions for the determination of tin were established. The precision of the extraction - spectrophotometric procedure, expressed in terms of relative standard deviation, was 1.4%.

It is shown that two different complexes (with $\lambda_{max.}$ 403 or 390 nm) can be extracted into the chloroform, depending on the presence or absence of chloride and on the pH of the solution.

The method has been tested on six standard lead-based samples with tin contents ranging from 0.05 to 1%. The average relative error (mean error) of the results lies within the range $\pm 1.4\%$, which shows that the accuracy is good and that systematic errors are absent.

Keywords: Tin determination; 5,7-dichloroquinolin-8-ol extraction; spectrophotometry; lead-based alloys

Most chromogenic reagents for the spectrophotometric determination of tin (dithiol,[1] phenylfluorone,[2] catechol violet,[3] haematoxylin, quercetin, gallein, etc.[4]) lack selectivity. As a result, the spectrophotometric determination of tin in metallic samples usually requires a preliminary separation of the tin. For example, distillation of the bromide or chloride is frequently used,[1,5] although this procedure is troublesome and not reproducible when microgram amounts of tin have to be separated.

Solvent-extraction methods have been extensively used for this purpose, especially the extraction of tin(IV) into toluene as tin(IV) iodide, which gives very good recoveries and has been applied successfully as a preliminary step in the spectrophotometric determination of tin in steel.[6] Other techniques used to achieve a preliminary separation are based on coprecipitation [*e.g.*, with manganese(IV) oxide] and ion exchange.

However, the advantage of liquid - liquid extraction is that it permits not only the separation of the desired constituent of the sample, or an increase in the sensitivity of the determination by a simple process of concentration, but also spectrophotometric determination directly in the non-aqueous phase by selection of an organic reagent that forms coloured neutral chelate complexes with the cation, *e.g.*, the extraction - spectrophotometric methods using quinolin-8-ol and its derivatives.

Gentry and Sherrington[7] reported that tin(IV) is extracted quantitatively with quinolin-8-ol in chloroform over the pH range 2.5–5.5. Owing to the poor selectivity of this procedure, Eberle and Lerner[8] recommended the extraction - spectrophotometric determination of tin(IV) with quinolin-8-ol at pH 0.85 in the presence of chloride ions. The use of this acidic medium made the extraction procedure much more selective.

It is well known that substitution by negative radicals of the hydrogen atoms in the quinolinol nucleus can result in increased selectivity of the reagent, as was shown for the dihalogen derivatives.[9] Several of these derivatives have been used for the gravimetric or spectrophotometric determination of cations.[10] In particular, the 5,7-dibromo derivative has been investigated for the analytical separation and spectrophotometric determination of tin.[11,12]

Previous work by the present authors[13] on the behaviour of five different dihalogen derivatives of quinolinol as reagents for niobium(V) showed that tin(IV) can also be extracted with an excess of the 5,7-dichloro derivative in chloroform from 2 M hydrochloric acid. This

acidity differs significantly from the optimum value of pH 1 given by Ruf[11] and Matsuo and Funayama[12] using 5,7-dibromoquinolin-8-ol and so could produce increased selectivity. In a more strongly acidic medium the tendency for the weaker metal complexes to be formed is minimised because the ionisation of the reagent is virtually suppressed. This fact, along with the better solubility of the dichloro derivative in chloroform,[13] encouraged the investigation of the 5,7-dichloroquinolin-8-ol as an extraction - spectrophotometric reagent for tin(IV).

A method for the selective spectrophotometric determination of tin(IV) by extracting it from 2 M sulphuric acid with 5,7-dichloroquinolin-8-ol in chloroform and direct measurement of the absorbance of the organic extract at 403 nm has been developed. The method has been applied successfully to the determination of tin in lead and lead-based alloys.

Experimental

Reagents

All of the reagents were of analytical-reagent grade.

Tin(IV) stock solution, 1000 μg ml^{-1}. Dissolve 1.000 g of pure tin in 50 ml of concentrated sulphuric acid with heating. When it has dissolved, add a further 150 ml of the acid and carefully pour the solution into 500 ml of distilled water. Cool this solution and dilute it to 1 l in a calibrated flask.

Dilute standard tin(IV) solutions are prepared by diluting this stock solution with the necessary volume of 3.25 M sulphuric acid.

5,7-Dichloroquinolin-8-ol solution, 1% *m/V in chloroform.*

Ammonium chloride solution, 2 M.

Ammonia solution, 10 M.

Nitric acid, 50% *V/V*.

Tartaric acid solution, 50% *m/V*.

Nitric acid - tartaric acid mixture. Mix 100 ml of 50% *V/V* nitric acid with the same volume of 50% *m/V* tartaric acid solution.

Equipment

Spectrophotometers. A Beckman, Model DU, single beam, for absorbance measurements, and a Beckman, Model DK-2A, for automatic recording of the spectra, each with 10-mm glass cells.

pH meter. Metrohm, Model E-516, with glass electrode and saturated calomel reference electrode.

Separating funnels. Capacity 100 ml.

Procedure

Dissolution of lead samples

Dissolve an appropriate amount (0.2–2 g for samples with tin contents ranging from 3 to 0.3%) of lead by gently warming it with 20 ml of the nitric acid - tartaric acid mixture. Heat to fuming and boil until fumes are no longer evolved. Cool the solution and dilute to 100 ml with distilled water in a calibrated flask.[14] Determine the tin content as described under *General procedure.*

General procedure

Pipette a portion of the sample solution containing 40–150 μg of tin into a separating funnel and add sufficient sulphuric acid to ensure a final concentration of it in the aqueous phase of 1.5–2 M (better selectivity is attained by using a concentration of 2 M, which can be produced by adding $6 - n$ ml of 3.25 M sulphuric acid to n ml of the solution) and 1 ml of the ammonium chloride solution. Adjust the final volume of the aqueous phase to approximately 10 ml with distilled water. Add 10 ml of 1% 5,7-dichloroquinolin-8-ol solution in chloroform with gentle manual shaking to achieve a rapid distribution of the complexing reagent between the two phases, allow to stand for 5–10 min and finally extract the tin by shaking the funnel for 3–4 min and allowing the phases to separate. Filter the chloroform solution through a dry Whatman No. 1 filter-paper and measure the absorbance at 403 nm against a blank prepared by extracting all of the reagents in the absence of sample.

Prepare a calibration graph by taking portions of dilute standard tin solutions containing 40, 50, 60, 70, 80, 100, 120 and 140 μg of this metal, and extracting each of these by the procedure described above.

Results and Discussion

Spectral Characteristics of Complex

As can be seen from Fig. 1, the absorption spectrum of the complex tin(IV) - 5,7-dichloroquinolin-8-ol extracted by following the *General procedure* exhibits a maximum at 403 nm when measured against a similar blank. However, a hypsochromic effect was observed when decreasing the hydrogen-ion concentration of the aqueous phase before the extraction step.

Effect of pH on Extraction of Tin and Colour of Complex

A set of experiments was carried out in order to study the influence of pH on the extraction of tin. The results are given in Fig. 2 and demonstrate that when the pH was increased above pH 1 the maximum of the absorption spectrum started to shift towards shorter wavelengths, and hence from pH $\geqslant$ 3 the maximum appeared at 390 nm. The magnitude of such a variation for different pH values is given in Table I.

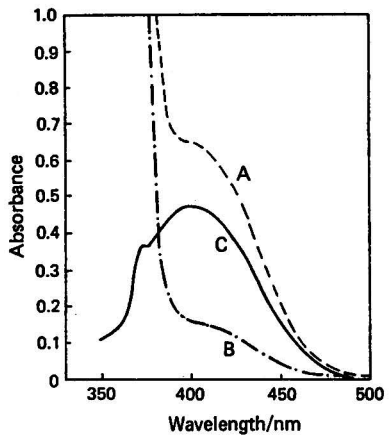

Fig. 1. Absorption spectra of: A, tin(IV) - 5,7-dichloroquinolin-8-ol complex, extracted into chloroform, measured against chloroform as reference; B, reagent blank (extracted under the same conditions) against chloroform; and C, tin(IV) - 5,7-dichloroquinolin-8-ol complex, extracted into chloroform, measured against reagent blank.

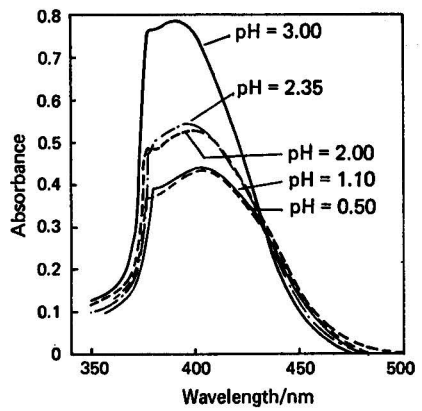

Fig. 2. Variation of the absorption spectra with pH.

All of the tests were carried out by using 100 μg of tin(IV), a 0.6-g total amount of ammonium chloride and 10 ml of the 1% 5,7-dichloroquinolin-8-ol solution in chloroform. The pH was adjusted with ammonia solution as the final step before shaking the separating funnel (this order of addition produces a higher reaction rate).[13]

As shown in Table I, the amount of tin(IV) extracted remained virtually constant (for the compound absorbing at 403 nm) down to pH 1 and the effect of higher acid concentrations was investigated, but sulphuric acid was used because the use of hydrochloric acid for this purpose gave too high absorbances for the blanks. The results are plotted in Fig. 3, which shows that over the range 0.5–2 M in sulphuric acid the amount of tin(IV) extracted reaches a virtually constant value. A sulphuric acid concentration of 1 M was initially used to optimise the experimental conditions.

TABLE I

EFFECT OF pH ON WAVELENGTH OF MAXIMUM ABSORBANCE AND ABSORBANCE AT THAT WAVELENGTH

pH	$\lambda_{max.}$/ nm	Absorbance		
		Sample*	Blank*	Sample†
4.00	390	1.400	0.280	1.120
3.10	390	1.000	0.250	0.790
2.35	397	0.720	0.150	0.547
2.10	400	0.620	0.100	0.530
1.10	403	0.535	0.055	0.442
0.70	403	0.520	0.057	0.435
0.60	403	0.517	0.072	0.445
0.40	403	0.536	0.075	0.469
0.20	403	0.550	0.085	0.465
0.10	403	0.626	0.145	0.452

* Absorbance of sample and of blank measured against chloroform as reference.
† Absorbance measured experimentally against blank as reference.

Tin(IV) Extraction in the Absence of Chloride

The effect of eliminating the ammonium chloride addition step in the *General procedure* was examined. The spectra of the organic extracts were similar to that obtained at pH > 3 with chloride ions present ($\lambda_{max.}$ 390 nm, as shown in Fig. 2). Tin(IV) was found to be extracted with 1% 5,7-dichloroquinolin-8-ol in chloroform in the total absence of chloride ions over the pH range 1–9, as shown in Fig. 4. The molar absorptivity of the extracted compound ($\lambda_{max.}$ 390 nm) is approximately double that of the compound extracted in the presence of halide ions ($\lambda_{max.}$ 403 nm).

All of the literature available claims that the presence of halide is necessary in order to achieve quantitative extraction of micro-amounts of tin(IV) with quinolin-8-ol[8] or with dibromoquinolin-8-ol.[12]

Although extraction in the absence of halide shows better spectrophotometric sensitivity, the higher pH needed for the quantitative extraction (Fig. 4) leads to a less selective extraction procedure than that with chloride present. This finding was confirmed experimentally by interference tests. The method given in the *General procedure* was chosen for the analysis of the actual lead samples.

Effect of Chloride Concentration on the Extraction of Tin(IV)

The extraction of tin(IV) in the presence of increasing halide concentrations was investigated by following the *General procedure* except that the sulphuric acid concentration was

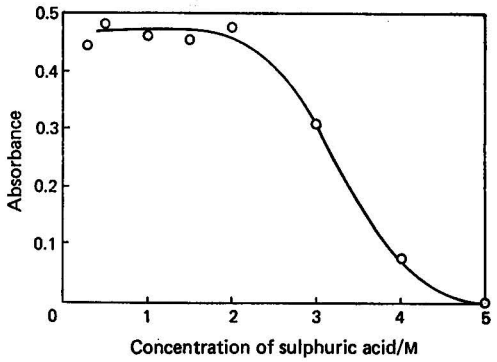

Fig. 3. Influence of the sulphuric acid concentration on the extraction of the tin(IV) complex.

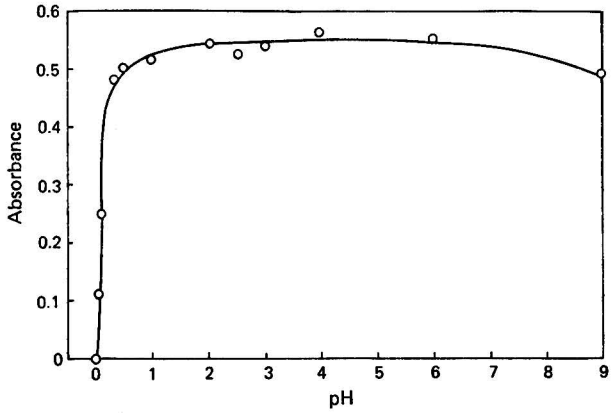

Fig. 4. Effect of pH on the extraction of the tin(IV) complex in the absence of chloride.

1 M (Table II). Tin(IV) is extracted in the absence of chloride ions as a complex with $\lambda_{max.}$ at 390 nm. As the chloride content of the aqueous phase increases, $\lambda_{max.}$ moves towards longer wavelengths to reach the value of 403 nm at a 10^{-2} M chloride concentration. A further increase in the halide concentration has no effect on the wavelength, although the absorbance increases slightly. A concentration of 2×10^{-1} M in chloride ions was selected as giving a sufficient excess to ensure the extraction of the maximum amount of tin as the complex with $\lambda_{max.}$ 403 nm.

TABLE II

EFFECT OF CHLORIDE CONCENTRATION ON THE EXTRACTION OF TIN FROM 1 M SULPHURIC ACID

Concentration of ammonium chloride/M	$\lambda_{max.}$/ nm	Absorbance		
		Sample*	Blank*	Sample†
0	390	0.740	0.160	0.630
10^{-3}	395	0.600	0.055	0.550
10^{-2}	403	0.510	0.020	0.495
10^{-1}	403	0.555	0.030	0.525
1	403	0.620	0.100	0.510

* Absorbance of sample and of blank measured against chloroform as reference.
† Absorbance measured experimentally against blank as reference.

Rate of Extraction and Stability of Colour

The plot of absorbance *versus* time of shaking the funnels reaches a constant, reproducible, maximum value after a relatively short time of about 3 min. The colour produced in the chloroform layer remained constant for at least 24 h against a similar blank when protected from exposure to direct sunlight.

Effect of Reagent Concentration

The influence of the concentration of 5,7-dichloroquinolin-8-ol in the chloroform was studied by extracting 100 μg of tin from 1 M sulphuric acid in a single extraction step. The absorbances were measured at 403 nm and plotted against the concentration of 5,7-dichloroquinolin-8-ol in chloroform (Fig. 5). The horizontal portion of the curve represents virtually 100% extraction. Although the use of 0.75% of reagent is apparently sufficient for the proposed procedure, a 1% concentration was selected in order to ensure an adequate excess.

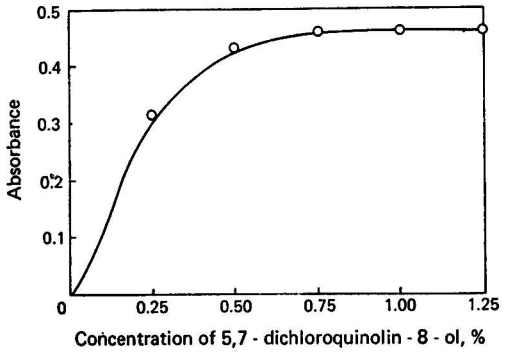

Fig. 5. Effect of 5,7-dichloroquinolin-8-ol concentration on the extraction of the tin(IV) complex in the presence of chloride.

Nature of the Complex

Published results[8] on the composition of the complex formed in the extraction of tin(IV) with quinolin-8-ol (oxH) in chloroform in the presence of chloride ions showed that the probable composition of the complex is $SnCl_2(ox)_2$. This formula is in agreement with the results reported by Hamaguchi *et al.*,[15] who determined large amounts of tin gravimetrically using quinolin-8-ol as the precipitating reagent. On the other hand, recently reported experiments[16] using different anionic compounds, *e.g.*, trichloroacetic acid instead of chloride ions, suggested the extraction of a mixed complex with a similar formula, $Sn(ox)_2(CCl_3COO)_2$. An analogous relationship between tin anion and reagent was found by Matsuo and Funayama[12] when extracting tin(IV) into carbon tetrachloride with 5,7-dibromoquinolin-8-ol.

As described above we have observed the presence of two different complexes when extracting tin(IV) with 5,7-dichloroquinolin-8-ol (Cl_2oxH) into chloroform, depending on the presence or absence of the halide anion. The analysis of the compound which had been obtained by following the procedure proposed in the present work (chloride present) suggests the formula $SnCl_2(Cl_2ox)_2$.

Precipitation experiments to establish the composition of the complex formed in the absence of halide, in which the $SnCl_2(Cl_2ox)_2$ complex was isolated, resulted in a mixture of $SnO_2.nH_2O$ and excess of reagent absorbed on the oxide. Continuous-variation and molar-ratio spectrophotometric methods using relatively concentrated tin(IV) solutions (2×10^{-3} M) and a pH of 2 for extraction in the absence of halide, led eventually to a ratio of tin to reagent of 1:3, which suggests the formula $Sn(Cl_2ox)_3$ for this complex.

It therefore appears that at higher pH values the two monodentate halide ions are replaced by a third bidentate reagent molecule (see Fig. 2).

Calibration Graph

The solution of the complex obeys Beer's law over a range of concentrations corresponding to 1–12 μg ml^{-1} of tin in the organic phase. The sensitivity of the determination, expressed in terms of molar absorptivity at 403 nm, was 4.7×10^3 l mol^{-1} cm^{-1}.

The reproducibility of the determination under the optimum conditions was established by carrying out 11 determinations on 100 μg of tin in a freshly prepared test solution. The set of absorbance values obtained was used to evaluate the precision of the method, which, expressed in terms of relative standard deviation, was found to be $\pm 1.4\%$.

Interferences

The effect of those potentially interfering elements that are present with tin in the lead samples was initially investigated by extracting 50 μg of tin from 1 M sulphuric acid in the presence of 500 μg of aluminium(III), copper(II), antimony(III), iron(III), lead(II) or bismuth(III). Aluminium, bismuth and lead did not interfere, even when present in greater excess, but iron, antimony and copper did interfere.

It was thought that there could be a gain in selectivity[13] by increasing the acid concentration as it was possible to extract tin from a more acidic medium without losing sensitivity (Fig. 3) and all further tests were carried out using a 2 M sulphuric acid medium.

Table III lists 15 foreign elements investigated under these conditions and their effect on the determination of 100 μg of tin. As can be seen, the procedure is highly selective, iron(III), copper(II) and antimony(III) being the only interfering elements that formed a coloured extractable reaction product. The use of masking agents to eliminate these interferences was investigated to see if it would be possible to overcome them without recourse to a preliminary separation technique. The masking agents investigated were fluoride, EDTA and tartaric acid. As shown in Table III, fluoride and EDTA, when added to the aqueous phase, inhibited the tin(IV) extraction with the reagent and thus only tartaric acid could be used as masking agent. The concentration of tartaric acid in the acid solution could be as high as 1 M without affecting the determination of 100 μg of tin. In the presence of 1 M tartaric acid iron(III) and antimony(III) could be masked when present in small amounts (up to 200 μg), but the masking action was insufficient if the amount of interferent was greater than five times the tin(IV) concentration.

TABLE III

EFFECT OF SOME COMMON IONS ON THE DETERMINATION OF TIN BY THE GENERAL PROCEDURE

Amount of tin/μg	Element or anion added	Compound	Amount tolerated/mg*
50	Al	$Al(NO_3)_3.9H_2O$	5.0
100	Pb	$Pb(NO_3)_2$	100
100	Bi	$BiONO_3.H_2O$	50
100	Ag	$AgNO_3$	0.5
100	Mn	$MnSO_4$	1.5
100	Zn	$ZnSO_4$	0.5
100	Ni	$Ni(NO_3)_2$	0.5
100	Mg	$Mg(NO_3)_2.6H_2O$	1.5
100	Co	$Co(NO_3)_2$	0.5
100	Si	SiO_2	0.05
100	Ti	$TiOSO_4$	0.25
100	Sb	$SbCl_5$	0.50
100	Sb	Sb_2O_3	Interfered
100	Fe	$Fe_2(NH_4)_2(SO_4)_3$	Interfered
100	Cu	$CuSO_4.5H_2O$	Interfered
100	Nitrate	$Pb(NO_3)_2$	0.05 M
100	Tartrate	$(CHOH.COOH)_2$	1.00 M
100	Sulphate	H_2SO_4	2.00 M
100	Chloride	NH_4Cl	1.00 M
100	EDTA	$Na_2.EDTA.2H_2O$	Interfered
100	Fluoride	NaF	Interfered

* The tolerances given correspond to the maximum amount of the foreign element or anion investigated in each instance.

In order to eliminate interferences in such instances, a selective pre-washing step was devised, taking advantage of the fact that tin(IV) is not extracted from a 2 M sulphuric acid medium in the absence of chloride ions (Fig. 4). By pre-extracting the sample solution in 2 M sulphuric acid, in the total absence of chloride ions, with a 1% 5,7-dichloroquinolin-8-ol solution in chloroform, a clear colourless extract is eventually obtained and large amounts of iron(III) or copper(II) can be removed. A single washing step eliminated the interference of up to 100 μg of copper(II) and 100 μg of iron(III) in the determination of 100 μg of tin(IV). The ammonium chloride was added after the washing step and tin(IV) was finally extracted with a fresh chloroform solution of the reagent by following the *General procedure*.

Antimony(III) showed similar extraction behaviour to tin(IV) and was extracted only in the presence of halide; it therefore could not be removed by the pre-washing technique. It was demonstrated that antimony(V) was not extracted under the *General procedure* conditions and thus the interference of antimony could be avoided by oxidising it to the non-interfering state before carrying out the extraction of tin(IV). On account of the practical

importance of antimony in commercial tin samples, a preliminary oxidation based on the use of sodium nitrite was tested for increasing antimony to tin ratios, the procedure being as follows: 0.5 g of sodium nitrite was added to the acidic sample solution containing the mixture of antimony(III) and tin(IV). After boiling for 10–15 min, 0.2 g of urea was added to destroy nitrogen oxides and excess of nitrite. After the solution had cooled, tin was determined by following the general extraction - spectrophotometric procedure. The results obtained are given in Table IV and show that amounts of antimony of up to twenty times the tin content can be tolerated by this procedure.

TABLE IV

ELIMINATION OF INTERFERENCE FROM ANTIMONY BY A PRELIMINARY OXIDATION WITH SODIUM NITRITE

Solution contained 100 μg of tin.

Sb added/μg	Sb: Sn ratio	Absorbance	Amount of Sn found/μg
0	0	0.412	100.0
100	1:1	0.412	100.0
200	2:1	0.415	100.7
500	5:1	0.425	103.1
1 000	10:1	0.420	101.9
2 000	20:1	0.430	104.3
5 000	50:1	0.455	110.4
10 000	100:1	0.600	145.6

Determination of Tin in Lead-based Samples

The recommended extraction - spectrophotometric procedure was tested by applying it to the determination of tin in six lead samples.

The results are given in Table V along with the certified values of the tin content in the different samples. It can be seen that the accuracy of the method, considered on the basis

TABLE V

TIN CONTENTS OF CERTIFIED LEAD SAMPLES

Sample number	Mass taken/g	Tin content, % Determined	Determined average	Certified	Relative error, %
I	1.578 4	0.307			
	1.757 8	0.327	0.319	0.315*	+1.3
	1.535 4	0.325			
II	1.020 3	0.490			
	0.945 5	0.491	0.495	0.500*	−1.0
	1.214 0	0.506			
III	2.429 6	0.094 1			
	2.030 8	0.097 8	0.097 5	0.100†	−2.0
	2.788 0	0.100 8			
IV	0.487 6	0.970			
	0.502 6	0.984	0.985	1.00†	−1.5
	0.547 1	1.00			
V	1.250 4	0.078			
	1.136 3	0.077	0.078	0.079‡	−1.3
	1.243 7	0.080			
VI	2.001 0	0.049			
	1.802 6	0.050	0.050	0.052‡	−3.8
	1.601 1	0.052			

* Commercial lead alloy for pipes. (Composition: lead containing Bi, Ag, Cu, Sb, Fe, Zn, Cd in amounts ranging from 0.005% for Ag to 0.1% for Sb, in addition to the Sn contents specified above.) Certified by Instituto del Hierro y del Acero (CENIM), Spain.

† Lead melted with the appropriate amount of pure tin, obtained from tin contents certified by Instituto del Hierro y del Acero (CENIM), Spain.

‡ Commercial lead from Peñarroya (Spain).

of the calculated average relative error, was satisfactory for tin contents above 0.05%. There was a variation within ±1.4%, corresponding to the mean relative error, for the five lead samples analysed that had tin contents above 0.05%. For samples with tin contents below 0.05% the method gave low results, probably caused by adsorption of these small amounts of tin on the surface of the precipitated lead sulphate.

As the precision of the extraction - spectrophotometric procedure itself was 1.4%, as shown above, it can be seen that there are no systematic errors in the tin contents.

When dissolving samples with high tin contents it is recommended that the excess of nitrogen oxides formed is destroyed by addition of urea. Unless this is done the deep orange colour produced by the oxidation of the reagent causes an error in the results.

References

1. Farnsworth, M., and Pekola, J., *Analyt. Chem.*, 1954, **26**, 735.
2. Luke, C. L., *Analyt. Chem.*, 1956, **28**, 1276.
3. Ross, W. J., and White, J. C., *Analyt. Chem.*, 1961, **33**, 421.
4. Marczenko, Z., "Spectrophotometric Determination of Elements," John Wiley, New York, 1976, p. 546.
5. Sandell, E. B., "Colorimetric Determination of Traces of Metals," Second Edition, Interscience, New York, 1959, 852.
6. Ashton, A., Fogg, A. G., and Thorburn Burns, D., *Analyst*, 1973, **98**, 202.
7. Gentry, C. H. R., and Sherrington, L. G., *Analyst*, 1950, **75**, 17.
8. Eberle, A. R., and Lerner, M. W., *Analyt. Chem.*, 1962, **34**, 627.
9. Irving, H., Butler, E. J., and Ring, M. F., *J. Chem. Soc.*, 1949, 1489.
10. Hollingshead, R. G. W., "Oxine and its Derivatives," Volume 4, Butterworths, London, 1956.
11. Ruf, E., *Z. Analyt. Chem.*, 1958, **162**, 9.
12. Matsuo, T., and Funayama, K., *J. Chem. Soc. Japan, Pure Chem. Sect.*, 1966, **87**, 433.
13. Sanz-Medel, A., *Revta Acad. Cienc. Zaragoza*, 1973, Serie 2, **28**, No. 2, 208.
14. Jimenez, J. L., Gomez, A., and Dorado, M. T., *Rev. Metal. Madrid*, 1969, **5**, 603.
15. Hamaguchi, H., Ikeda, N., and Osawa, K., *Bull. Chem. Soc. Japan*, 1959, **32**, 656.
16. Rakovskii, E. E., and Krylova, T. D., *Zh. Analit. Khim.*, 1974, **29**, 910.

Received *May 27th*, 1977
Amended *November 28th*, 1977
Accepted *March 17th*, 1978

Analyst, October, 1978, Vol. 103, pp. 1046–1052

Method for the Determination of Methanol in Binary Methanol - Water Mixtures by Use of Ion-selective Electrodes

G. J. Kakabadse, H. Abdulahed Maleila, M. N. Khayat, G. Tassopoulos and A. Vahdati

Department of Chemistry, University of Manchester Institute of Science and Technology, P.O. Box 88, Manchester, M60 1QD

For a given concentration of indicator ion X (X = F^-, Cl^-, Br^-, I^-, OH^-, S^{2-}, Ag^+ or H^+), the systematic change of cell potential, E, with variation in the concentration of methanol provides a graphical method for the rapid determination of methanol in methanol - water mixtures. Readings obtained by direct potentiometry show good reproducibility and stability. In 99.0–99.9% *m/m* methanol, containing 10^{-3} M hydrochloric acid, trace amounts of water can be determined accurately owing to a potential "anomaly."

Keywords: *Methanol determination*; *methanol - water mixtures*; *ion-selective electrodes*; *trace water determination*

The effect of organic solvents on the potentials of ion-selective electrodes is well known.[1–6] The use of this effect in the determination of solvents, first reported in 1975,[7] has been tested on a number of binary water - organic solvent mixtures and the method is explained for the methanol - water system.

In the system ISE|X, 0–*n*% methanol|RE (ISE is the ion-selective electrode = AgCl, AgBr, AgI, Ag_2S, LaF_3 or pH glass electrode; X = F^-, Cl^-, Br^-, I^-, OH^-, S^{2-}, Ag^+ or H^+; $n < 100$; RE is the reference electrode), for a given concentration of indicator ion X and a given reference electrode the electrode potential decreases systematically with an increase in the concentration of methanol when X is an anion and the reverse is observed when X is a cation. With the pH glass electrode an initial decrease in potential is reversed at higher concentrations of methanol.

Experimental and Results

Apparatus and Experimental Conditions

Measurements of potential were made with solutions stirred magnetically (at a constant rate throughout) at a temperature of 25 ± 0.5 °C by using an Orion, Model 801, digital pH/millivolt meter with a potential range of ±1000 mV and a discrimination of ±0.1 mV. Potentials were recorded on a Servoscribe potentiometric recorder, Type RE 511. A Hewlett-Packard 9862A calculator/plotter was used for drawing the graphs.

Orion solid-state lanthanum fluoride, silver halide and silver sulphide electrodes, and EIL and Beckman pH glass electrodes were used. The concentration of X was about 10^{-4} M and that of the background electrolyte was 10^{-1} M. Analytical-reagent grade chemicals were used throughout.

Preparation of Calibration Graphs

Direct method

A series of solutions having the same concentration of X (and of background electrolyte, when used) and different concentrations of methanol (0–*n*% *m/m*) were prepared by accurate weighing. Measurements of potential were made in an enclosed system in order to prevent the evaporation of solvent. Each solution was placed in a 250-ml three-necked round-bottomed flask fitted with indicator and reference electrodes and measurements were recorded over a period of several minutes so as to allow for equilibration (see Table I and Figs. 1–3).

TABLE I

POTENTIAL RESPONSE OF METHANOL TO DIFFERENT ION-SELECTIVE ELECTRODES

ISE	X ion	Measured range of methanol concentration, % *m/m*	Corresponding change in potential, ΔE*/mV	Range of methanol concentration showing linear response to *E*, % *m/m*	Corresponding change in potential, ΔE*/mV
LaF_3	F^-	0–95	−129	0–84	−119
AgCl	Cl^-	0–75	−81	<50	
	Ag^+	0–94	97	<50	
AgBr	Br^-	0–75	−65	<50	
AgI	I^-	0–75	−33	<50	
	Ag^+	0–75	32	0–54	21
Ag_2S	S^{2-}	0–64	−32	0–64	−32
	Ag^+	0–87	54	0–65	34
EIL pH glass electrode	OH^-	0–80	−33	0–60	−28.5
		80–98	4		
EIL pH glass electrode	H^+	0–63	−11 (ΔE_1)	0–60	−10
		63–99	94 (ΔE_2)		
		99–99.9	20 (ΔE_3)	99–99.9	20

* ΔE for 0% *m/m* methanol is taken arbitrarily as zero.

Indirect method

The reversibilities of the systems were checked by constructing Nernstian-type graphs for solutions of the same concentration of methanol and different concentrations of X (in the approximate range 10^{-6}–10^{-3} M X). Known increments of a stock solution of X were added to the methanol - water mixture (plus background electrolyte) in a 250-ml three-necked round-bottomed flask. After each addition potentials were recorded for a period of 3–5 min so as to allow for equilibration. The electrode slopes are listed in Table II. From a series of 7–10 Nernstian-type graphs (corresponding to a series of methanol - water mixtures) potentials

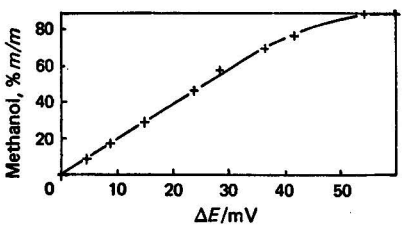

Fig. 1. Change in potential, ΔE, in solutions 10^{-4} M in silver nitrate, 0.1 M in sodium nitrate and of various methanol concentrations, measured by using silver sulphide and double-junction electrodes.

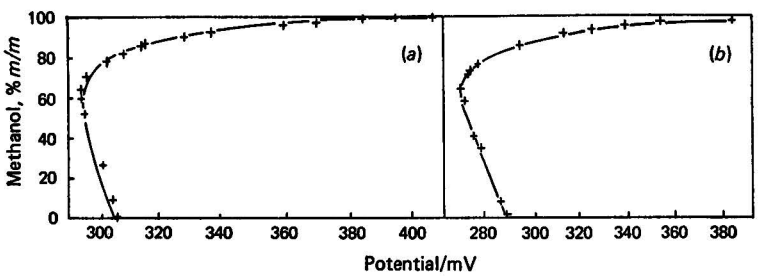

Fig. 2. Potential response in solutions of various methanol concentrations and 10^{-2} M in hydrochloric acid measured by using: (*a*), an EIL pH glass electrode and a double-junction reference electrode; and (*b*), a Beckman pH glass electrode and a double-junction reference electrode.

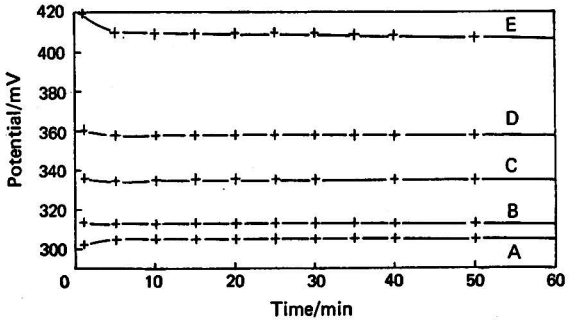

Fig. 3. Graphs of time *versus* potential for methanol - water mixtures in 10^{-2} M hydrochloric acid. Potential measured by using an EIL pH glass electrode and a double-junction reference electrode. Concentration of methanol: A, 0; B, 85.7; C, 92.6; D, 96.3; and E, 99.9%.

for the same concentration of X were abstracted and then plotted against the percentage by mass of methanol. Fig. 4 shows a typical graph. From a series of such graphs the one with the best linearity provided the optimum value for the concentration of X for use in the direct method.

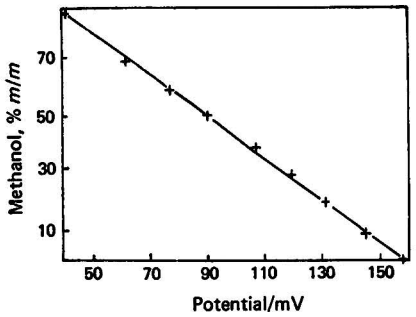

Fig. 4. Potential response (obtained by the indirect method) in solutions 10^{-4} M in sodium fluoride, 0.1 M in potassium chloride and of various methanol concentrations, measured by using lanthanum fluoride and silver - silver chloride electrodes.

Reproducibility Measurements

Measurements of potential on solutions used in the direct method were repeated 7–10 times, allowing 5 min for each measurement. The results, expressed as standard deviations, are shown in Table II.

Stability of Potentials

All of the solutions used in the direct method were submitted to measurements of potential for a period of 60 min and the millivolt readings were recorded on a chart. Fig. 3 shows typical results.

Discussion

Several experimental parameters must be considered when assessing the suitability of the proposed method for the determination of methanol in a binary mixture with water. As the systems investigated were restricted to solutions used for the preparation of calibration graphs no systematic bias was observed.

Electrochemical Reversibility

As non-aqueous solvents have a pronounced effect on ionic activities[8,9] and, hence, on electrode potentials, the electrochemical reversibility was checked by establishing the electrode slope for each system. The results in Table II show that the mean values of the slopes for fluoride ion, silver ion and hydrogen ion are close to the theoretical Nernstian values.

TABLE II

ELECTRODE SLOPES FOR SOLUTIONS HAVING A CONSTANT CONCENTRATION OF METHANOL AND ELECTROLYTE AND A VARYING CONCENTRATION OF X (INDIRECT METHOD) AND STANDARD DEVIATIONS OF POTENTIAL READINGS FOR SOLUTIONS HAVING A CONSTANT CONCENTRATION OF X AND A VARYING CONCENTRATION OF METHANOL (DIRECT METHOD)

	X ion					
	F^- (LaF_3)		Ag^+ (Ag_2S)		H^+ (Glass electrode)	
Concentration of methanol, % *m/m*	Electrode slope/−mV, per decade	Standard deviation, σ/mV	Electrode slope/mV per decade	Standard deviation, σ/mV	Electrode slope/mV per decade	Standard deviation, σ/mV
0	58.5	0.69	59.5	0.43	60.0	0.13
10	58.0	0.41	58.5	0.02	60.0	0.36
20	58.5	0.69	59.0	0.31	59.5	—
30	57.5	0.69	58.5	0.59	61.5	0.22
40	57.5	0.84	58.5	0.14	60.25	—
50	58.0	0.75	58.5	0.21	—	0.28
60	57.0	0.75	58.0	0.84	61.5	0.34
70	57.0	0.81	58.0	0.30	60.0	0.45
80	58.5	0.69	58.0	0.16	60.0	0.45
87	—	—	58.0	0.45	—	0.48
99.9	—	—	—	—	—	0.52
Mean values	57.8	0.70	58.5	0.35	60.3	0.36

Response Time and Stability of Potentials

In general both response time and stability were satisfactory (Fig. 3). Steady potentials were obtained after 1–2 min but the response time increased to 2–5 min at high concentrations of methanol. Long-term stabilities over periods of more than 1 h were also good (Fig. 3).

Reproducibility and the Magnitude of ΔE

The standard deviations given in Table II clearly indicate the reproducibilities of the results, which were always reasonable when compared with the performance of the same ion-selective electrodes in aqueous solutions.

For a given concentration of methanol and a given standard deviation, the magnitude of ΔE is important: the greater the magnitude the more accurate the results.

Coefficient of Variation, Sensitivity and Relative Uncertainty

These three parameters, listed in Table III, are a useful guide when comparing the performance of different ion-selective electrodes. While the coefficient of variation indicates the relative error in the determination of methanol ($100\sigma/\Delta E\%$, varying from $\pm 0.6\%$ for the fluoride system to $\pm 3.4\%$ for the hydrogen ion system in the 0–60% methanol range), it does not take into account the sensitivity of a given cell to the change in concentration of methanol. A more realistic estimate of the electrode performance is therefore given by the relative uncertainty parameter, incorporating both σ and ΔE/(concentration of methanol). For linear regions of the graph the best performance is shown by the hydrogen ion system in the 99.0–99.9% *m/m* methanol range, followed in decreasing order of accuracy by the fluoride ion and silver ion systems, all three having relative uncertainty values of less than 1.

TABLE III

COMPARISON OF COEFFICIENT OF VARIATION, SENSITIVITY AND RELATIVE UNCERTAINTY FOR METHANOL - WATER MIXTURES IN THE PRESENCE OF A CONSTANT CONCENTRATION OF FLUORIDE, SILVER AND HYDROGEN IONS USING FLUORIDE, SILVER SULPHIDE AND GLASS ELECTRODES, RESPECTIVELY

Electrode	Indicator ion	Range of methanol concentration, % *m/m*	Coefficient of variation ($\pm 100\sigma/\Delta E$), %	Sensitivity, $S[\Delta E/$(concentration of methanol)$]$/mV	Relative uncertainty (σ/S)
Fluoride	F^-	0–84	0.59	1.42	0.49
Silver sulphide ..	Ag^+	0–65	1.03	0.52	0.67
		65–87*	1.75	0.91	0.38_5
Glass	H^+	0–60	3.43	0.17_8	2.06
		63–99*	0.38	2.61	0.14
		99–99.9	1.80	22.22	0.02

* Non-linear region of the graph.

The pH glass electrode can also be used for the determination of trace amounts of water in methanol, which is of considerable practical interest.

The problem of overlapping ranges of potential, ΔE_1 and ΔE_2, in the hydrogen ion system (see Table I and Fig. 2) can be resolved as the addition of water to a methanol - water mixture would increase the potential in ΔE_1 but decrease it in ΔE_2.

"Hypersensitivity" of the pH Glass Electrode

Measurements obtained with an EIL pH glass electrode were repeated in 10^{-2} M hydrochloric acid, using a Beckman pH 0–14 glass electrode. While the over-all response was similar [Fig. 2(*b*)], differences occurred in the magnitude of ΔE measured in millivolts for the individual ranges of methanol concentration (EIL data in parentheses): 0–63% methanol, $\Delta E_1 = -19$ (−11); 63–99% methanol, $\Delta E_2 = 83.5$ (94); 99–99.9% methanol, $\Delta E_3 = 30.5$ (20). The observed large increase in ΔE in acid solution at high concentrations of methanol is in agreement with results obtained by other workers.[10–12]

Several factors may contribute to the hypersensitivity phenomenon of the pH electrode. There is an increase in conductivity in the range 80–100 mol % methanol[13] in a methanol - water mixture. A comparison of the "acidity potentials" of acid - base conjugate pairs in methanol and water has shown $CH_3OH_2^+$ to be more acidic than H_3O^+.[14] Further, an increase in the concentration of methanol may lead to gradual dehydration of the gel layer on the outer glass surface,[17] causing in turn a large shift in the equilibrium between the gel layers of the outer and inner glass surfaces.

The effect of methanol on the potential of the hydrogen cell, E^H, is well documented.[15–17] Using a combined glass - hydrogen cell over the range 0–100% of methanol, the observed changes in potential, ΔE^H (where $\Delta E^H = E^H_{H_2O} - E^H_{CH_3OH}$), were between 40 and 100 mV, depending on the glass composition of the pH electrode.[17]

Effect of Reference Electrode

The presence of a liquid junction (between the solution inside the reference electrode and the test solution) of variable potential (liquid-junction potential, E_j) gives rise to some uncertainty in measurements of potential.[18,19] The change in the liquid-junction potential, ΔE_j, with the concentration of methanol is probably a substantial factor.[7,10] Further, there appears to be a considerable variation in E_j between reference electrodes of a different type, as illustrated in Table IV. In the fluoride system, replacing a silver - silver chloride electrode (Beckman 39403 Futura) with a conventional mercury - mercury(I) sulphate electrode caused a reduction of $-\Delta E$ by nearly 31 mV (from −119.0 to −88.2 mV). On the other

hand, the variation between different reference electrodes of the same type has, in the authors' experience with several Orion double-junction reference electrodes, no significant effect on ΔE.

TABLE IV

EFFECT OF REFERENCE ELECTRODE ON POTENTIAL CHANGE, ΔE, FOR (0–80)% *m/m* METHANOL IN THE SYSTEM 2×10^{-4} M SODIUM FLUORIDE + 10^{-1} M SODIUM CHLORIDE

Reference electrode	Ag - AgCl (Beckman 39403 Futura)	Ag - AgCl (Orion double-junction)	Ag - AgCl (Orion single-junction)	S.C.E	Hg - Hg_2SO_4
ΔE/mV ..	119.0	114.1	113.4	106.6	88.2

Effect of X

A given ion X can be used over a fairly wide concentration range, the upper limit of which is set by the solubility of the ion in methanol and the lower limit by the limit of the Nernstian response of the ion-selective membrane in question.

If the test (methanol) sample already contains a particular X ion as contaminant, one can determine the concentration of this ion and either prepare standard solutions with an identical concentration of X ion or increase the concentration of X ion in the test solution to match that present in the already existing standard solutions. Alternatively, a known amount of a different X ion (absent in the test sample) can be added to methanol and an appropriate ion-selective electrode used.

Different Types of Graph

The potential *versus* percentage by mass of methanol graphs show linear and non-linear regions (Figs. 1 and 2 and Tables I and III). While the observed linearity is useful analytically, it must be accepted as empirical in nature. The extent of the linear range is probably a function of the properties of ions in solution and of liquid-junction potentials.

Conclusions

When limited to binary methanol - water mixtures, the proposed method is fast, reasonably accurate and simple to operate. Judging by the literature data, this method compares favourably with several other methods for the determination of methanol in methanol - water mixtures, *e.g.*, colorimetric,[20] dichromate,[21] mass-spectrometric,[22] infrared[23] and specific-gravity[24] methods, but is inferior to gas chromatography.[25]

An added advantage of the proposed method is its adaptability to continuous monitoring.

The authors gratefully acknowledge discussions with the following: Professor K. Burger (L. Eötvös University of Budapest); Professor J. de O. Cabral (University of Oporto), Mr. J. Dwyer (UMIST), Professor M. C. R. Symons (University of Leicester) and Dr. J. D. R. Thomas (UWIST).

References

1. Lingane, J. J., *Analyt. Chem.*, 1968, **40**, 935.
2. Wells, C. F., *J. Chem. Soc., Faraday Trans. I*, 1974, **70**, 694.
3. Kazarjan, N. A., and Pungor, E., *Analytica Chim. Acta*, 1970, **51**, 213.
4. Covington, A. K., and Thain, J. M., *J. Chem. Soc., Faraday Trans. I*, 1975, **71**, 78.
5. Ficklin, W. H., and Gottshall, W. C., *Analyt. Lett.*, 1973, **6**, 217.
6. Bennetto, H. P., and Spitzer, J. J., *J. Chem. Soc., Faraday Trans. I*, 1973, **69**, 1491.
7. Elbakai, A. M., Kakabadse, G. J., Khayat, M. N., and Tyas, D., *Proc. Analyt. Div. Chem. Soc.*, 1975, **12**, 83.
8. Bates, R. G., and Robinson, R. A., *in* Conway, B. E., and Barradas, R. G., *Editors*, "Chemical Physics of Ionic Solutions," John Wiley, New York, 1966, p. 211.
9. Parsons, R., "Handbook of Electrochemical Constants," Butterworths, London, 1959.

10. DeLigny, C. L., and Rehbach, M., *Recl Trav. Chim. Pays-Bas Belg.*, 1960, **79**, 727.
11. Johansson, G., Karlberg, B., and Wikby, A., *Talanta*, 1975, **22**, 953.
12. Nikolski, B. P., Schul'z, M. M., and Beljustin, A. A., *Wiss. Z. Tech. Hochsch. Chem. Leuna-Merseb.*, 1976, **18**, 573.
13. Bockris, J. O'M., and Conway, B. E., *Editors*, "Modern Aspects of Electrochemistry," No. **3**, Butterworths, London, 1964, p. 86.
14. Bates, R. G., *in* Lagowski, J. J., *Editor*, "The Chemistry of Non-Aqueous Solvents," Volume 1, Academic Press, London, 1966, p. 103.
15. Oiwa, I. T., *J. Phys. Chem.*, 1956, **60**, 754.
16. Paabo, M., Bates, R. G., and Robinson, R. A., *Analyt. Chem.*, 1965, **37**, 462.
17. Shul'z, M. M., and Ivanovskaya, I. S., *Sov. Electrochem.*, 1967, **3**, 506.
18. Covington, A. K., *in* Durst, R. A., *Editor*, "Ion-Selective Electrodes," National Bureau of Standards, Washington, D.C., 1969, p. 127.
19. Bailey, P. L., "Analysis with Ion-Selective Electrodes," Heyden, London, 1976, p. 23.
20. Boos, R. N., *Analyt. Chem.*, 1948, **20**, 964.
21. Welcher, F. J., *Editor*, "Standard Methods of Chemical Analysis," Sixth Edition, Volume II, Part B, D. Van Nostrand, New York, 1963, p. 2143.
22. Gifford, A. P., Rock, S. M., and Comaford, D. J., *Analyt. Chem.*, 1949, **21**, 1026.
23. Kaye, W., *Spectrochim. Acta*, 1954, **6**, 257.
24. Snell, F. D., and Ettre, L. S., *Editors*, "Encyclopedia of Industrial Chemical Analysis," Volume **16**, Interscience, New York, 1972, p. 107.
25. Blustein, C., and Posmanter, H. N., *Analyt. Chem.*, 1966, **38**, 1865.

Received *July 27th*, 1977
Amended *April 11th*, 1978
Accepted *May 17th* 1978

Analyst, October, 1978, Vol. 103, pp. 1053–1060

Potentiality of Seaweed as a Resource: Analysis of the Pyrolysis Products of *Fucus serratus*

Phillip J. Morgan and Keith Smith

Department of Chemistry, University College of Swansea, Singleton Park, Swansea, SA2 8PP

As a prelude to the investigation of the potentiality of seaweeds as a future source of organic chemicals or fuel, the products of pyrolysis under nitrogen of *Fucus serratus* (serrated wrack) have been analysed. The pyrolysis produces large amounts of charcoal, water and carbon dioxide with smaller amounts of an oil, pitch, hydrocarbon gases, carbon monoxide, ammonia and carboxylic acids. The oil proved to be a complex mixture of heterocyclic bases, phenols, aromatic hydrocarbons, nitrogen and oxygen heterocyclic compounds and small amounts of aliphatic compounds. A variety of analytical techniques have been employed to analyse the pyrolysis products, with gas chromatography and mass spectrometry being the most widely applicable.

Keywords: *Seaweed pyrolysis*; Fucus serratus; *gas chromatography*; *mass spectrometry*

There has recently been concern over the rate of depletion of world reserves of fossil fuels, especially crude oil. In addition to making the major contribution to world energy production, fossil fuels provide the basic feedstock for most of the organic chemicals industry. In the future it will be necessary to utilise alternative organic feedstocks and renewable biomass would appear to be an attractive prospect. In view of the large areas of ocean, the rapid growth rates of some species of kelp (sometimes more than 1 ft per day) and the success being achieved in the artificial cultivation of seaweeds,[1] the latter may be considered as a promising source of biomass for large-scale utilisation. We have therefore considered means of converting seaweed into more readily usable products. While others are investigating the microbiological production of methane,[2] we have mainly considered the possibilities for chemical conversion using combinations of elevated temperatures and/or pressures, with or without additional reactants or catalysts, and with or without preliminary treatment with other reagents.

It has been known for over a century that dry distillation of seaweed produces oily products,[3] but it was in the period prior to about 1930 that attempts were made to identify the nature of the distillation products,[4–7] the incentive at that time being a possible increase in profits in the potash production industry. Although some of the compound classes were recognised,[4–7] the detailed composition of the distillates remained obscure and, when seaweed was no longer used as a source of potash, research along these lines was discontinued. We have therefore carried out a much more detailed analysis, using modern techniques, of the pyrolysis products from *Fucus serratus* in order to establish a basis for comparison when seaweed is treated by different methods.

Experimental

Samples

Fucus serratus (serrated wrack) was collected from Limeslade Bay, Swansea. The whole plants were air dried, crushed manually and then ground in an electric grinder. Thermogravimetric analysis and oven drying showed that the air-dried seaweed contained 15% of residual moisture.

Gas-chromatographic supports and stationary phases were standard commercial materials.

Apparatus

A cylindrical (about 30 × 5 cm) electrically heated furnace (Severn Science) with a Eurotherm 021 temperature controller (adjustable to 1000 °C) was equipped with a B34

jointed quartz test-tube. The test-tube was connected by standard Pyrex glassware to a series of cooled traps.

Gas-chromatographic analyses were carried out using a Pye 104 gas chromatograph equipped with a flame-ionisation detector and facilities for link-up to an AEI MS9 mass spectrometer. The thermal analyses were carried out on a Linseis thermogravimetric analysis apparatus and the X-ray powder diffraction patterns were obtained on a para-focusing Guinier de Wolff No. II camera.

Pyrolysis Procedure

The quartz test-tube was charged with about 60 g of dried, crushed seaweed and then connected to a series of three standard traps (each with a capacity of about 150 ml), which were cooled successively in solid carbon dioxide, liquid nitrogen and liquid nitrogen. The outlet of the third trap was connected to a rotary pump - nitrogen cylinder - mercury bubbler arrangement leading to a soda-lime tower, and from there to a large (10-l) bell-jar for collection of the gases over water. The whole apparatus was evacuated and filled with nitrogen prior to the start of pyrolysis.

The desired maximum temperature was pre-set and the distillation was allowed to continue until no further volatile products were formed. In the high-temperature (800 °C) distillations, this point was reached at a temperature of about 600 °C, but the temperature was allowed to increase to the pre-set maximum.

When pyrolysis was complete, the apparatus was allowed to equilibrate to ambient temperature. A solid residue remained in the quartz test-tube and the gases were collected over water, carbon dioxide being removed in the soda-lime tower. The liquid distillates were directly redistilled from the traps under nitrogen to a maximum temperature of 300 °C. This procedure gave a light oil and an aqueous solution, which formed two layers in the receiver, and a pitch which remained in the traps. The distillates from all of the traps were combined.

Separation and Analysis of the Pyrolysis Products

An over-all scheme of the methods of separation of the products is given in Fig. 1, and details are given below.

Solid residue

The solid residue was extracted in a continuous extractor (Soxhlet) using water as the solvent. On cooling, the aqueous solution precipitated a solid, which was shown by X-ray powder diffraction to be calcium carbonate, while the mother liquor contained primarily potassium chloride and sodium chloride (identified by X-ray powder diffraction after evaporation). The insoluble residue was termed charcoal, although it undoubtedly also contained a small amount of ash.

Liquid distillates

Redistillation of the liquid distillates at 300 °C gave three fractions: a residual pitch and a liquid consisting of an aqueous fraction and an oil. The aqueous - oil mixture was separated by extraction with diethyl ether into the aqueous fraction and an ether solution (A) that contained the oil.

Aqueous fraction (B)

The aqueous fraction (B) was found to be alkaline (pH about 8.5) and was made more alkaline by addition of excess of sodium hydroxide. Extraction of this strongly alkaline solution with diethyl ether gave a fraction containing organic bases, which was combined with a similar fraction obtained from the ether layer (A) (see below). Distillation of the remaining aqueous layer under reduced pressure gave an aqueous ammonia distillate, which was analysed by titration and converted into ammonium chloride, this being identified by X-ray powder diffraction. The residual salts after the last distillation were acidified with excess of concentrated orthophosphoric acid and then a further distillation under reduced pressure was carried out to give a concentrated aqueous distillate containing carboxylic acids,

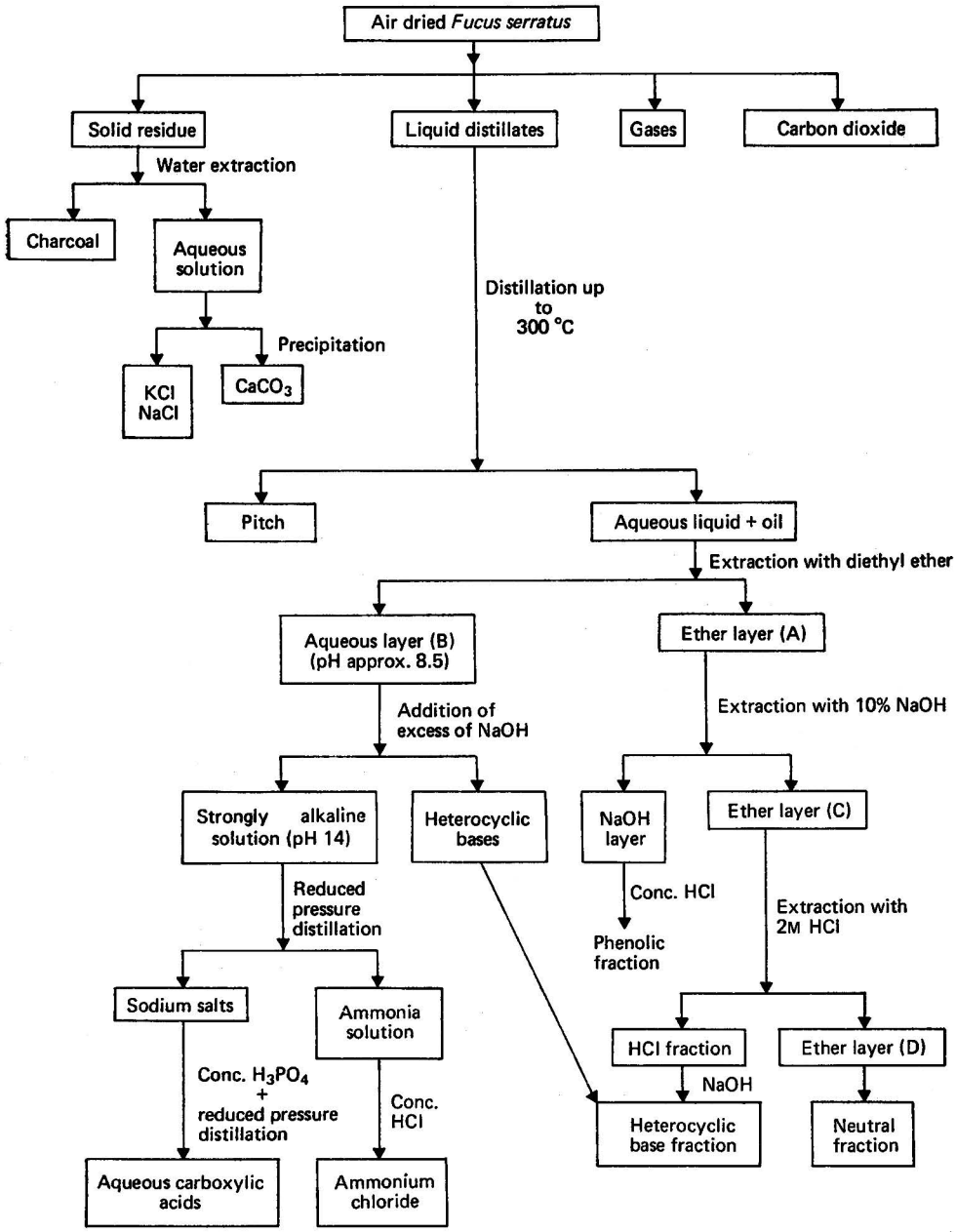

Fig. 1. Scheme for separation of pyrolysis products.

which were identified and determined by gas chromatography.[8] The salts were found to be mixed with a small amount of an ether-insoluble oil that was decomposed by the action of the orthophosphoric acid.

Oil

The ether layer (A) was extracted with 10% sodium hydroxide solution to give an alkaline layer from which phenols were extracted on acidification. These phenols were identified by

their mass spectra and determined by gas chromatography, using cyclohexanol as an internal standard. Extraction of the remaining ether layer (C) with dilute hydrochloric acid gave an acid layer from which heterocyclic bases were liberated on basification. These bases were combined with those obtained from the aqueous fraction (B) and were analysed by gas chromatography - mass spectrometry using a gas-chromatographic column packed with Carbowax 20M - potassium hydroxide.[9]

The residual ether layer (D) contained a large number of neutral components, including aromatic hydrocarbons, heteroaromatic compounds and some aliphatic compounds. The major components were identified by gas chromatography - mass spectrometry using standard mass spectra documentation tables and co-injection of samples when possible.

Pitch

The pitch was briefly examined using an Iatroscan quantitative thin-layer chromatography system and by gas chromatography, but it showed few discrete compounds, consisting mainly of polar polymeric material.

Gases

Carbon dioxide was removed from the gases by the use of a soda-lime tower and was determined by direct measurement of the increase in mass. The other gases were found to consist of a mixture of carbon monoxide, hydrocarbon gases, nitrogen and small amounts of hydrogen sulphide. Carbon monoxide was determined by titration of the iodine liberated when aliquots of the gases were passed over diiodine pentoxide heated at 150 °C in a stream of nitrogen,[10] the iodine formed being trapped in potassium iodide solution and determined by titration against standard thiosulphate solution.

Hydrocarbon gases present in the mixture were determined by gas chromatography on a column of alumina deactivated with liquid paraffin.[11] Mass spectrometry indicated the virtual absence of hydrogen.

Gas-chromatographic Identification and Determination

Details of the columns used for the gas-chromatographic identifications and determinations are given in Table I.

TABLE I

GAS-CHROMATOGRAPHIC COLUMNS AND CONDITIONS

		Conditions		
Stationary phase	Support	Temperature/°C	Column length/m	Uses and comments
OV-17 (5%)	Chromosorb G, 60–80 mesh, AW, DMCS	100	1.5	Phenols. Cyclohexanol is a convenient standard
Apiezon N (8%)	Chromosorb G, 100–120 mesh, AW, DMCS	65–200	3.5	Neutral compounds
Carbowax 20M - TPA (5%)	Chromosorb G, 60–80 mesh, AW, DMCS	110	3.5	Carboxylic acids. Cyclohexanol is a convenient standard
Carbowax 20M (8%) - KOH (2%)	Chromosorb G, 60–80 mesh, AW, DMCS	100	1.5	Organic bases
Liquid paraffin (4%) ..	Alumina, 100–120 mesh	50	1.5	Light hydrocarbons

Results and Discussion

Pyrolyses were carried out at three maximum temperatures (300, 450 and 800 °C) and Table II records the breakdown of products by class at the three temperatures.

TABLE II

PYROLYSIS PRODUCTS OBTAINED AT DIFFERENT TEMPERATURES

Figures are expressed as percentage of air-dried seaweed. Figures in parentheses are expressed as percentages of the organic material in seaweed. Air-dried seaweed contains 15% of moisture and 15% of inorganic salts.

Product	Temperature/°C 800*	450	300
Hydrocarbon gases	1.7 (2.4)	0.74 (1.0)	<0.01 (0)
Carbon monoxide	1.5 (2.1)	1.3 (1.9)	0.50 (0.70)
Carbon dioxide	12.0 (17)	11.0 (16)	7.0 (10)
Nitrogen and oxygen†	10.8 (15.5)	5.0 (7.1)	5.0 (7.1)
Total gases	26 (37)	18 (26)	12.5 (17.8)
Oil (F) Phenolics	0.16 (0.23)	0.16 (0.23)	0.0 (0.0)
Oil (F) Bases	0.16 (0.23)	0.13 (0.19)	0.1 (0.14)
Oil (F) Neutral compounds‡	3.7 (5.3)	3.7 (5.3)	2.5 (3.6)
Pitch	5.0 (7.1)	4.0§ (5.7)	0.0‖ (0.0)
Ammonia	0.18 (0.26)	0.19 (0.27)	0.10 (0.14)
Carboxylic acids	0.75 (1.1)	0.64 (0.91)	0.67 (0.96)
Water†	32 (24.3)	35 (28.6)	29.1 (20.1)
Total liquid distillates	42 (38.5)	44 (41.2)	32.5 (25.0)
Inorganic salts	15	15	15
Charcoal¶	17 (24.5)	23 (32.8)**	40 (57.2)**
Total residue	32 (24.5)	38 (32.8)	55 (57.2)

* Distillation complete by about 600 °C.
† By difference.
‡ By difference, fraction contaminated by polymer formation and precipitation, making direct determination difficult.
§ A further 1% of pitch remained with the residue.
‖ Does not distil but about 1% of pitch was extracted from the residue.
¶ In high-temperature pyrolyses this is mainly carbon, but includes undecomposed organic material in low-temperature pyrolyses.
** Includes about 1% of pitch.

The products of the distillation at 800 °C were subjected to a more detailed study. Table III gives the relative amounts of components within each fraction.

The neutral and organic base fractions are complex mixtures, but most of the major components have been identified by gas chromatography - mass spectrometry (comparison with literature standard mass spectra) and when possible confirmed by co-injection with authentic materials. Chromatograms are shown in Figs. 2 and 3.

Similar detailed studies of the components of the various fractions from pyrolyses at 300 and 450 °C showed qualitatively similar results, although quantitative differences were noted. Phenols were found to be almost absent from the products of pyrolysis at 300 °C, whereas there was a large increase in the amount of acetylfuran, which became the major component in the neutral fraction. Small amounts of cyclic dienes such as cyclohexadiene and methylcyclopentadiene were indicated by the mass spectral data. These compounds would be aromatised at the higher temperatures. Hydrocarbon gases were essentially absent. These features indicate a lower degree of decomposition of the seaweed and its initial decomposition products at the lower temperature.

Microanalysis of the raw air-dried *Fucus serratus*, after correction for moisture and inorganic salts, gave the following results: C 45.5, H 5.7, N 3.3 and O 45.5%. These figures are similar to those for cellulose, which is reasonable for a material that contains large amounts of carbohydrates. The bulk of the organic compounds formed in the pyrolyses have a higher C:H ratio, with a large part of the hydrogen (about 50%) present in the seaweed being used in the formation of large amounts of water. The major organic products are either aromatic or contain large amounts of oxygen (*e.g.*, formic acid). This is not

TABLE III

PRODUCTS OF THE DISTILLATION AT 800 °C

Product	Fraction	Components	Proportion of fraction, %	Proportion of product, %	Product as a proportion of total, %
Oil	Phenolics	Phenol	40	1.6	4
		Cresols	40	1.6	
		Xylenols	20	0.8	
	Neutral*	—	—	92	
	Heterocyclic bases†	—	—	4	
Pitch	—	—	—	—	5
Aqueous layer (B)	Carboxylic acids	Acetic acid	70	2	33
		Formic acid	17		
		Propionic acid	12		
		Higher acids	1		
	Ammonia	—	—	0.5	
	Water	—	—	97.5	
Charcoal	—	—	—	—	17
Salts	Soluble	KCl, NaCl	Combined	97	15
	Insoluble	$CaCO_3$	—	3	
Gases	CO	—	—	10.6	14
	Hydrocarbons	Methane	80	11.6	
		Ethane	12		
		Ethylene	6		
		Propane	1		
		Propene	1		
	Nitrogen and oxygen	—	—	77.8	
CO_2	—	—	—	—	12

* See Fig. 2.
† See Fig. 3.

surprising as the oxygen content of seaweed is high, and this is also responsible for the considerable production of carbon dioxide and water, which together constitute over 40% of the decomposition products from the organic material.

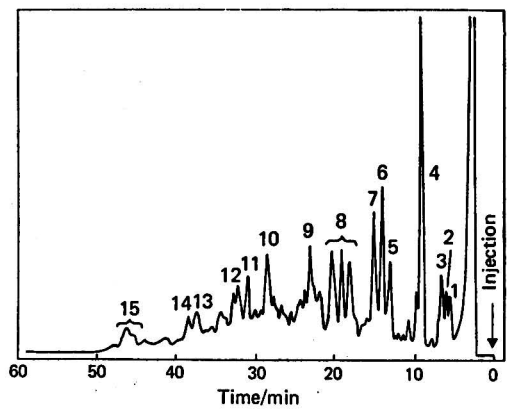

Fig. 2. Chromatogram of neutral fraction on 8% Apiezon N on 100–120-mesh Chromosorb G. Temperature programmed from 60 to 200 °C at 4 °C min^{-1}; carrier gas (nitrogen) flow-rate, 10 ml min^{-1}. Peaks: 1, butanone; 2, benzene; 3, pyrrole; 4, toluene; 5, acetylfuran; 6, xylene; 7, xylene + styrene; 8, trimethylbenzenes; 9, indene; 10, unknown; 11, naphthalene; 12, indole; 13, 2-methylnaphthalene; 14, 1-methylnaphthalene; and 15, dimethylnaphthalenes.

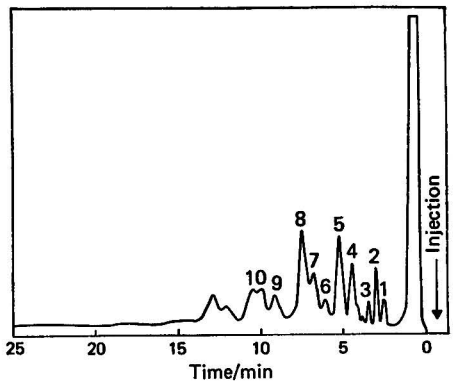

Fig. 3. Chromatogram of organic base fraction on 8% Carbowax 20M + 2% KOH, on 60–80-mesh Chromosorb G at 100 °C; carrier gas (nitrogen) flow-rate, 40 ml min^{-1}. Peaks: 1, pyridine; 2, α-picoline; 3, 2,6-lutidine; 4, β- + γ-picolines; 5, a dimethylpyridine; 6, 2,4,6-collidine + a dimethylpyridine; 7, a trimethylpyridine* + a trimethyldiazine*; 8, a trimethyldiazine*; 9, a dimethylpyrazine*; and 10, tetramethylpyrazine. Compounds marked with asterisks were identified by their mass spectrum only.

The results obtained in these pyrolyses broadly match those of earlier reports but provide greater detail. However, we were unable to detect the significant amounts of hydrogen recorded in earlier work. The results of pyrolyses at 800 and 450 °C were very similar, indicating that a pyrolysis temperature of about 500 °C would suffice to maximise product formation. Pyrolysis temperatures of about 300 °C appear to be of little value.

Conclusion

An extensive analysis of the components of seaweed pyrolysates should serve as an important basis for comparison in future studies of the possibilities of the conversion of seaweed into useful chemical components. Direct pyrolysis produces useful organic products, such as hydrocarbon gases, phenols, carboxylic acids, organic bases and neutral molecules, and also some valuable inorganic by-products, such as ammonia, carbon monoxide and potassium chloride. However, the larger organic fractions (*e.g.*, neutral distillates) are complex mixtures and would probably be of little direct value, and in any event the total amount of organic materials is small. It therefore seems unlikely that simple pyrolysis would be an economic prospect in the foreseeable future.

A large proportion of the carbon content is converted into hydrogen-deficient species such as charcoal, carbon dioxide and carbon monoxide, which is not unexpected in view of the high oxygen and low hydrogen content of the raw seaweed. It is likely that the products would have greater economic value if reducing agents, such as hydrogen or an alcoholic solvent, were present in the pyrolysis mixture. Pre-treatment of the seaweed is another possibility for improving the economics of the process. We are currently investigating such possibilities.

We thank the Science Research Council and BP Ltd. for a CASE studentship (to P. J. M.), and Mr. E. V. Whitehead, Dr. D. Brooks and Dr. A. Barwise (BP Ltd.) for valuable assistance and discussions. We are grateful to Dr. J. A. Ballantine of University College, Swansea, for guidance and assistance with all gas chromatographic - mass spectrometric work reported.

References

1. Jackson, G. A., and North, W. J., Final Report, Contract No. N60530-73-MV176, US Naval Weapons Center, China Lake, Calif., October 1973.
2. Wilcox, H. A., and Leese, T. M., *Hydrocarb. Process.*, 1976, **86**.
3. Stanford, E. C. C., *Chem. News, Lond.*, 1862, **5**, 167.
4. Hoagland, D. R., *J. Ind. Engng Chem.*, 1915, **7**, 673.
5. Turrentine, J. W., and Shoaff, P. S., *J. Ind. Engng Chem.*, 1919, **11**, 864.
6. Spencer, G. C., *J. Ind. Engng Chem.*, 1920, **12**, 786.
7. Tupholme, C. H. S., *Chem. Metall. Engng*, 1926, **33**, 81.
8. Baker, R. A., *J. Gas Chromat.*, 1966, **4**, 418.
9. Smith, E. D., and Radford, R. D., *Analyt. Chem.*, 1961, **33**, 1160.
10. Scott, W. W., and Furman, N. H., "Standard Methods of Chemical Analysis," Fifth Edition, Technical Press, London, 1939, p. 2406.
11. Jeffery, P. G., and Kipping, P. J., "Gas Analysis by Gas Chromatography," Second Edition, Pergamon Press, Oxford, 1972, p. 114.

Received *February 20th*, 1978
Accepted *April 14th*, 1978

Analyst, October, 1978, Vol. 103, pp. 1061–1065

Determination of Theophylline in Plasma: Comparison of High-performance Liquid Chromatography and an Enzyme Multiplied Immunoassay Technique

M. L. Eppel, J. S. Oliver and Hamilton Smith
Department of Forensic Medicine, Glasgow University, Glasgow, G12 8QQ

A. Mackay
MRC Blood Pressure Unit, Western Infirmary, Glasgow, G11 6NT

and L. E. Ramsay
Department of Medicine, Western Infirmary, Glasgow, G11 6NT

Plasma theophylline concentrations have been determined by both high-performance liquid chromatography and the enzyme multiplied immunoassay technique (EMIT). Comparison of the results showed a good correlation between the techniques. The faster processing time and smaller sample size makes EMIT the preferred technique when routine batch assays for theophylline are required.

Keywords: Theophylline determination; plasma; high-performance liquid chromatography; enzyme multiplied immunoassy technique

Theophylline (1,3-dimethylxanthine), a bronchodilator, has been used in the treatment of asthma for many years. The optimum therapeutic effect has been found when plasma concentrations are in the range 10–20 μg ml^{-1}.[1,2] Therefore, it is of interest to be able to monitor drug levels in plasma rapidly.

In the late 1940s, Schack and Waxler[3] developed an assay for the drug using ultraviolet spectrophotometry. This technique lacks specificity in that theobromine and barbiturates interfere. A modification by Jatlow[4] improved the assay although theobromine and theophylline metabolites still interfered. Separation techniques using gas - liquid chromatography[5–7] and high-performance liquid chromatography[8–10] have been developed and used successfully.

An assay procedure using the enzyme multiplied immunoassay technique (EMIT) has recently become available. The results obtained by using this method and high-performance liquid chromatography (HPLC) to monitor theophylline levels in plasma are presented and compared in this paper.

Experimental

Enzyme Multiplied Immunoassay Technique

The assay kit and standards were supplied by Syva (UK) Ltd. The instrumentation was the basic EMIT package based on the Gilford Stasar III spectrometer.

All of the reagents, standards and samples were kept at room temperature before use. Analysis of the standards supplied and the standards prepared for liquid chromatography as described below showed that the technique gave a linear response over the range 1–40 μg ml^{-1}.

When using the reagents supplied with the EMIT kit, 50 μl of standard or sample were diluted with 250 μl of pH 9 buffer. This mixture was diluted a second time in a similar manner and 50 μl of reagent A (antibody) diluted with 250 μl of buffer were added, followed by 50 μl of reagent B (enzyme-labelled drug) diluted with the same volume of buffer. The resultant solution was aspirated into the spectrometer and the difference in absorbance measured over a period of 30 s.

High-performance Liquid Chromatography

The pump used was the Pye Unicam LC 20 separator. The drug was detected by using a Cecil CE212 spectrophotometer set to monitor the effluent from the column at 273 nm, which is the absorbance maximum for theophylline. A 100 × 5.00 mm i.d. stainless-steel column packed with ODS-Hypersil (average particle size 5 μm) was used. Earlier work had been carried out with a column packed with μBondapak C_{18} (average particle size 10 μm). However, this packing material was discarded in favour of ODS-Hypersil because the resolution obtained with the former material was poorer.

The column was eluted with a solution of 7% of acetonitrile in 0.01 M sodium acetate trihydrate solution (adjusted to pH 4 with glacial acetic acid). This solvent was similar to those used by Franconi *et al.*[9] and by Orcutt.[11] A flow-rate of 1.6 ml min^{-1} was found to be suitable with the column used at room temperature.

A stock solution of theophylline in plasma (40 μg ml^{-1}) was prepared by dissolving a weighed amount of the drug in a few drops of ethanol and adding the solution to drug-free plasma. Other standards with concentrations ranging from 2.5 to 20 μg ml^{-1} (the expected therapeutic range) were prepared by diluting the stock solution with plasma. By injecting these standards containing a known amount of internal standard a linear relationship between peak height and drug concentration was demonstrated.

The internal standard used was β-hydroxyethyltheophylline. A concentration of 20 μg ml^{-1} was found to be suitable. A number of materials were considered for use as internal standards (Table I) but all except β-hydroxyethyltheophylline were rejected because of interference problems or the possibility of their presence in the samples submitted for analysis.

TABLE I

HPLC RETENTION TIMES OF XANTHINE COMPOUNDS

Compound	Retention time/min
Xanthine	<1.5
Hypoxanthine	<1.5
Uric acid	<1.5
Theobromine	2.1
Theophylline	3.1
Diprophylline	3.5
β-Hydroxyethyltheophylline	4.2
Caffeine	6.1
Proxyphylline	7.6
Millophylline	Retained on column

Determination of Theophylline

Three techniques were examined for the determination of theophylline in plasma by HPLC.

1. An extraction assay was designed by modifying the techniques of Manion *et al.*[12] and Sitar *et al.*[13] A 0.5-ml sample of plasma was acidified with 1.0 ml of 1 M hydrochloric acid, 0.5 ml of internal standard solution was added and the drugs were extracted from the resulting mixture by shaking for 20 min, using a rolling and rocking device, with 10 ml of chloroform - propan-2-ol (95 + 5). The phases were separated by centrifuging and the organic layer was filtered through Whatman 1PS phase-separating paper before being evaporated to dryness using a heating block at 30 °C and a stream of nitrogen. The residue was dissolved in 0.5 ml of methanol and 10-μl portions of this solution were chromatographed.

2. Protein was precipitated from plasma by the addition of trichloroacetic acid (TCA). Jusko and Poliszczuk[14] used 20% TCA but a weaker (10%) solution in water was found to be of sufficient strength for this purpose. A 0.5-ml volume of the internal standard solution was added to 0.5 ml of sample followed by 0.5 ml of 10% TCA solution. After mixing and centrifuging a clear supernatant layer was obtained; 10-μl samples of this solution were used for chromatography.

3. A direct injection technique was tried. Equal volumes (0.2 ml) of plasma and internal standard solution were mixed and 10-μl aliquots of the resulting solution were used directly for chromatography.

Quantification of the results was carried out by measuring peak-height or peak-area ratios and comparing the results with those for standards, which were plotted against the known concentrations of theophylline.

Results

EMIT standards and prepared standards were analysed over a period of 2 weeks when the known concentrations of the theophylline were plotted against the change in absorbance. A linear response was observed over the range 0–40 $\mu g\ ml^{-1}$ when using the specially calibrated paper supplied.

HPLC-extracted standards were analysed over a similar period and gave reproducible results. The values obtained were used to plot a standard graph of concentration against the ratio of drug to internal standard. This graph proved to be linear over the measured range (0–40 $\mu g\ ml^{-1}$).

HPLC standards subjected to the protein precipitation technique were treated in a similar fashion and gave the same results.

The EMIT system was tested for cross-reactivity with caffeine and theobromine, which are two xanthine compounds commonly found in the human diet. The former compound is consumed in tea and coffee and the latter in chocolate. No cross-reactivity was observed at levels up to 20 $\mu g\ ml^{-1}$ of caffeine and theobromine, which more than covers the expected levels.

Fig. 1 shows the separation achieved by HPLC between the above substances, theophylline and β-hydroxyethyltheophylline (the internal standard). There is no mutual interference and if necessary all three drugs can be measured by this method.

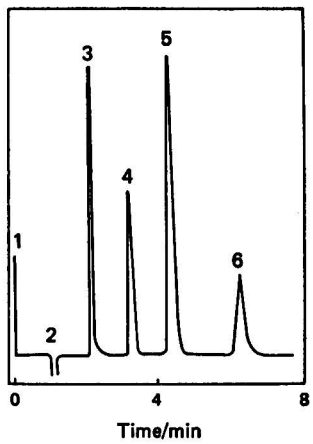

Fig. 1. HPLC separation of theophylline. 1, Injection point; 2, solvent; 3, theobromine; 4, theophylline; 5, β-hydroxyethyltheophylline; and 6, caffeine.

The results of precision studies carried out for EMIT and all three HPLC techniques are given in Table II. As a further test, both EMIT and HPLC with protein precipitation were used to analyse 58 samples so that a comparison of the results under working conditions could be made. The results shown in Fig. 2 have an average difference of 4.3%.

Discussion

Of the three HPLC techniques employed (extraction, protein precipitation and direct injection), protein precipitation was preferred although the precision for all three methods was acceptable.

The extraction technique yielded the cleanest product but sample preparation was lengthy (1½–2 h). The recovery of theophylline from plasma was found to be 80 ± 6% over the range 0–40 μg ml^{-1}. The use of the internal standard that has the same extraction characteristics automatically compensates for this loss.

TABLE II

COMPARISON OF PRECISIONS OF THE ANALYTICAL PROCEDURES FOR THEOPHYLLINE

	HPLC*					EMIT*	
	Extraction		Protein precipitation		Direct analysis: sample		
	Standard	Sample	Standard	Sample		Standard	Sample
Concentration of theophylline/ μg ml^{-1}	20.0	12.2	20.0	9.7	9.7	20.0	11.3
No. of samples	10	10	10	10	5	10	10
Coefficient of variation, % ..	4.5	4.9	1.2	2.6	1.1	2.1	2.1

* The samples analysed were different for each technique.

No sample preparation was required for the direct injection approach but the column life was extremely short (about five analyses), possibly owing to protein contamination. Peak-area measurements were necessary for this procedure because deteriorating resolution and peak shape made peak-height measurements inconsistent.

Precipitation of the protein in the plasma enabled large numbers of samples to be chromatographed without contamination and subsequent deterioration of the column. As sample preparation was relatively rapid, this technique was useful for the routine determination of theophylline in plasma. In all three HPLC methods no extraneous material from the plasma was found to interfere in the assay.

EMIT required no sample preparation and each assay was performed in less than 1 min.

The methods of choice for the determination of theophylline in plasma are HPLC with protein precipitation and EMIT. Both methods are acceptably precise, rapid and easy to use. The comparison of the methods (Fig. 2) shows that the results by both techniques are in reasonable agreement even when run under routine batch analysis conditions. The average difference is 4.3% but there does not appear to be any bias towards either method. HPLC has the advantage of the ability to measure the related materials at the same time but a smaller amount of manipulation is required when EMIT is used.

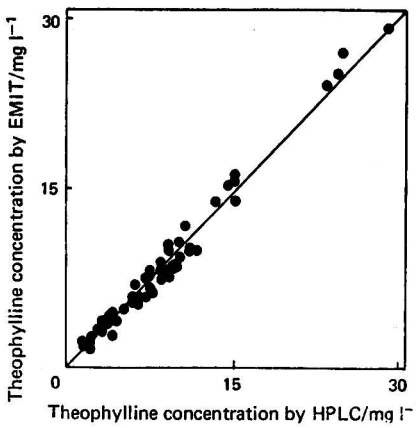

Fig. 2. Comparison of results for concentration of theophylline in plasma, obtained by HPLC and by EMIT.

Conclusion

All three methods of HPLC described and EMIT are acceptable methods of analysis but direct injection of plasma rapidly destroys the chromatographic column. HPLC following protein precipitation and EMIT are suitably precise and rapid for use as routine analytical techniques but the greater ease of handling and greater rapidity (one sample in under 1 min) make EMIT the method of choice for routine batch work. The related materials caffeine and theobromine, which can be detected and measured by the HPLC technique, do not interfere in either method.

The authors thank Syva (UK) Ltd. for the gift of the EMIT assay kit and standards and M. L. E. thanks the N.G.R.C. for financial support.

References

1. Jenne, J. W., Wyze, E., Rood, F. S., and Macdonald, F. M., *Clin. Pharmac. Ther.*, 1972, **13**, 349.
2. Mitenko, P. A., and Ogilvie, R. I., *New Engl. J. Med.*, 1973, **289**, 600.
3. Schack, J. A., and Waxler, S. H., *J. Pharmac. Exp. Ther.*, 1949, **97**, 283.
4. Jatlow, P., *Clin. Chem.*, 1975, **21**, 1518.
5. Shah, V. P., and Riegelman, S., *J. Pharm. Sci.*, 1974, **63**, 1283.
6. Johnson, G. F., Dechtiaruk, W. A., and Solomon, H. M., *Clin. Chem.*, 1975, **21**, 144.
7. Least, C. J., Jr., Johnson, G. F., and Solomon, H. M., *Clin. Chem.*, 1976, **22**, 765.
8. Adams, R. F., Vandemark, F. L., and Schmidt, G. J., *Clin. Chem.*, 1976, **22**, 1903.
9. Franconi, L. C., Hawk, G. L., Sandmann, B. J., and Haney, W. G., *Analyt. Chem.*, 1976, **48**, 372.
10. Peat, M. A., and Jennison, T. A., *J. Analyt. Toxicol.*, 1977, **1**, 204.
11. Orcutt, J., *Ann. Allergy*, 1976, **36**, 289.
12. Manion, C. V., Shoeman, D. W., and Azarnoff, D. L., *J. Chromat.*, 1974, **101**, 169.
13. Sitar, D. S., Piafsky, K. M., Rangno, R. E., and Ogilvie, R. I., *Clin. Chem.*, 1975, **21**, 1774.
14. Jusko, W. J., and Poliszczuk, A., *Am. J. Hosp. Pharm.*, 1976, **33**, 1193.

Received *April 26th*, 1978
Accepted *June 5th*, 1978

Analyst, October, 1978, Vol. 103, pp. 1066–1073

Optical Emission Spectrometry with an Inductively Coupled Radiofrequency Argon Plasma Source and Sample Introduction with a Graphite Rod Electrothermal Vaporisation Device

Part I. Instrumental Assembly and Performance Characteristics

A. M. Gunn, D. L. Millard and G. F. Kirkbright
Chemistry Department, Imperial College, London, SW7 2AY

A system is described in which a graphite rod electrothermal vaporisation device is employed for the introduction of microlitre liquid samples, after desolvation, into an inductively coupled argon plasma source for atomisation and excitation for optical emission spectrometry. The analytical performance of the system has been studied and detection limits for 16 elements at the sub-nanogram level are presented.

Keywords: *Optical emission spectrometry; inductively coupled radiofrequency argon plasma; graphite rod electrothermal atomisation*

A number of workers[1–4] have demonstrated that the high-frequency inductively coupled argon plasma (ICP) provides an effective excitation source for the simultaneous multi-element determination of metals and metalloids over a wide concentration range in solutions of samples. The ICP source can allow detection limits at the parts per 10^9 level for many metals, linear dynamic concentration ranges of typically five orders of magnitude and freedom from chemical condensed phase and vapour phase interferences. The most commonly used technique for the introduction of sample solutions into the ICP is based on the injection of a liquid aerosol generated by either a pneumatic or an ultrasonic nebuliser. Desolvation of the sample aerosol prior to its injection has also been employed. The major advantages of the ultrasonic nebuliser are the substantial improvement in the detection limits obtained, this improvement being typically a factor of ten or greater, the greater freedom of choice of sample injection rate and the need for only small sample volumes. Coupled with these very significant advantages are a number of disadvantages, *e.g.*, the use of high injection rates may necessitate desolvation of the aerosol prior to its passage into the plasma, which is inconvenient and may give rise to so-called "desolvation interference," and the magnitude of any matrix effect may then increase correspondingly. These disadvantages, and the high cost and possibly less convenient operation of the ultrasonic nebuliser, tend to mitigate against the advantages so that pneumatic nebulisation may frequently be preferable for rapid routine analysis.

Kleinmann and Svoboda[4] have reported direct vaporisation of samples into a low-power ICP source from a graphite disc support mounted directly within the body of the plasma torch. Nixon *et al.*[5] have described the use of a tantalum filament electrothermal vaporisation (TFV) apparatus as a sample introduction device for the inductively coupled plasma and reported detection limits for 16 elements in the range between nanograms and micrograms per litre for 100-μl samples. They pointed out that this TFV - ICP system gave an improvement in detection limits of one to two orders of magnitude, comparing these results with those obtained using pneumatic nebulisation of solutions into the inductively coupled argon plasma. The reason for this significant improvement in detection power has been attributed to the result of the increased concentration of the analyte, already desolvated and vaporised by the tantalum filament, passing as a pulse of sample through the axial channel of the plasma and giving rise to a transient analyte atomic-emission signal.

This paper describes the application of a graphite filament electrothermal vaporisation apparatus as a sample introduction system for optical emission spectrometry with an inductively coupled argon plasma source. Detection limits obtained with this system for small (10-μl) aqueous sample solutions are presented for 16 elements and some characteristics of the method of interfacing between the graphite filament and ICP source are discussed.

Experimental

The graphite rod vaporisation apparatus employed is shown in Fig. 1. A graphite rod (about 70 mm in length and 3 mm in diameter) was positioned between the terminals of the power supply in the shielded chamber (in the position of the dotted lines); the terminals were cooled with tap water. The unit was contained within a cylindrical glass manifold (about 100 mm in diameter and 210 mm long) of the shape shown. The total volume of the manifold was approximately 1 l and the distance from the top of the manifold to the plasma

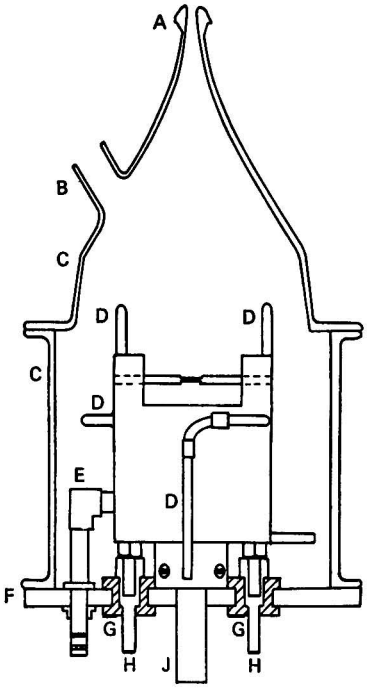

Fig. 1. Graphite rod vaporisation apparatus: A, ball joint to plasma torch sample inlet; B, sample delivery port; C, cylindrical glass manifold; D, water cooling link; E, argon sample transport gas inlet; F, circular brass base; G, Tufnol insulating blocks; H, electrode terminals; and J, mounting pillar.

was about 0.5 m. The enclosure was fitted with a conical top containing two ports. Port A was fitted with a ground-glass ball joint allowing the argon sweep gas carrying the vaporised sample to be transported to the injector tube of the ICP source, and port B was fitted with a polypropylene stopper and was positioned to allow the delivery by a micropipette of sample solution to the depression on the graphite rod. The filament was heated by a low-voltage, high-current power supply fitted with a programmer allowing variation of the power and time during desolvation, ashing and vaporisation procedures (A3370 electrothermal atomiser, Shandon Southern Instruments Ltd.).

Plasma Instrumentation

The instrumental system utilised a 2-kW crystal-controlled generator with an output frequency of 27.12 MHz (International Plasma Corp., Hayward, Calif., USA, Model 120-27). A schematic diagram of the system is shown in Fig. 2. A 1-m plane grating monochromator

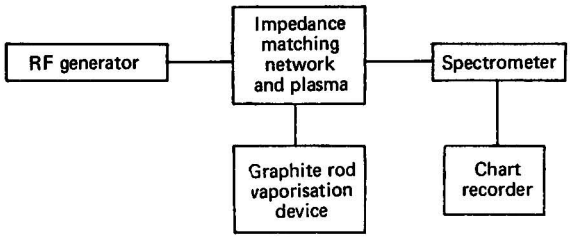

Fig. 2. Schematic diagram of experimental facilities.

(Monospek 1000, Rank Hilger Ltd., Margate, Kent, reciprocal linear dispersion 0.8 nm mm^{-1}) and a 13-stage end-window photomultiplier tube (EMI 6256B) were employed. A potentiometric chart recorder (Servoscribe, Model RE 541-20) was used for signal registration. Further details of the instrumentation used are given in Table I.

TABLE I

EXPERIMENTAL FACILITIES AND OPERATING CONDITIONS

Plasma power supply ..	International Plasma Corp., Model 120-27; operating frequency 27.12 MHz; power output 0–2 kW, continuously variable. Work coil, 1½ turns, 6 mm o.d. copper tubing.
Spectrometer	Hilger Monospek 1000; Czerny - Turner scanning monochromator with grating (1200 lines mm^{-1}) blazed for 300 nm; reciprocal linear dispersion, 0.8 nm mm^{-1}.
Optics	Plasma imaged in 1:1 ratio on to entrance slit with two 7.5 cm focal length, 5 cm diameter fused silica lenses.
Readout	Signal from EMI 6256B photomultiplier tube displayed on Servoscribe chart recorder.
Plasma torch	Demountable fused silica fitting into brass base. Coolant gas tubing, 21 mm o.d.; plasma gas tubing, 17 mm o.d.; injector tubing, 6 mm o.d., 1.5 mm i.d.
Filament power supply ..	Shandon Southern Instruments, Model A3370, electrothermal atomiser; the temperatures and times of desolvation and vaporisation were set at 100 °C for 30 s and 2400 °C for 1.5 s, respectively.
Filament	Single-depression graphite rods were constructed to be of 70 mm length and 3 mm diameter; the depression for the sample was a channel length of 8 mm and depth 1.0 mm; maximum sample volume, 20 μl.
Gas flow-rates	Argon flow-rates of 11, 1.0 and 0.8 l min^{-1} were used for the coolant, plasma and injector tubing, respectively.
Sample introduction ..	A 10-μl Eppendorf micropipette with a disposable polypropylene tip was used to introduce 10-μl volumes of sample solution on to the graphite rod.
Standard solutions	All stock solutions were prepared by dissolving analytical-reagent grade salts in dilute mineral acid or distilled water. Working solutions were prepared daily from these stock solutions.

Procedure

After the plasma had been generated and stabilised, the flow-rate of the argon was adjusted to the value established as optimal for simultaneous multi-element detection and the monochromator was set at the desired wavelength for the element concerned.

Sample solutions (10 μl) were deposited on the depression on the graphite rod. After desolvation, when the rod temperature increased to approximately 2400 °C, the analyte together with the matrix elements were vaporised into the argon carrier stream and swept into the plasma. The emission intensity for the selected line of the element of interest was then recorded at the monochromator and detector system.

Results and Discussion

The mode of operation of a graphite rod electrothermal vaporisation device for introduction of the sample into the inductively coupled plasma source is different from that required in the use of this type of device in atomic-absorption spectrophotometry. In the latter technique, the graphite rod (or tube) electrothermal device is required both to release the analyte from the surface of the graphite (vaporisation) and also to effect atomisation of the analyte so that free atomic species are available above the graphite surface for measurement by atomic-absorption spectrophotometry. In the use of the graphite rod as described here for the introduction of discrete samples into the ICP source, however, the atomisation requirement is not necessary. The electrothermal device is required only to release a discrete pulse of analyte material from the sample transferred to it; this may be released alone or together with the components of the sample matrix and may also be released bound in molecular form, as finely divided particulate material or as free atoms. Atomisation (and excitation for optical emission spectrometry) is then provided subsequently by passage of the analyte through the axial channel of the core of the ICP source. Provided, therefore, that no problems arise from premature loss of analyte during the desolvation and/or ashing stages of the temperature cycle employed with the graphite rod device, the requirement for close control of the final temperature of vaporisation used to remove different analyte elements from the graphite rod is not as critical as is encountered in atomic-absorption spectrophotometry. It is necessary only to provide a sufficiently high heating rate to the rod to ensure a rapid rate of removal of analyte from the surface and a discrete pulse of sample material above the surface of the rod for transport to the plasma source for excitation. For the elements studied in this work, a satisfactory compromise vaporisation temperature for the graphite rod was found to be 2400 °C. All further work was therefore undertaken at this vaporisation temperature. More important, for the purposes of attaining high sensitivity and precision in the technique employed, was careful optimisation of the parameters controlling sample transport to the ICP source.

Sample Transport from Graphite Rod to ICP Source

The principal parameters governing the rate and efficiency of sample transport from the graphite rod manifold to the ICP source were shown to be the length of the polythene connecting tube interface between the two units and the flow-rate of the argon injector gas used to sweep the analyte from the manifold into the source. The effects of these parameters on the analytical performance of the system were studied by using silver as the test element and monitoring the transient atomic-emission signal at 328.1 nm produced on vaporisation of 400-pg amounts of silver from the graphite rod at 2400 °C after desolvation of 10-μl aliquots of an aqueous 0.04 p.p.m. silver solution.

Fig. 3 shows the effect on the analytical signals obtained for silver of variation of the length of the tubing connecting the graphite rod manifold to the plasma torch injector gas inlet; the injector gas flow-rate was maintained constant at 1.3 l min^{-1} for this experiment. The traces represent the variation in observed emission intensity at 328.1 nm with time from the initiation of the filament vaporisation step. It is apparent that the vaporised analyte can be transported effectively over a considerable distance to the plasma (even utilising a 20.5-m length of connecting tubing a useful analytical signal is recorded for silver) and that, as expected, the appearance of the signal is delayed after the start of the vaporisation cycle for a period proportional to the distance over which it must be transported to the plasma source. In addition, as the length of the connecting tubing is increased, the analytical peak height decreases and the duration of the signal increases; this effect is attributed to progressive mixing and dilution of the analyte particles with the argon injector gas to cause "tailing." It is worth noting, however, that the leading edge of the analyte sample pulse remains relatively well defined even with a length of connecting tubing as much as a 10.5 m. Integration of the analyte emission signal revealed that the use of a greater length of tubing does not appear to decrease the sample transport efficiency very greatly. Some analyte is undoubtedly lost by deposition on to the walls of the manifold cover and the part of the connecting tubing nearest to the manifold as the vaporised material cools and aggregates; after this has occurred as the primary process that lowers the sample transport efficiency,

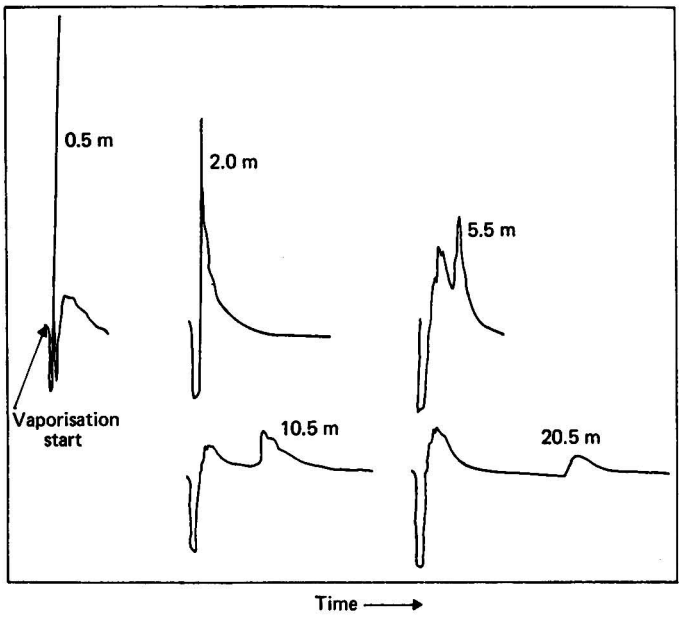

Fig. 3. Effect of variation of the length of connecting tubing on the analytical signal at 328.1 nm obtained from 400 pg of silver. Aliquots of 10 μl of 0.04 μg ml^{-1} silver solution. Injector gas flow-rate, 1.3 l min^{-1}.

however, little further loss of analyte material by deposition occurs. At the initiation of the vaporisation step a decrease in plasma background intensity is observed. This is caused by the pressure pulse that occurs as the argon carrier gas in the sample manifold is heated by its passage over the hot graphite rod and gives rise to an instantaneous temporary increase in the injector gas flow-rate at the plasma via a "piston effect"; for short tubing lengths this occurs just before the analyte material arrives at the plasma and for longer tubing this event is well separated in time from the analyte signal. The background returns to its initial value as the rod cools after the vaporisation heating step.

Fig. 4 shows the results of experiments conducted to examine the variation of the observed peak emission intensity for silver with injector gas flow-rate for various lengths of connecting tubing between the sample manifold and plasma torch. For a given length of connecting tubing there is an optimum injector gas flow-rate for maximum peak emission intensity; at gas flow-rates lower than this the reduced signal intensity is probably caused by a decreased sample transport efficiency, whereas at high gas flow-rates the signal intensity is again reduced owing to dilution of the analyte concentration in the gas stream. For the best signal to background and signal to noise ratio conditions, all further work was undertaken with connecting tubing of length 0.5 m, which represented the shortest practicable length for convenience of access and operation of the graphite rod system, and an injector gas flow-rate of 0.8 l min^{-1}.

Effect of Viewing Height and Plasma Operating Power

With a flow-rate of argon injector gas of 0.8 l min^{-1} the effect of variation in the height above the work coil at which the analyte emission intensity was viewed by the spectrometer was investigated over a range of applied forward power settings of the generator. With the particular system employed, maximum signal to background and signal to noise ratios were observed for a number of elements using a viewing height of 20 mm above the work coil and a forward power setting of 1.0 kW. These conditions were employed in all further studies.

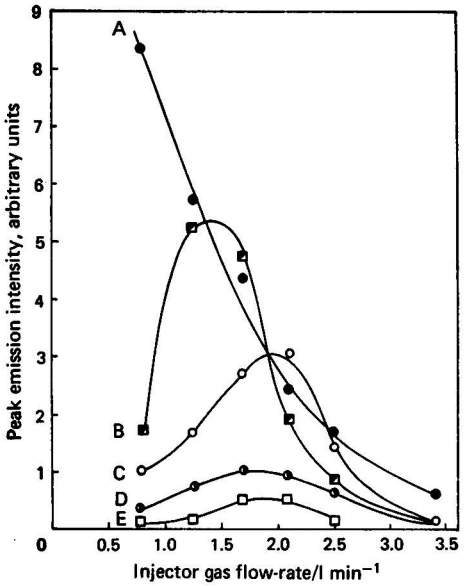

Fig. 4. Effect of variation of peak emission intensity obtained at 328.1 nm from 400 pg of silver with injector gas flow-rate using various lengths of connecting tubing: A, 0.5; B, 2.0; C, 5.5; D, 10.5; and E, 20.5 m.

Analytical Calibration Graphs and Detection Limits

Fig. 5 shows typical calibration graphs obtained using the graphite rod vaporisation device described here for the introduction of 10-μl aqueous samples into the ICP source for optical emission spectrometry. The graphs for silver and cadmium at their atomic resonance lines at 328.1 and 228.8 nm, respectively, are seen to be linear over four orders of magnitude

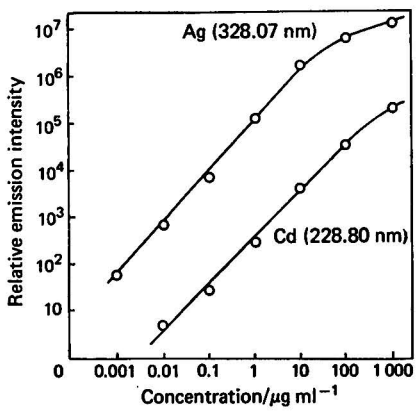

Fig. 5. Relative emission intensity *versus* concentration of cadmium and silver.

of concentration range up to 10 μl of an approximately 100 p.p.m. analyte solution. The graphs shown were drawn from a factor of 10 above the detection limit for silver and a factor of 3 above the detection limit for cadmium so that for these, and other, elements a linear dynamic concentration range of four to five orders of magnitude is possible with the system employed.

Under the optimum operating conditions of injector gas flow-rate, forward power and viewing height established earlier, and employing a maximum vaporisation temperature of the graphite rod of 2400 °C, the detection limits attainable for 16 elements whose determination is of particular interest in our laboratory were established. The detection limit for each analyte was defined as that concentration of the element in aqueous solution that produced an atomic-emission signal at the wavelength employed equal to twice the noise level observed in the plasma background emission. The relative detection limits expressed in terms of analyte concentration for 10-μl aqueous samples, and the corresponding absolute detection limits expressed as mass of analyte, are given in Table II. It is clear that, with the exception of arsenic, sub-nanogram amounts of each of the elements studied can be detected and that for several elements (silver, beryllium, lithium and manganese) the detection limits are in the picogram range. In order to minimise loss of analyte during desolvation in the determination of mercury, stabilisation was effected by the addition of aqueous sodium sulphide solution to the analyte solution on the graphite rod before commencing the desolvation stage. Where possible, the detection limits for the elements studied are compared in Table II with those obtained by Nixon *et al.*[5] using a tantalum filament vaporisation system and by Dahlquist *et al.*[6] using a graphite yarn thermal atomisation system for the introduction of samples into an ICP source; in most instances a superior power of detection was obtained with the graphite rod system employed here.

TABLE II

RELATIVE AND ABSOLUTE DETECTION LIMITS OBTAINED FOR ELEMENTS INVESTIGATED

All data at: power, 1000 W; viewing height, 20 mm; coolant gas flow-rate, 11 l min^{-1}; plasma flow-rate, 1 l min^{-1}; injector gas flow-rate, 0.8 l min^{-1}; atomisation temperature, 2400 °C

Element	Line/nm	Detection limit, p.p.m. (10 μl)	Detection limit/pg	Detection limit with TFV - ICP/pg*	Detection limit with graphite yarn atomiser - ICP/pg†
Ag ..	I 328.1	0.0001	1	10	300
As ..	I 228.8	0.2	2000	1000	500
Au ..	I 267.6	0.001	10	—	—
Be ..	I 234.9	0.0001	1	2	—
Cd ..	I 228.8	0.003	30	600	200
Ga ..	I 417.2	0.001	10	—	—
Hg ..	I 253.7	0.006	60‡	200	1000
In ..	I 325.6	0.002	20	—	—
Li ..	I 670.8	0.0004	4	—	—
Mn ..	II 257.6	0.0001	1	3	6
P ..	I 213.6	0.02	200	2000	—
Pb ..	I 405.8	0.01	100	300	80
Re ..	I 346.0	0.01	100	—	—
Sb ..	I 259.8	0.03	300	100	—
Tl ..	I 535.0	0.006	60	300	—
Zn ..	I 213.8	0.002	20	—	200

* From ref. 5.
† From ref. 6.
‡ Na_2S stabilisation technique employed.

Precision

The reproducibility of the graphite rod technique for introduction of samples into the ICP source was evaluated by using silver as the analyte element. Aliquots of 10 μl of a solution containing 0.4 p.p.m. of silver were introduced repetitively (15 times) on to the graphite rod for vaporisation and the peak emission intensity observed at 328.1 nm was recorded. The relative standard deviation obtained for these determinations was 0.06 (*i.e.*, 6%). Similar relative standard deviations were observed for other elements. These precision values reflect not only the reproducibility of the instrumental technique employed but also that of the sampling procedure using the micropipette for introduction of the sample on to the graphite rod.

Matrix and Inter-element Effects

Optical emission spectrometry using the ICP source and introduction of liquid samples using conventional pneumatic nebulisation is relatively free from condensed phase and vapour phase chemical inter-element and matrix effects, and the introduction of a dry particulate aerosol of sample material into the plasma source by the technique described here would be expected to be similarly free of such effects on atomisation and excitation when the sample has reached the plasma. With the system employed, however, interference effects are possible owing to the effect of concomitant substances upon the rate of vaporisation of analyte from the graphite rod and upon the efficiency of sample transport to the plasma. A number of complex effects of this type have been observed with the system described here; these have been the subject of an extensive study that will be described in Part II.

Conclusions

The graphite rod vaporisation technique provides an effective method for the application of optical emission spectrometry with the inductively coupled argon plasma to the determination of trace elements in small liquid samples; the technique allows high sensitivity and adequate precision to be obtained. The ability to transport the sample material for distances as far as 20 m to the ICP source for excitation may prove valuable for remote sampling in on-site applications. Matrix effects caused by the effect of concomitant substances on the rate of vaporisation of analyte from the graphite rod have been observed; these effects, and the effects of concomitant substances on the sample transport efficiency, form the subject of Part II.

This work was supported by the Employment Medical Advisory Service, Health and Safety Executive. We also acknowledge the assistance given by L. N. Opheim.

References

1. Fassel, V. A., and Kniseley, R. N., *Analyt. Chem.*, 1974, **46**, 1110A and 1155A.
2. Greenfield, S., McGeachin, H. McD., and Smith, P. B., *Talanta*, 1976, **23**, 1.
3. Boumans, P. W. J. M., and de Boer, F. J., *Proc. Analyt. Div. Chem. Soc.*, 1975, **12**, 140.
4. Kleinmann, I., and Svoboda, V., *Analyt. Chem.*, 1969, **41**, 1029.
5. Nixon, D. E., Fassel, V. A., and Kniseley, R. N., *Analyt. Chem.*, 1974, **46**, 210.
6. Dahlquist, R. L., Knoll, J. W., and Hoyt, R. E., paper presented at the 26th Pittsburgh Conference on Analytical Chemistry and Applied Spectroscopy, Cleveland, Ohio, 1975.

Received *April 28th*, 1978
Accepted *May 12th*, 1978

SHORT PAPERS

Determination of Antimony by Stibine Generation and Atomic-absorption Spectophotometry Using a Flame-heated Silica Furnace

D. L. Collett, D. E. Fleming and G. A. Taylor

Government Chemical Laboratories, Food and Industrial Hygiene Division, 30 Plain Street, Perth, Western Australia 6000

Keywords: Antimony determination; atomic-absorption spectrophotometry; hydride generation; flame-heated silica furnace

Considerable difficulty has been experienced in obtaining reliable results in the determination of antimony in blood and urine when using the method cited by Sandell,[1] involving extraction with benzene. The recovery and reproducibility were poor.

Good recoveries and reliable results have been obtained by using a procedure similar to that described for arsenic determination by Fleming and Taylor,[2] with a modified apparatus. Three modifications were made, as follows.

(i) A change was made in the design of the silica furnace, which is applicable also to arsenic determinations. The furnace is now T-shaped and consists of a silica tube 195 mm long, 10 mm i.d. and 12 mm o.d., with a side-arm of the same diameter welded in the middle of the tube, to serve as an inlet. This is mounted centrally above a Varian Techtron air - acetylene H/S burner (10-cm slit length).

(ii) The stainless-steel needle fitted to the 2-ml plastic syringe was replaced with 1 mm i.d. PTFE tubing. The tubing remained in the Supelco septum permanently and the end protruding above the septum was cut at an angle of 45° so that the delivery end of the full syringe could be fitted over the tubing with a twisting motion before each injection. (The internal diameter of the delivery end matched the external diameter of the tubing, *viz.*, 2 mm.)

(iii) The nitrogen flow-rate was changed to 0.9 l min^{-1}.

Experimental

Standard Solutions

An antimony potassium tartrate stock solution, containing 100 mg l^{-1} of antimony in 9 N sulphuric acid, was diluted to give working standards containing 0.002, 0.01, 0.03 and 0.05 mg l^{-1} of antimony in 9 N sulphuric acid.

Procedure

Digestion of the blood or urine was carried out by essentially the method described by Sandell,[1] such that after making up to volume the final solution was 9 N in sulphuric acid and contained 0–0.05 mg l^{-1} of antimony.

The Varian Techtron AA1200 atomic-absorption spectrophotometer settings were as follows: wavelength, 217.6 nm; slit width, see below; and lamp current, 5 mA.

When making up the 1% *m/V* sodium tetrahydroborate(III) (sodium borohydride) solution[2] one pellet of analytical-reagent grade potassium hydroxide per gram of sodium tetrahydroborate(III) was used.

Results and Discussion

Typical results obtained by one analyst on blood and another analyst on urine are given below.

Blood

A 150-ng amount of antimony was added to 1 g of blood (≡15 μg per 100 ml). After digestion the final volume was 20 ml, giving a theoretical concentration of added antimony of 7.5 μg l^{-1}. The slit width was 0.5 nm. The results are given in Table I.

TABLE I

RESULTS FOR DETERMINATION OF ANTIMONY IN BLOOD

Material	Antimony content/ng	Absorbance	Range	Absorbance—blank	Antimony recovered/ng	Recovery, %
Standards	0	0.010	0.010–0.016	—	—	—
	2	0.037	0.034–0.039	0.027	—	—
	10	0.129	0.127–0.131	0.119	—	—
	30	0.351	0.347–0.353	0.341	—	—
Blood samples ..	0*	0.010	0.009–0.010	—	—	—
	7.5*	0.092	0.090–0.093	0.082	6.7	89
	7.5*	0.097	0.095–0.099	0.087	7.1	95
	7.5*	0.102	0.099–0.105	0.092	7.5	100

* Antimony added.

The calibration graph was rectilinear.

Urine

A 500-ml volume spiked with 15 μg of antimony, giving 30 ng ml^{-1} of added antimony, was used. A 50-ml aliquot was digested to give a final volume of 50 ml. The slit width was 0.2 nm. The results are given in Table II.

TABLE II

RESULTS FOR DETERMINATION OF ANTIMONY IN URINE

Material	Antimony content/ng	Absorbance	Range	Antimony recovered/ng	Recovery, %
Standards	0	0.014	0.010–0.018	—	—
	10	0.234	0.226–0.240	—	—
	30	0.540	0.528–0.545	—	—
	50	0.840	0.835–0.846	—	—
Urine samples ..	0*	0.067	0.066–0.068	1	—
	30*	0.518	0.499–0.524	28	90
	30*	0.517	0.512–0.521	28	90
	30*	0.515	0.512–0.517	28	90

* Antimony added.

The calibration graph was rectilinear from 7 to 50 ng.

The reproducibility within a run is good, as indicated by the results in Tables I and II. The difference in sensitivity when using the two different slit widths for blood and urine can be explained by a variation in the absorbance - band width profile for antimony.[3]

We thank the Director, Government Chemical Laboratories, for permission to publish this paper.

References

1. Sandell, E. B., "Colorimetric Metal Analysis," Third Edition, Volume 3, Interscience, New York, 1959, p. 275.
2. Fleming, D. E., and Taylor, G. A., *Analyst*, 1978, **103**, 101.
3. "Hollow Cathode Lamp Data," Varian Techtron, 1972, p. 1.

Received *May 2nd*, 1978
Accepted *May 15th*, 1978

Quantitative Determination of Steroids in Semi-solid Pharmaceutical Preparations by Using High-performance Liquid Chromatography

Monir Amin* and Peter W. Schneider

Schering A.G., Department Galenik/Department Allgemeine Physikochemie, Müllerstrasse 170–178, 1000 Berlin 65, Germany

Keywords: High-performance liquid chromatography; quantitative steroid determination; semi-solid pharmaceutical preparations

The efficiency of high-performance liquid chromatography (HPLC) for the separation of mixtures of compounds with various properties is well documented[1–4] and has been exploited for numerous compounds of therapeutic interest.[5–12] The determination of such active compounds in pharmaceutical preparations, however, is often complicated by the chemical nature and the large excess of the pharmaceutical excipients. In this paper, methods are described for the quantitative determination of steroids, using creams, fatty ointments and fatty suppositories as examples of semi-solid preparations. In particular, it is shown that many of the detrimental effects of these auxiliary compounds on the quantitative determination of the active ingredients can be overcome by the use of HPLC.

Experimental

Materials and Reagents

Preparation A. Oil - water emulsion cream on the basis of paraffinic components containing 0.1% *m/m* of 11β-hydroxy-3,20-dioxopregna-1,4-diene-21-acid butyl ester (compound 1).

Preparation B. Water - oil emulsion cream on the basis of paraffins and waxes containing 0.5% *m/m* of 11β,17-dihydroxy-3,20-dioxopregna-1,4-diene-21-acid butyl ester (compound 2).

Preparation C. Fatty ointment on the basis of Plastibase containing 0.5% *m/m* of 6α-fluoro-11β-hydroxy-3,20-dioxo-16α-methylpregna-1,4-diene-21-acid butyl ester (compound 3).

Preparation D. Suppository on the basis of fatty components with 4.0 mg (per suppository) of compound 3.

Eluents. Methanol - water (3 + 7 *V/V*) for preparation A and methanol - water (1 + 1 *V/V*) for preparations B–D.

Reference solutions. For preparation A: 6.46 mg of compound 1 and 6.36 mg of compound 2 (internal standard) were weighed to 0.01 mg and dissolved in 50 ml of methanol.

For preparation B: 2.80 mg of compound 2 and 5.80 mg of clocortolone caproate (compound 4) as internal standard were weighed to 0.01 mg and dissolved in 50 ml of methanol.

For preparations C and D: 4.85 mg of compound 3 and 7.35 mg of compound 4 (internal standard) were weighed to 0.01 mg and dissolved in 50 ml of methanol. Ten-microlitre volumes of these solutions were injected into the HPLC column.

Apparatus and Conditions

A Du Pont, Model 841, liquid chromatograph with an ultraviolet detector (254 nm) and a column of Du Pont Zipax ETH Permaphase, 100 cm × 2.1 mm i.d., was used.

The mobile phase pressure was 10.3 MPa for preparations A and C, 6.5 MPa for preparation B and 13.7 MPa for preparation D, giving flow-rates of approximately 0.5–1 ml min^{-1}.

The chromatograms were evaluated by addition of an internal standard. Typical chromatograms are shown in Figs. 1 and 2.

* To whom correspondence should be addressed.

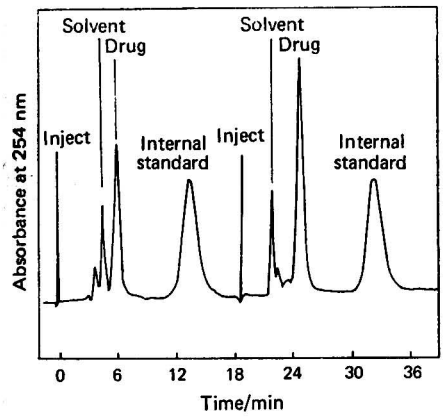

Fig. 1. Typical liquid chromatogram of preparation B: left, reference chromatogram; right, chromatogram of preparation.

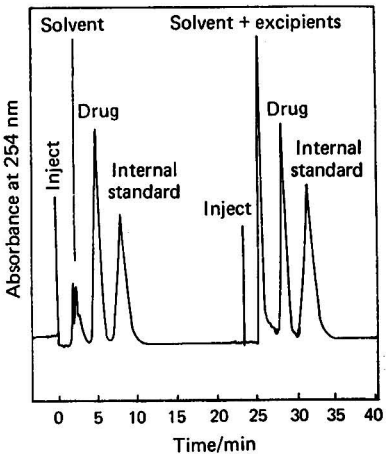

Fig. 2. Typical liquid chromatogram of preparation C: left, reference chromatogram; right, chromatogram of preparation.

Procedure

Sample preparation

For preparations A and B: 1.0 g of cream A (corresponding to 1.0 mg of compound 1) or 129.4 mg of cream B (corresponding to 0.647 mg of compound 2) were accurately weighed. In order to remove the water from the preparations, the samples were dissolved in 20 ml of a 1 + 1 mixture of chloroform and methanol and the solution was evaporated to dryness using a rotary evaporator at 30–40 °C. The residues were dissolved in 20–30 ml of warm methanol and the solution was cooled to 20–30 °C. The fatty components solidified and were filtered off and treated twice more by following the same procedure. The combined filtrates were evaporated to dryness and the residue was taken up in methanol containing the internal standard (1 mg of compound 2 in 10 ml of methanol for preparation A and 1.05 mg of compound 4 in 10 ml of methanol for preparation B).

It is more convenient and efficient to extract the active components from the above preparations by employing a fully automatic method developed in our laboratories.[13]

For preparations C and D: 0.4 g of fatty ointment C (corresponding to 2.0 mg of active substance) or one suppository (corresponding to 4.0 mg of active substance) was dissolved in warm methanol and treated as described above. A solution of compound 4 in methanol was added as internal standard, such that its final concentration was 3.4 mg per 20 ml and 4 mg per 25 ml for preparations C and D, respectively.

Thin-layer chromatography (TLC)

Reference solutions and extracts from the samples (see *Sample preparation*) were chromatographed on 20 × 20 cm silica gel plates (F_{254}, Merck); the amounts of solution applied were such that they contained 1–5 μg of the active substances. The plates were developed as follows.

Preparations A and B: a preliminary elution to remove fats was carried out with hexane - diethyl ether (1 + 1 *V/V*) for a development time of approximately 90 min. The plates were dried in a stream of warm air before the analytical separation in cyclohexane - ethyl acetate (1 + 1 *V/V*), when the elution time was approximately 90 min.

Preparations C and D: a preliminary elution to remove fats was carried out with benzene - chloroform (1 + 1 *V/V*) for approximately 90 min, after which the plates were dried and the analytical separation was carried out as described for preparations A and B.

The developed spots were quantitatively evaluated by reflectance measurement at the appropriate wavelengths using a Model PMQ II spectrophotometer - densitometer (Zeiss, Oberkochen) and standardisation against an external standard.[14] The results are given in Table I.

TABLE I

ANALYSIS OF PREPARATIONS A–D BY THIN-LAYER CHROMATOGRAPHY

The results given are the means of eight determinations.

Preparation	Amount of active substance present in preparation	Amount of active substance found: Mean value	Standard deviation of the individual values	Coefficient of variation, %
A	0.1% *m/m*	0.103%	0.003%	2.9
B	0.5% *m/m*	0.512%	0.031%	6.0
C	0.5% *m/m*	0.507%	0.029%	5.7
D	4.0 mg per suppository	3.88 mg	0.160 mg	4.1

Elution of excipients from the HPLC column

Following the freezing-out procedure, some of the excipients still remain, and these require multiple elution techniques for separation by TLC as described above. It was shown by TLC that these components do not accumulate on the HPLC column. For this purpose a placebo cream, analogous to preparation B, was treated as described under *Sample preparation*. It was found that approximately 7% of the excipients were not removed. This residue was taken up in methanol - chloroform (1 + 1 *V/V*) and examined by TLC using dichloromethane as eluent and made visible by spraying with 5% ethanolic dodecamolybdophosphoric acid. The individual components were spotted for reference (Fig. 3). Part of the placebo residue was injected into the HPLC system and the following fractions were collected and examined by TLC to demonstrate that all of the excipients had been eluted from the column (Fig. 4): fraction (a), eluent prior to injection of sample; fraction (b), 6 ml (12 min) after injection of placebo residue; fraction (c), 25 ml (12–62 min) after collection of fraction (b); and fraction (d), 20 ml (62–102 min) after collection of fraction (c).

Discussion

Quality control and the determination of long-term stability data of pharmaceutical preparations require, for the quantitative determination of the active compounds, analytical methods that are reliable in the presence of a large excess of complex mixtures of excipients. In the examples of oil - water and water - oil emulsions, fatty ointments and suppositories discussed in this paper, a freezing-out method is used to remove the bulk of the excipients, but there are still sufficient components left behind to interfere seriously in a gas - liquid chromatographic (GLC) method, even if the active compounds are amenable to separation by GLC. Some of the excipients not removed yield GLC peaks that interfere in the detection of the active compounds while others are not sufficiently volatile and accumulate on the column, shortening the column life and changing its separation characteristics. The fatty preparations, however, can be analysed by TLC, but the remaining excipients require the use of multiple elution techniques and thus a considerable investment in time and technical supervision. The HPLC system described here offers a number of advantages over GLC and TLC. An important advantage is that the active compounds can be separated and determined in a short time, with the fatty components not interfering and not irreversibly altering the column performance. These components are eluted quantitatively from the column by the same eluent that is used for the separation of the active compounds (Figs. 3 and 4). There is no alteration in retention times and, as the excipients do not absorb ultraviolet light at 254 nm, there is no interference in the detection of the active compounds (Figs. 1 and 2). As summarised in Tables II and III, speed, accuracy and sensitivity make HPLC a valuable tool for the analysis of complex pharmaceutical formulations.

It is possible to perform several analyses simultaneously on one TLC plate. Thus, the rather long development times given in Table II should not be interpreted as giving HPLC preference over TLC in every instance. It is still the responsibility of the analyst to consider and decide which technique is to be preferred for a given problem.

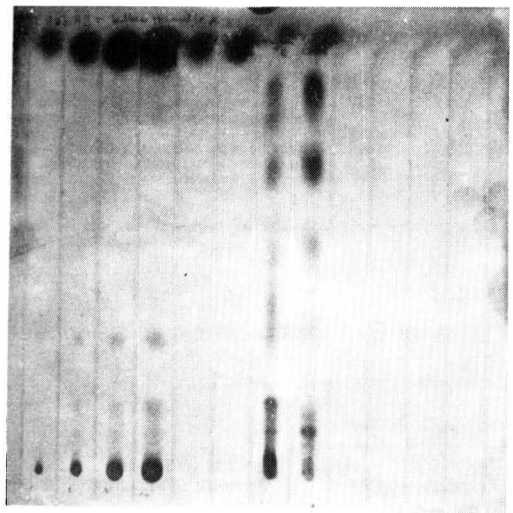

Fig. 3. Thin-layer chromatogram showing the components of the excipients of preparation B and the components not removed by the freezing-out procedure. Amounts of 1, 2, 5 and 10 μl of the residue were spotted on the four tracks to the left of the TLC plate. The four tracks on the right of the plate show the individual components of the excipients.

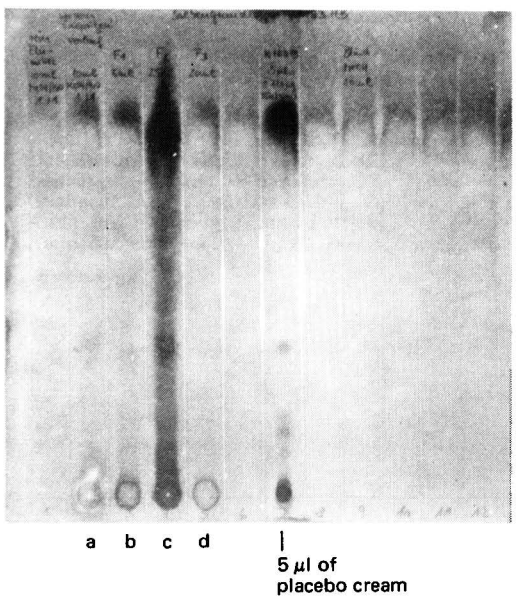

Fig. 4. Thin-layer chromatogram showing that all components of the excipients from preparation B are eluted from the HPLC column.

[To face p. 1078

TABLE II

COMPARISON OF HIGH-PERFORMANCE LIQUID CHROMATOGRAPHIC AND THIN-LAYER CHROMATOGRAPHIC PROCEDURES

	Preparation							
	A		B		C		D	
Parameter	HPLC	TLC	HPLC	TLC	HPLC	TLC	HPLC	TLC
Approximate time for sample application* ..	5 s	5 min	5 s	5 min	5 s	5 min	5 s	5 min
Approximate time for development of chromatograms*	30 min	3 h	24 min	3 h	12 min	3 h	10 min	3 h
Approximate time for quantitative evaluation*	5 min	15 min	5 min	15 min	5 min	15 min	5 min	15 min
Lower limit for quantitative evaluation (approximately 10× noise level at peak maximum)/μg	0.1	1	0.1	1	0.1	1	0.1	1

* Several tracks are developed on one TLC plate simultaneously. This is a great advantage of TLC over the other methods, particularly in routine analysis.

TABLE III

ANALYSIS OF PREPARATIONS A–D BY HIGH-PERFORMANCE LIQUID CHROMATOGRAPHY

The results given are the means of eight determinations.

		Amount of active substance found			Calibration factor		
Preparation	Amount of active substance present	Mean	Standard deviation	Coefficient of variation, %	Mean	Standard deviation	Coefficient of variation, %
A	0.1% *m/m*	0.101%	0.002%	2.2	1.122	0.019	1.7
B	0.5% *m/m*	0.505%	0.026%	5.2	0.956	0.016	1.8
C	0.5% *m/m*	0.501%	0.027%	5.6	0.694	0.019	2.8
D	1 mg per suppository	0.972 mg	0.036 mg	3.8	0.680	0.033	5.0

References

1. Amin, M., and Schneider, P. W., *Analyst*, 1978, **103**, 728.
2. Kirkland, J. J., *Editor*, "Modern Practice of Liquid Chromatography," Wiley-Interscience, New York, London, Sydney and Toronto, 1971.
3. Hadden, N., and Baumann, F., "Basic Liquid Chromatography," Varian Aerograph, Walnut Creek, Calif., 1971.
4. Perry, S. L. G., Amos, R., and Brewed, P. I., "Practical Liquid Chromatography," Plenum Press, New York, 1972.
5. Wragg, J. S., and Johnson, G. W., *Pharm. J.*, 1974, **213**, 601.
6. Salmon, J. R., and Wood, P. R., *Analyst*, 1976, **101**, 611.
7. Cobb, P. H., *Analyst*, 1976, **101**, 768.
8. Weddle, O. H., and Mason, W. D., *J. Pharm. Sci.*, 1977, **66**, 874.
9. Owen, B. J., and Wilkie, S. V., *J. Pharm. Sci.*, 1977, **66**, 877.
10. Das Gupta, V., and Ghanekar, A. G., *J. Pharm. Sci.*, 1977, **66**, 895.
11. Das Gupta, V., and Sachanandani, S., *J. Pharm. Sci.*, 1977, **66**, 897.
12. Ghanekar, A. G., and Das Gupta, V., *Am. J. Hosp. Pharm.*, 1977, **34**, 651.
13. Amin, M., Korbakis, Z., and Petrick, D., *Z. Analyt. Chem.*, 1976, **279**, 283.
14. Amin, M., and Jakobs, U., *Z. Analyt. Chem.*, 1974, **268**, 119.

Received *February 3rd*, 1978
Accepted *April 14th*, 1978

Determination by Gas Chromatography - Single-ion Monitoring Mass Spectrometry of Phthalate Contaminants in Intravenous Solutions Stored in PVC Bags

G. A. Ulsaker and R. M. Hoem
National Centre for Medicinal Products Control, Sven Oftedals vei 8, Oslo 9, Norway

Keywords: Phthalate contaminants; intravenous solutions; poly(vinyl chloride) bags; gas chromatography - single-ion monitoring mass spectrometry

Poly(vinyl chloride) (PVC) plasticised with phthalate esters, *e.g.*, bis(2-ethylhexyl) phthalate, has been used for many years in the manufacture of medical accessories such as storage bags for intravenous solutions, transfusion assemblies and haemodialysis units. Small amounts of bis(2-ethylhexyl) phthalate may leach out when these articles are brought into contact with solvents. Special attention has been given to the concentration of this compound in blood and plasma (for example, references 1 and 2). The presence of bis(2-ethylhexyl) phthalate in intravenous solutions such as physiological saline and glucose solutions stored in PVC bags has also been reported.[3]

Intravenous solutions dispensed in PVC bags are heat-sterilised and may be stored for a few years in contact with the plasticised PVC wall. Little published information is available, however, concerning the possible hydrolysis of bis(2-ethylhexyl) phthalate into the corresponding alcohol and acid. Phthalic acid and 2-ethylhexan-1-ol have been identified in anticoagulant citrate dextrose (ACD) solutions.[4] Contaminants of a different origin than the plasticiser may also occur. Recently, cyclohexanone has been detected in intravenous solutions.[5]

Gas chromatography has been one of the most frequently used methods in analyses for phthalates.[6] Mass fragmentography, however, has developed as a selective and sensitive method for trace analyses. The electron-impact mass spectra of phthalate esters have been extensively studied.[7,8] Dimethyl phthalate and methyl 2-ethylhexyl phthalate have base peaks at *m/e* 163. Bis(2-ethylhexyl) phthalate has only a minor fragment at *m/e* 163. After treatment with diazoethane, bis(2-ethylhexyl) phthalate, phthalic acid, butyl hydrogen phthalate and 2-ethylhexyl hydrogen phthalate have base peaks at *m/e* 149.

In this paper a new method is described, based on gas chromatography - single-ion monitoring mass spectrometry, for the simultaneous determination of phthalic acid, 2-ethylhexyl hydrogen phthalate and bis(2-ethylhexyl) phthalate, using butyl hydrogen phthalate as internal standard. The ethyl ester derivatives of the phthalates are eluted at different times from the gas chromatograph, as shown by monitoring the common base peak of the phthalates. A new method for the determination of 2-ethylhexan-1-ol from the hydrolysis of bis(2-ethylhexyl) phthalate is also described. The method is based upon single-ion monitoring of the base peak of the alcohol at *m/e* 57. The isomeric octan-1-ol is used as internal standard, having a major fragment at *m/e* 57.

Experimental

Apparatus

The scanning of mass spectra and the single-ion monitoring were carried out by using an LKB 2091 gas chromatograph - mass spectrometer. The mass marker on the instrument was used for stabilising the magnetic field on a pre-selected value. The electron-impact ion source was operated at 20 eV when recording the single-ion traces and at 70 eV when scanning the mass spectra.

In the determination of the phthalates a glass column (1.5 m × 2 mm i.d.) packed with 3% SE-30 on Supelcoport (80–100 mesh) was used. The injector, the separator and the ion source were all maintained at 250 °C. The temperature of the column oven was maintained at 140 °C for 2 min after injection and then increased at a rate of 20 °C min^{-1} to 240 °C. The helium flow-rate was 25 ml min^{-1}.

When 2-ethylhexan-1-ol was determined, a glass column (1.5 m × 2 mm i.d.) packed with 10% SP-1000 on Supelcoport (80–100 mesh) was used. The injector, the separator and the ion source were maintained at 160 °C. The temperature of the column was 110 °C and the helium flow-rate was 40 ml min^{-1}.

Reagents

All reagents used were of the highest available purity. The glassware was rinsed with a solution of potassium dichromate in concentrated sulphuric acid and then with distilled water in order to reduce potential interferences to a minimum.

2-Ethylhexyl hydrogen phthalate. Synthesised according to the method given in reference 9.

Butyl hydrogen phthalate. Synthesised according to the method given in reference 9.

Esterifying reagent. An ethereal solution of diazoethane was prepared.[10]

Caution—Work should be carried out in a well ventilated fume hood. Prevent contact with skin and eyes.

Samples. The intravenous solutions dispensed in plasticised PVC bags were commercial samples.

Procedures

Determination of phthalates

Hydrogen chloride (5.0 ml, 6 N), methanol (4.0 ml) and a solution of internal standard (1.0 ml of a 100 mg l^{-1} solution of butyl hydrogen phthalate in methanol) were added to 250 ml of the intravenous solutions (bags a–d, Table I). After mixing, the sample was extracted with 2.0 ml of chloroform. The extract was then treated for 15 min with excess of an ethereal solution of diazoethane (0.5 ml) at 0 °C. After evaporation of the solvent the residue was dissolved in chloroform (1.0 ml) and a suitable aliquot (2 μl) was injected into the instrument, monitoring the base peak of the phthalate esters (*m/e* 149). For the ACD and CPD (anticoagulant citrate phosphate dextrose) solutions (bags e and f, Table I), 50 ml of solution and 6.0 ml of hydrogen chloride (6 N) were used.

TABLE I

DETERMINATION OF PHTHALATE CONTAMINANTS IN INTRAVENOUS SOLUTIONS

Bag	Solution	Age/ years	Concentration/mg l^{-1}			
			Phthalic acid	2-Ethylhexyl hydrogen phthalate	Bis(2-ethyl-hexyl) phthalate	2-Ethylhexan-1-ol
a	500 ml of 0.9% saline solution	2½	0.08	0.1	0.01	0.04
b	500 ml of 5% glucose solution	3½	0.07	0.03	0.02	0.02
c	500 ml of 5% glucose - 0.9% saline solution	2½	0.08	0.03	0.01	0.02
d	500 ml of Ringer lactate solution	4½	0.03	0.15	0.01	
e	76.5 ml of ACD solution	1½	0.05	0.20	—*	0.28
f	63 ml of CPD solution	½	0.59	2.25	—*	0.27

* Results unreliable (see text).

A standard matrix was prepared for each sample. Known amounts of phthalic acid, 2-ethylhexyl hydrogen phthalate, bis(2-ethylhexyl) phthalate and 2-ethylhexan-1-ol, each dissolved in 1.0 ml of methanol, were added to a portion of the matrix. Calibration graphs for the phthalates in each sample were constructed, treating the standard preparation as described above. Retention times were 130 s for diethyl phthalate, 222 s for the internal standard, 324 s for ethyl 2-ethylhexyl phthalate and 540 s for bis(2-ethylhexyl) phthalate. Single-ion monitoring traces for the ethyl ester derivatives of phthalates in CPD solution are shown in Fig. 1.

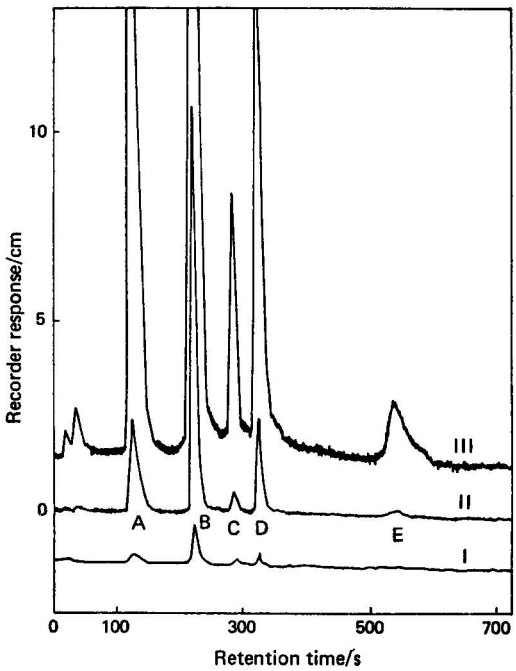

Fig. 1. Single-ion monitoring traces (m/e = 149) of ethyl ester derivatives of phthalates in CPD solution. A, Diethyl phthalate; B, internal standard; C, unknown compound; D, ethyl 2-ethylhexyl phthalate; and E, bis(2-ethylhexyl) phthalate. The intensity ratios between traces I, II and III are 1 : 10 : 100.

Alternative standard-additions procedure[11]

The contents of five bags of CPD solution were mixed. Internal standard was added to a 50-ml portion of the resulting solution and extraction and derivatisation were carried out. To three further 50-ml portions were added internal standard and 2-ethylhexyl hydrogen phthalate in methanol solution to levels of 2, 4 and 6 mg l^{-1}. After mixing each portion of sample was treated as described above.

Determination of 2-ethylhexan-1-ol

Sodium hydrogen carbonate (0.5 g), methanol (4.0 ml) and a solution of internal standard (1.0 ml of a 100 mg l^{-1} solution of octan-1-ol in methanol) were added to 250 ml of the intravenous solutions (bags a–d, Table I). After mixing, the sample was extracted with 1.5 ml of chloroform and an aliquot of the extract (1 μl) was injected into the instrument, monitoring the base peak of 2-ethylhexan-1-ol (m/e 57). For the ACD and CPD solutions (bags e and f, Table I), 50 ml of solution and 1.0 g of sodium hydrogen carbonate were used.

Calibration graphs for each sample were constructed by using standard preparations. Retention times were 150 s for 2-ethylhexan-1-ol and 210 s for the internal standard.

Precision

The phthalates in a physiological saline solution to which had been added 0.1 mg l^{-1} of phthalic acid, 0.1 mg l^{-1} of 2-ethylhexyl hydrogen phthalate, 0.01 mg l^{-1} of bis(2-ethylhexyl) phthalate and 0.03 mg l^{-1} of 2-ethylhexan-1-ol were determined. The relative standard deviation was 8% for phthalic acid, 6% for 2-ethylhexyl hydrogen phthalate and 10% for bis(2-ethylhexyl) phthalate (n = 8). When 2-ethylhexan-1-ol was determined the relative standard deviation was 6% (n = 8).

Results and Discussion

For the CPD solution, phthalic acid and 2-ethylhexyl hydrogen phthalate were identified after extraction and derivatisation by comparing retention times and fragmentation with those of authentic samples. An underivatised sample revealed neither diethyl phthalate nor ethyl 2-ethylhexyl phthalate. In the other samples (bags a–e, Table I) the identification of phthalic acid, 2-ethylhexyl hydrogen phthalate and bis(2-ethylhexyl) phthalate is based upon retention times and monitoring of the base peak at *m/e* **149**. Correspondingly, 2-ethylhexan-1-ol was identified by monitoring the base peak at *m/e* **57**. All the contaminants were detected in the samples investigated and the results of the determinations are given in Table I.

The concentrations of phthalic acid, 2-ethylhexyl hydrogen phthalate and 2-ethylhexan-1-ol are higher than the concentration of bis(2-ethylhexyl) phthalate, but the concentrations of all the impurities are low for bags a–d. Bags e and f, however, gave higher values for the contaminants. In particular, the CPD solution contained a much larger amount of 2-ethylhexyl hydrogen phthalate (2.25 mg l^{-1}). About 1 year later a sample of the same batch number was analysed by using the standard-additions procedure, the result obtained being 2.6 mg l^{-1}.

The contaminants listed in Table I may be decomposition products of bis(2-ethylhexyl) phthalate produced during heat-sterilisation and storage, or they may be extraction products from a contaminated plasticiser.

In the blank solutions no background corresponding to phthalic acid, 2-ethylhexyl hydrogen phthalate and 2-ethylhexan-1-ol could be detected. At the beginning of the work any background due to bis(2-ethylhexyl) phthalate was negligible but as work progressed an increasing background due to this compound was observed, rendering its quantification unreliable for bags e and f. High blank values have been reported previously in determinations of bis(2-ethylhexyl) phthalate.[12]

References

1. Jaeger, R. J., and Rubin, R. J., *New Engl. J. Med.*, 1972, **287**, 1114.
2. Fayz, S., Herbert, R., and Martin, A. M., *J. Pharm. Pharmac.*, 1977, **29**, 407.
3. Weisenberg, E., Schoenberg, Y., and Ayalon, N., *Analyst*, 1975, **100**, 857.
4. Guess, W. L., Jacob, J., and Autian, J., *Drug Intell.*, 1967, **1**, 120.
5. Ulsaker, G. A., and Korsnes, R. M., *Analyst*, 1977, **102**, 882.
6. Fishbein, L., and Albro, P. W., *J. Chromat.*, 1972, **70**, 365.
7. Hites, R. A., *Environ. Hlth Perspect.*, 1973, **3**, 17.
8. Stalling, D. L., Hogan, J. W., and Johnson, J. L., *Environ. Hlth Perspect.*, 1973, **3**, 159.
9. Albro, P. W., Thomas, R., and Fishbein, L., *J. Chromat.*, 1973, **76**, 321.
10. Müller, E., *Editor*, "Methoden der Organischen Chemie," Fourth Edition, Volume X/4, Georg Thieme, Stuttgart, 1968, p. 539.
11. Ewing, G. W., "Instrumental Methods of Chemical Analysis," Third Edition, McGraw-Hill, New York, 1969, pp. 299 and 520.
12. Rubin, R. J., *Lancet*, 1972, **1**, 965.

Received *March 20th*, 1978
Accepted *May 16th*, 1978

Thin-layer Chromatographic Behaviour of Barbiturates Under Various Conditions

R. Abu-Eittah, A. Osman and A. El-Behare*

Department of Chemistry, Faculty of Science, Cairo University, Giza, Egypt

Keywords: *Barbiturate determination*; *thin-layer chromatography*

The major problem in the determination of non-volatile organic drugs (for example barbiturates) in body fluids and tissues is usually the separation and purification of the active

* Medico-legal Department, Ministry of Justice, Cairo, Egypt.

ingredients from the extraneous biological material. Different chromatographic techniques have been used for the separation, identification and determination of barbiturates.[1–8] Chromatograms on fibre-glass sheets impregnated with silica gel and on glass and aluminium foil have been investigated.[9,10] Many reagents have been proposed for the detection of barbiturates by use of the thin-layer chromatographic technique,[11–14] the sensitivity of the method varying between 5 and 0.4 μg. Machata[15] and Machata and Battista[16] have combined thin-layer with gas chromatography for the detection and determination of barbiturates. Several methods of identification of barbiturates by using one-dimensional[17–19] and two-dimensional[20] thin-layer chromatography have been reported, while the quantitative determination of barbiturates with thin-layer chromatographic techniques has also been investigated.[21–23]

In this work a thin-layer chromatographic investigation has been conducted on the separation and identification of some barbiturates and one thiobarbiturate using some new approaches, such as mixing the slurry with an alkali in solution and/or with cobalt(II) ions.

Experimental

Materials

Barbitone (5,5-diethylbarbituric acid) and phenobarbitone (5-ethyl-5-phenylbarbituric acid) were BDH reagents obtained as pure samples. Allobarbitone (5,5-diallylbarbituric acid) and cyclobarbitone [5-(1-cyclohexenyl)-5-ethylbarbituric acid] were Merck chemicals. Brevinarcon [5-ethyl-5-(1-methylpropyl)-2-thiobarbituric acid] was precipitated from the commercially available sodium salt. The solvents, inorganic salts and other reagents were of analytical-reagent grade; silica gel GF_{254} according to Stahl (Merck) was used.

Method

Slurry 1 was prepared by mixing silica gel with water, slurries 2, 3 and 4 were prepared by mixing silica gel with aqueous (1–3%) solutions of potassium hydroxide and slurry 5 was prepared by mixing silica gel with 1% cobalt perchlorate solution. The plates, after being covered with the slurries, were heated at 100 °C for 1 h. The samples were applied to the plates in the conventional manner, the developers being either mercury(II) or cobalt(II) solutions. Two types of mercury(II) reagents were used: firstly, a 1 + 1 (*V*/*V*) mixture of 2% mercury(II) chloride solution in methanol and 0.05% diphenylcarbazone solution in chloroform; and secondly, a solution of 5 g of yellow mercury(II) oxide in 100 ml of 2% sulphuric acid (sp. gr. 1.84), diluted to 250 ml with distilled water. The plate was sprayed with this solution, followed by spraying with 0.05% diphenylcarbazone solution in chloroform. The cobalt(II) reagent consists of a 1% cobalt perchlorate solution in methanol (cobalt chloride, nitrate or acetate could be used).

When the plates that had been coated with slurry 1 were sprayed with cobalt(II) reagent, the colour developed only after spraying with 1% methanolic lithium hydroxide or exposure to ammonia vapour. If slurry 5 was used no spraying reagent was needed when using a developing solvent containing ammonia.

The thin-layer chromatographic study was conducted on chemically pure barbiturates, on barbiturates extracted from commercially available pharmaceutical preparations and from body organs and fluids. The results obtained for extracted barbiturates were identical with those for chemically pure specimens. The developing solvents used were: E_1, chloroform - acetone (1 + 1 *V*/*V*); E_2, chloroform - acetone (9 + 1 *V*/*V*); E_3, chloroform - acetone (1 + 4 *V*/*V*); E_4, chloroform - butanol (4 + 1 *V*/*V*); E_5, chloroform - diethyl ether (3 + 1 *V*/*V*); E_6, hexane - acetone (1 + 1 *V*/*V*); E_7, hexane - acetone (4 + 1 *V*/*V*); E_8, ethyl acetate - benzene (1 + 2 *V*/*V*); E_9, ethyl acetate - benzene (1 + 1 *V*/*V*); E_{10}, ethanol - methanol - 25% ammonia solution (85 + 10 + 5); and E_{11}, acetone - benzene - 25% ammonia solution (20 + 80 + 0.5).

Results and Discussion

R_F Values of the Barbiturates

The R_F values of the barbiturates studied were determined and the results are given in Table I.

TABLE I

R_F VALUES OF THE BARBITURATES

Plate prepared using slurry 1.

Developing solvent	R_F value*				
	B	P	C	A	TB
E_1	0.79	0.76	0.80	0.81	0.94
E_2	0.39	0.37	0.45	0.49	0.96
E_4	1.00	1.00	1.00	1.00	1.00
E_5	0.55	0.51	0.57	0.60	0.93
E_6	0.69	0.68	0.72	0.70	0.83
E_7	0.19	0.17	0.21	0.19	0.39
E_8	0.54	0.57	0.60	0.63	0.85
E_9	0.63	0.67	0.68	0.70	0.86
E_{10}	0.71	0.70	0.71	0.73	0.77
E_{11}	0.29	0.30	0.35	0.35	0.58

* B = Barbitone; P = phenobarbitone; C = cyclobarbitone; A = allobarbitone; and TB = brevinarcon.

Table I shows that, as expected from the eluotropic series,[24] R_F values for barbiturates undergoing thin-layer chromatography increase with decreasing polarity of the developing solvent. The chromatograms resulting from the use of slurry 1 are shown in Fig. 1.

The effect of the properties of the adsorbent (stationary phase) on the rate of migration of the barbiturates has been investigated by determining the R_F values using slurries 2, 3 and 4. Table II gives the results for barbitone. Raising the pH of the slurry led to a reduced rate of migration, *i.e.*, has increased the relative adsorption of the sample. Silica is commonly regarded as an acidic adsorbent and its surface hydroxyl groups do exhibit weak acidity.[24] The adsorptive properties of silica depend almost exclusively on the superficial hydroxyl groups. These groups interact with polar or unsaturated molecules by hydrogen bonding. Mixing silica with an alkali will inactivate the acid sites. As the concentration of alkali increases acidic hydrogens are removed and the sample is adsorbed strongly on the negatively charged oxygen. This effect explains the decrease in the R_F

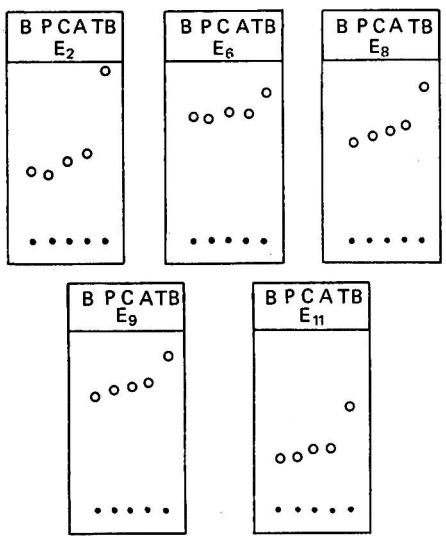

Fig. 1. Chromatograms of barbiturates on plates coated with slurry 1 and developed with solvents E_2, E_6, E_8, E_9 and E_{11}. B, Barbitone; P, phenobarbitone; C, cyclobarbitone; A, allobarbitone; and TB, brevinarcon.

values of both barbiturates and thiobarbiturate as the pH of the slurry increases. Thiobarbiturates, being less polar than their oxo analogues, should show higher R_F values; brevinarcon shows this to be the case.

TABLE II

COMPARISON OF THE R_F VALUES OF BARBITONE USING DIFFERENT SLURRIES AND DEVELOPING SOLVENTS

Developing solvent	R_F value			
	Slurry 1	Slurry 2	Slurry 3	Slurry 4
E_1	0.79	0.76	0.40	0.25
E_2	0.39	0.37	—	—
E_3	—	—	0.49	0.25
E_4	1.00	0.86	0.56	0.39
E_5	0.55	—	—	—
E_6	0.69	0.66	0.35	0.25
E_7	0.19	—	—	—
E_8	0.54	0.34	0.06	0.07
E_9	0.63	0.49	0.14	0.09
E_{10}	0.71	0.75	0.69	0.75
E_{11}	0.29	0.19	0.09	0.05

The barbiturates on the chromatograms were detected by spraying with either cobalt(II) or mercury(II) solutions, except when using slurry 5. The coloured spot observed resulted from the formation of a complex between the metal ion and the enol form of the drug. The formation of the mixed-ligand complex between cobalt(II), barbiturate and ammonia has been closely investigated.[25] The keto form of the drug does not appear to form a complex with the metal ion as the coloured spot does not appear on a neutral slurry unless the plate is sprayed with ammonia solution or lithium hydroxide solution. A similar conclusion has been reported previously.[26]

The sensitivity of the determination is 10 μg of drug when using cobalt(II) reagent and 1.0 μg when using mercury(II) reagent, which increases to 0.5 μg when using an alkaline slurry.

The results given in Table I suggest a simple and fairly accurate scheme for barbiturate detection. In addition, slurry 2 and solvent E_{11} differentiate between brevinarcon (R_F = 0.55) and all of the barbiturates studied (R_F = 0.25–0.19), and slurry 3 and solvent E_6 differentiate between cyclobarbitone (R_F = 0.18) and all other barbiturates (R_F = 0.35–0.42). For a mixture of barbiturates and brevinarcon, adequate separation of the components is achieved by using slurry 2 and solvent E_9. The chromatogram is shown in Fig. 2.

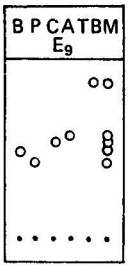

Fig. 2. Chromatogram of barbiturates on plate coated with slurry 2, and developed with solvent E_9. M, Mixture of the five barbiturates; the other abbreviations are the same as in Fig. 1.

References

1. Constantinescu, T., and Enache, S., *Farmacia, Buc.*, 1970, **18**, 45.
2. Gupta, R. C., and Kofoed, J., *Nature, Lond.*, 1963, **198**, 384.
3. Ebel, S., Holtz, H., and Lerche, H., *Dt. ApothZtg*, 1968, **108**, 779.
4. Bush, M. T., *Microchem. J.*, 1961, **5**, 73.
5. Ioannides, C., Chakraborty, J., and Parke, D. V., *Chromatographia*, 1974, **7**, 351.
6. Larebau, S., and Saux, M. C., *J. Eur. Toxicol.*, 1973, **6**, 139.
7. Weissman, N., Lowe, M., Beattie, J. M., and Demetriou, J. A., *Clin. Chem.*, 1971, **17**, 875.
8. Rosenthal, W. A., Kaser, M. M., and Milewski, K. N., *Clinica Chim. Acta*, 1971, **33**, 51.
9. Itiaba, K., Crawhall, J. C., and Sin, C. M., *Clin. Biochem.*, 1970, **3**, 287.
10. Kreysing, G., and Frahm, M., *Dt. ApothZtg*, 1970, **110**, 1133.
11. Goenechea, S., *J. Chromat.*, 1969, **40**, 182.
12. Melzacka, M., and Kahl, W., *Chemia Analit.*, 1969, **14**, 453.
13. Amal, H., Tulus, S., and Sanli, L., *Istanbul Univ. Eczacilik Fak. Mecmuasi*, 1968, **4**, 23.
14. Curry, A. S., and Fox, R. H., *Analyst*, 1968, **93**, 834.
15. Machata, G., *Mikrochim. Acta*, 1960, **1**, 79.
16. Machata, G., and Battista, H. J., *Chromatographia*, 1968, 104.
17. Sohn, D., *US Pat.* 3832134; *Chem. Abstr.*, 1974, **81**, 164454z.
18. Hishida, S., Ueda, M., Tanabe, T., Mizoi, Y., and Kobe, J., *Med. Sci., Tokyo*, 1972, **18**, 1.
19. Kenison, L. T., Loveridge, E. L., Gronlund, J. A., and Elmowafi, A. A., *J. Chromat.*, 1972, **71**, 165.
20. DeZeeuw, R. A., and Wijsbeek, J., *Pharm. Weekbl.*, 1969, **104**, 901.
21. Kammerl, E., and Mutschler, E., *Pharm. Ind., Berl.*, 1973, **35**, 146.
22. Wang, R. I. H., and Mueller, M. A., *J. Pharm. Sci.*, 1973, **62**, 2047.
23. Garceau, Y., Philopoulos, Y., and Hasegawa, J., *J. Pharm. Sci.*, 1973, **62**, 2032.
24. Snyder, L. R., *in* Heftmann, E., *Editor*, "Chromatography," Van Nostrand Reinhold, New York, 1967, pp. 52 and 59.
25. Osman, A., *PhD Thesis*, Department of Chemistry, University of Cairo, Egypt, 1977.
26. Morvay, J., "Study of Transition Metal Thiobarbiturate Complexes," Edit. Universitas Scientiarum Medicinae Szegedinensis, Szeged, 1972.

Received *July 28th*, 1977
Amended *March 7th*, 1978
Accepted *April 6th*, 1978

Book Reviews

FUNDAMENTALS OF RIA AND OTHER LIGAND ASSAYS. A PROGRAMMED TEXT. By JEFFREY C. TRAVIS. Pp. viii + 168. Anaheim, Calif.: Scientific Newsletters, Inc. 1977. Price $25.

The use of immunoassay techniques has expanded very rapidly in recent years, and their potential is enormous, not only in clinical chemistry, but also in environmental analysis, food analysis and other fields. Analysts not familiar with these methods, students of analytical chemistry and their teachers would therefore welcome the publication of a book that explains the principles and practice of immunoassays clearly and concisely. Unfortunately, this book cannot be warmly recommended as its disadvantages outweigh its merits. It has the advantage of being up-to-date, for example, in its inclusion of fluorescence immunoassays and of references dated 1977. Its other advantages include a fairly clear description of the principles of competitive binding assays, a good balance between theory and practice and a useful appendix dealing with counting theory and including a glossary of relevant terms.

On the other hand, the layout of the book as a programmed text must be regarded as a failure. The questions for the would-be student are asked immediately after the information first appears in the text, and the answers generally appear just below the question; this arrangement is perhaps too small a trial of the reader's memory, and too great a trial of his honesty! The extra space involved in making the reader *think* by setting him multiple-choice questions, and by putting the answers on separate pages, would have been well worth while. The book's American origin is also a disadvantage to European readers. Expressions such as "to beef up a precipitate" will irritate some readers and merely amuse others, but the safety regulations described inevitably relate to US legislation, and this is a more serious drawback. There are a number of misprints, some of them unfortunately placed where they seriously hamper understanding of the text (for example, in the crucial Fig. 2). The technical errors probably arise largely from a well intentioned desire to keep the book concise: thus there are a number of simplifications, such as the synonymous use of the terms "antigenic" and "immunogenic," and the rather astonishing statement that "most plasma proteins have a single binding site." Strangely, there is hardly any reference to the widespread use of radioimmunoassays in the determination of very low concentrations of macromolecules (*e.g.*, IgE and α-fetoprotein). Another inexplicable error is the repeated misuse of the term "inversely proportional," even when the accompanying graphs clearly show a curvilinear relationship. Finally, and this is not merely a repetition of the now routine reviewer's complaint, the price: in this instance, although by its nature the book is clearly designed for individual use, one is asked to pay $25 (about £15) for a paperback book containing 168 pages and poorly printed on coarse paper. To add insult to injury, my copy started to disintegrate as soon as I opened it. On a number of grounds, therefore, one must regretfully conclude that there still remains a need for a satisfactory introductory text in this field. J. N. MILLER

WATER ANALYSIS: SOME REVISED METHODS FOR LIMNOLOGISTS. By F. J. H. MACKERETH, J. HERON and J. F. TALLING. *Scientific Publication No.* 36. Pp. 122. Far Sawrey, Ambleside: Freshwater Biological Association. 1978. Price £2.50 (non-members).

This small handbook is sub-titled "Some Revised Methods for Limnologists," but its contents immediately make this sub-title inadequate, for this is a small gem of a book good enough to be in every laboratory that deals with water analysis. It is obviously written by experts for those of us who have occasion to require to analyse water as a non-routine but frequently occurring assay, and for whom the more complex systems of automation for repetitive analysis of large numbers of samples are not economically viable.

The general remarks in the introductory chapter reveal the wealth of practical experience of the authors and the pragmatism that pervades the whole of this volume.

It might be argued that this book lacks a consideration of the theoretical background of the methods quoted; this may be so, and it can also be stated that it does not give values in SI units and still talks about normalities of solutions; these may be faults, but they fade into significance before the commonsense approach of this book. I enjoyed reading it—I shall enjoy using it.

L. S. BARK

Potentiality of Seaweed as a Resource: Analysis of the Pyrolysis Products of *Fucus serratus*

As a prelude to the investigation of the potentiality of seaweeds as a future source of organic chemicals or fuel, the products of pyrolysis under nitrogen of *Fucus serratus* (serrated wrack) have been analysed. The pyrolysis produces large amounts of charcoal, water and carbon dioxide with smaller amounts of an oil, pitch, hydrocarbon gases, carbon monoxide, ammonia and carboxylic acids. The oil proved to be a complex mixture of heterocyclic bases, phenols, aromatic hydrocarbons, nitrogen and oxygen heterocyclic compounds and small amounts of aliphatic compounds. A variety of analytical techniques have been employed to analyse the pyrolysis products, with gas chromatography and mass spectrometry being the most widely applicable.

Keywords: *Seaweed pyrolysis*; Fucus serratus; *gas chromatography*; *mass spectrometry*

PHILLIP J. MORGAN and KEITH SMITH

Department of Chemistry, University College of Swansea, Singleton Park, Swansea, SA2 8PP.

Analyst, 1978, **103**, 1053–1060.

Determination of Theophylline in Plasma: Comparison of High-performance Liquid Chromatography and an Enzyme Multiplied Immunoassy Technique

Plasma theophylline concentrations have been determined by both high-performance liquid chromatography and the enzyme multiplied immunoassay technique (EMIT). Comparison of the results showed a good correlation between the techniques. The faster processing time and smaller sample size makes EMIT the preferred technique when routine batch assays for theophylline are required.

Keywords: *Theophylline determination*; *plasma*; *high-performance liquid chromatography*; *enzyme multiplied immunoassy technique*

M. L. EPPEL, J. S. OLIVER and HAMILTON SMITH

Department of Forensic Medicine, Glasgow University, Glasgow, G12 8QQ.

A. MACKAY

MRC Blood Pressure Unit, Western Infirmary, Glasgow, G11 6NT.

and L. E. RAMSAY

Department of Medicine, Western Infirmary, Glasgow, G11 6NT.

Analyst, 1978, **103**, 1061–1065.

Optical Emission Spectrometry with an Inductively Coupled Radiofrequency Argon Plasma Source and Sample Introduction with a Graphite Rod Electrothermal Vaporisation Device Part I. Instrumental Assembly and Performance Characteristics

A system is described in which a graphite rod electrothermal vaporisation device is employed for the introduction of microlitre liquid samples, after desolvation, into an inductively coupled argon plasma source for atomisation and excitation for optical emission spectrometry. The analytical performance of the system has been studied and detection limits for 16 elements at the sub-nanogram level are presented.

Keywords: *Optical emission spectrometry*; *inductively coupled radiofrequency argon plasma*; *graphite rod electrothermal atomisation*

A. M. GUNN, D. L. MILLARD and G. F. KIRKBRIGHT

Chemistry Department, Imperial College, London, SW7 2AY.

Analyst, 1978, **103**, 1066–1073.

Determination of Antimony by Stibine Generation and Atomic-absorption Spectrophotometry Using a Flame-heated Silica Furnace

Short Paper

Keywords: *Antimony determination*; *atomic-absorption spectrophotometry*; *hydride generation*; *flame-heated silica furnace*

D. L. COLLETT, D. E. FLEMING and G. A. TAYLOR

Government Chemical Laboratories, Food and Industrial Hygiene Division, 30 Plain Street, Perth, Western Australia 6000.

Analyst, 1978, **103**, 1074–1075.

Quantitative Determination of Steroids in Semi-solid Pharmaceutical Preparations by Using High-performance Liquid Chromatography

Short Paper

Keywords: *High-performance liquid chromatography*; *quantitative steroid determination*; *semi-solid pharmaceutical preparations*

MONIR AMIN and PETER W. SCHNEIDER

Schering A.G., Department Galenik/Department Allgemeine Physikochemie, Müllerstrasse 170–178, 1000 Berlin 65, Germany.

Analyst, 1978, **103**, 1076–1079.

Determination by Gas Chromatography - Single-ion Monitoring Mass Spectrometry of Phthalate Contaminants in Intravenous Solutions Stored in PVC Bags

Short Paper

Keywords: *Phthalate contaminants*; *intravenous solutions*; *poly(vinyl chloride) bags*; *gas chromatography - single-ion monitoring mass spectrometry*

G. A. ULSAKER and R. M. HOEM

National Centre for Medicinal Products Control, Sven Oftedals vei 8, Oslo 9, Norway.

Analyst, 1978, **103**, 1080–1083.

Thin-layer Chromatographic Behaviour of Barbiturates Under Various Conditions

Short Paper

Keywords: *Barbiturate determination*; *thin-layer chromatography*

R. ABU-EITTAH, A. OSMAN and A. EL-BEHARE

Department of Chemistry, Faculty of Science, Cairo University, Giza, Egypt.

Analyst, 1978, **103**, 1083–1087.

ANALAO 103 (1231) 1009–1088 (1978) October 1978
ISSN 0003–2654

THE ANALYST

THE ANALYTICAL JOURNAL OF THE CHEMICAL SOCIETY

CONTENTS

Printed by Heffers Printers Ltd Cambridge England
Entered as Second Class at New York, USA, Post Office